`

Supporting Information

Chemoselective synthesis of isolated and fused fluorenones and their photophysical and antiviral properties

Ismail Althagafi, Ranjay Shaw, Cheng-Run Tang, Rahul Kumar,Shally, Chanda Sinha,Amit Kumar, Yong-Tang Zheng, RamendraPratap

Table of content

`

Screening of reaction condition (scheme-2)

Table 1: Optimization of reaction condition for synthesis of teraryl.

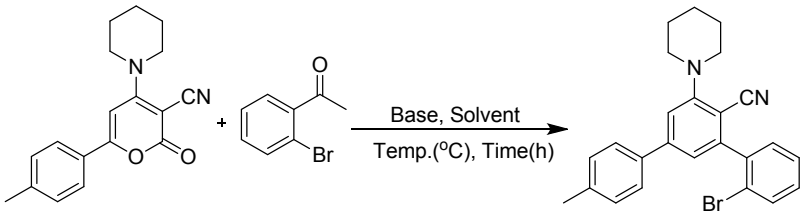

Entry	Base	Solvent	Temp.(°C)	Time(h)	Yield(%)[b]
1	KOH	EtOH	78	6	C.M.
2	KOH	DMF	RT[d]	9	46
3	KOH	DMF	80	5	28[c]
4	**KOH**	**DMSO**	**RT[d]**	**8**	**66**
5	KOH	DMSO	80	5	37[c]
6	KOH	THF	RT[d]	9	44
7	$NaNH_2$	DMF	RT[d]	9	47
8	$NaNH_2$	DMSO	RT[d]	9	56
9	$NaNH_2$	THF	RT[d]	9	33
10	NaH	DMF	RT[d]	9	60
11	NaH	DMF	60	6	53
12	NaH	DMSO	RT[d]	9	51

[a]The reaction was conducted with 6-(4-methyl)-2-oxo-4-(piperidin-1-yl)2H-pyran-3-carbonitrile (0.5 mmol), 2-bromoacetophenone (0.6 mmol)and base (1.0 mmol) in solvent(3.5 mL);
[b]Yieldofisolatedproduct;[c]Another product was also formed in very low yield. [d]Roomtemperaturevaries from 30-40°

`

X-ray Crystallography of 6d

Intensity data for the compound**6d** was collected at 298 K on an Agilent Xcalibur, Sapphire3 diffractometer using graphite monochromated Mo-Kα radiation λ = 0.71073 Å. Unit cell determination, data collection were performed with Oxford Diffraction DiffractometerCrysAlisPro.[1] The structure was solved by SHELXT program[2] and refined on F2 using all data by full matrix least-squares procedures with SHELXL-2014/7[3,4] and incorporated in OLEX2 crystallographic package.[5] The hydrogen atoms were placed at the calculated positions and included in the last cycles of the refinement.[6] The C-H, CH_2 and CH_3 hydrogen atoms were placed at their calculated positions (C-H = 0.93 Å,CH_2= 0.97 Å, CH_3= 0.96 Å) followed by their treatment using ariding model with U_{iso} (H, For CH and CH_2) = 1.2Ueq(C) and U_{iso} (For,CH_3) = 1.5Ueq(C). The graphics for publication was prepared by using Mercury software.[7]Crystallographic data collection and structure solution parameters are summarized in the Table S1. **CCDC**- contains the supplementary crystallographic data for this manuscript.

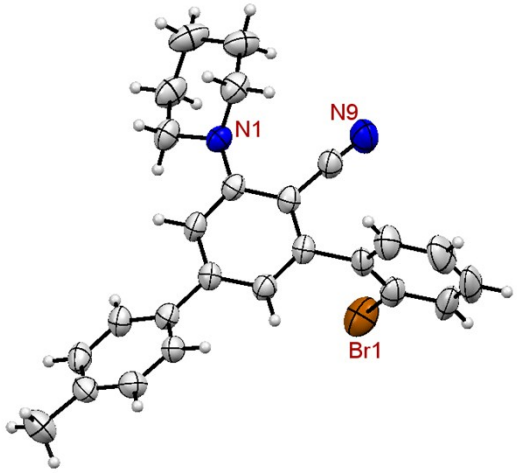

Fig. 1. ORTEP representation of **6d**. Thermal ellipsoids are 50% probability level.

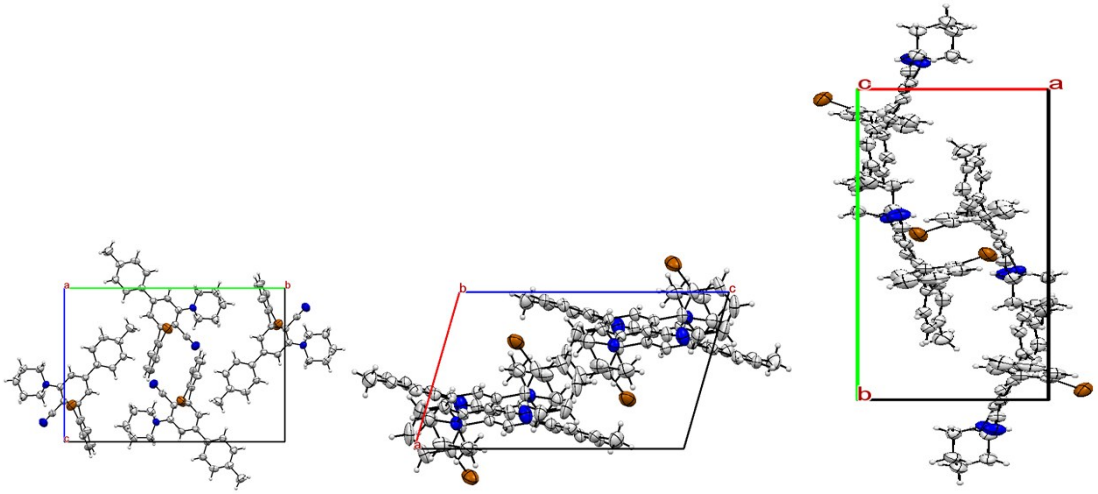

Fig.2. Crystal packing representation of **6d** along A-, B- and C-axis, respectively. Ellipsoids are shown at 50% probability level.

`

Table 2. Crystallographic data and structure refinement parameters for**6d**.

Empirical formula	$C_{25}H_{23}BrN_2$
CCDC	
Formula weight	*431.36*
Temperature/K	*293(2)*
Crystal system	*monoclinic*
Space group	$P2_1/n$
a/Å	*8.4375(6)*
b/Å	*19.2059(12)*
c/Å	*13.8112(10)*
α/°	*90*
β/°	*105.900(7)*
γ/°	*90*
Volume/Å³	*2152.5(3)*
Z	*40*
$\rho_{calc}g/cm^3$	*13.311*
μ/mm^{-1}	*19.217*
F(000)	*8880.0*
Crystal size/mm³	*0.5 × 0.5 × 0.5*
Radiation	*MoKα (λ = 0.71073)*
2Θ range for data collection/°	*6.492 to 50*
Index ranges	$-10 \le h \le 10, -22 \le k \le 22, -16 \le l \le 16$
Reflections collected	*25350*
Independent reflections	*3732 [R_{int} = 0.0549, R_{sigma} = 0.0409]*
Data/restraints/parameters	*3732/0/254*
Goodness-of-fit on F²	*0.984*
Final R indexes [I>=2σ (I)]	*R_1 = 0.0543, wR_2 = 0.1404*
Final R indexes [all data]	*R_1 = 0.0820, wR_2 = 0.1588*
Largest diff. peak/hole / e Å⁻³	*0.37/-0.45*

Table 3. Symmetry operator and derscription of the crystal structure of **6d**.

S.No.	**Symm. Op.**	**Description**
1	x,y,z	Identity
2	1/2-x,1/2+y,1/2-z	Screw axis (2-fold)
3	-x,-y,-z	Inversion centre
4	1/2+x,1/2-y,1/2+z	Glide plane

`

Biological Study

Sample and chemicals

All samples were dissolved in DMSO. AZT were purchased from USP and dissolved in serum-free RPMI-1640 medium.

Reagents

HEPES (N-2 (2-Hydroxyethyl)-piperazine-N'-(2-ethanesufonic acid), MTT (3,(4,5-dimethylthiazol-2-yl) -2,5-diphenyl tetrazolium bromide), DMF (N, N'-Dimethyl formamide), Penicillin, Streptomycin sulfate, Glutamine were purchased from Sigma; 2-ME (2-Mercaptoethanol) was purchased from Bio-Rad. RPMI-1640 and fetal bovine serum (FBS) were purchased from Gibco.

Cells and viruses

C8166 cell and HIV-1_{IIIB} were kindly donated by Medical Research Council, AIDS Regent Project. The cells were maintained at 37℃ in 5% CO_2 in RPMI-1640 medium supplemented with 10% heat-inactivating FBS (Gibco). HIV-$1_{IIIB}$was prepared from the supernatants of H9/HIV-1_{IIIB}cells. The 50% HIV-1 tissue culture infectious dose (TCID50) in C8166 cells was determined and calculated by Reed and Muench method. Virus stocks were stored in small aliquots at -70℃. The titre of virus stock was 1.0×10^8 TCID50 per ml.

Cytotoxicity assay

The cellular toxicity of compounds on C8166 was assessed by MTT colorimetric assay. Briefly, 100μL of 4×10^5 cells were plated into 96-well plates, 100 μL of various concentrations of compounds was added and incubated at 37 ℃ in a humidified atmosphere of 5% CO_2 for 72 h. Discard 100 μL supernatant, MTT reagent was added and incubated for 4 h, 100μL 50% DMF-15% SDS was added. After the formazan was dissolved completely, the plates were analyzed by a Bio-TekELx 800 ELISA reader at 570 nm/630 nm. 50% cytotoxicity concentration (CC_{50}) was calculated.

Inhibition of syncytia formation

The inhibition effect of samples on acute HIV-1 infection was measured by the syncytia formation assay. In the presence or absence of various concentrations of samples, 4×10^4 C8166 cells were infected with HIV-1 at a multiplicity of infection (MOI) of 0.04, and cultured in 96-well plates at 37℃ in 5% CO_2 for 3 days. AZT was used as a positive control. At 3 days post-infection, Cytopathic effect (CPE) was measured by counting the number of syncytia (multinucleated giant cell) in each well of 96-well plates under an inverted microscope (100×). The inhibitory percentage of syncytia formation was calculated by the percentage of syncytia number in treated

`

sample compared to that in infected control. 50% effective concentration (EC_{50}) was calculated.

Formula

According to the method described by Reed &Muench, 50% cytotoxic concentration (CC_{50}) and 50% effective concentration (EC_{50}) was determined from dose–response curve. Therapeutic index (TI) of anti-HIV activity is CC_{50}/EC_{50}.

Cell viability (% of control) = (OD test-OD blk)/(OD ctrl – OD blk)×100

CPE inhibition(%) = (1-CPEtest /CPE ctrl)×1

Table 4. Summary of cytotoxicity and anti-HIV-1 activities of compounds

Sample code	Experiment	Method	CC_{50} (μM)	EC_{50} (μM)	Therapeutic index (TI)
6b	Cytotoxicity assay	MTT	46.26	—	2.21
	Inhibition of syncytium Formation	CPE	—	20.95	
6d	Cytotoxicity assay	MTT	>200	-	>14.21
	Inhibition of syncytium Formation	CPE	—	14.07	
6e	Cytotoxicity assay	MTT	>200		>4.02
	Inhibition of syncytium Formation	CPE	—	49.76	
6g	Cytotoxicity assay	MTT	>200		>46.19
	Inhibition of syncytium Formation	CPE	—	4.33	
6h	Cytotoxicity assay	MTT	>200		-
	Inhibition of syncytium Formation	CPE	—	>200	
6i	Cytotoxicity assay	MTT	>200		-
	Inhibition of syncytium Formation	CPE	—	>200	

`

6j	Cytotoxicity assay	MTT	>200		>3.49
	Inhibition of syncytium Formation	CPE	—	57.25	
6k	Cytotoxicity assay	MTT	>200		>47.96
	Inhibition of syncytium Formation	CPE	—	4.17	
6l	Cytotoxicity assay	MTT	66		<0.33
	Inhibition of syncytium Formation	CPE	—	>200	
6m	Cytotoxicity assay	MTT	>200		>21.51
	Inhibition of syncytium Formation	CPE	—	9.30	
6n	Cytotoxicity assay	MTT	>200		>5.74
	Inhibition of syncytium Formation	CPE	—	34.85	
6o	Cytotoxicity assay	MTT	>200		>4.01
	Inhibition of syncytium Formation	CPE	—	49.90	
8b	Cytotoxicity assay	MTT	>200		>3.50
	Inhibition of syncytium Formation	CPE	—	57.09	
8d	Cytotoxicity assay	MTT	>200		>10.10
	Inhibition of syncytium Formation	CPE	—	19.80	
8e	Cytotoxicity assay	MTT	61.50		3.73
	Inhibition of syncytium Formation	CPE	—	16.47	
8g	Cytotoxicity assay	MTT	>200		>8.18

`

	Inhibition of syncytium Formation	CPE	—	24.44	
8h	Cytotoxicity assay	MTT	>200		>4.19
	Inhibition of syncytium Formation	CPE	—	47.71	
8i	Cytotoxicity assay	MTT	57.30		3.27
	Inhibition of syncytium Formation	CPE	—	17.54	
8j	Cytotoxicity assay	MTT	>200		>7.96
	Inhibition of syncytium Formation	CPE	—	25.13	
8k	Cytotoxicity assay	MTT	>200		>9.80
	Inhibition of syncytium Formation	CPE	—	20.41	
8l	Cytotoxicity assay	MTT	>200		>2.60
	Inhibition of syncytium Formation	CPE	—	76.79	
8m	Cytotoxicity assay	MTT	71.05		3.17
	Inhibition of syncytium Formation	CPE	—	22.41	
8n	Cytotoxicity assay	MTT	>200		>13.74
	Inhibition of syncytium Formation	CPE	—	14.56	

^{1}H and ^{13}C NMR spectra

6a. 2''-bromo-5'-(piperidin-1-yl)-[1,1':3',1''-terphenyl]-4'-carbonitrile

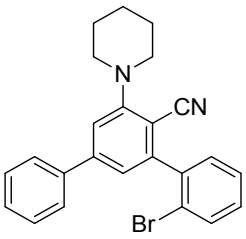

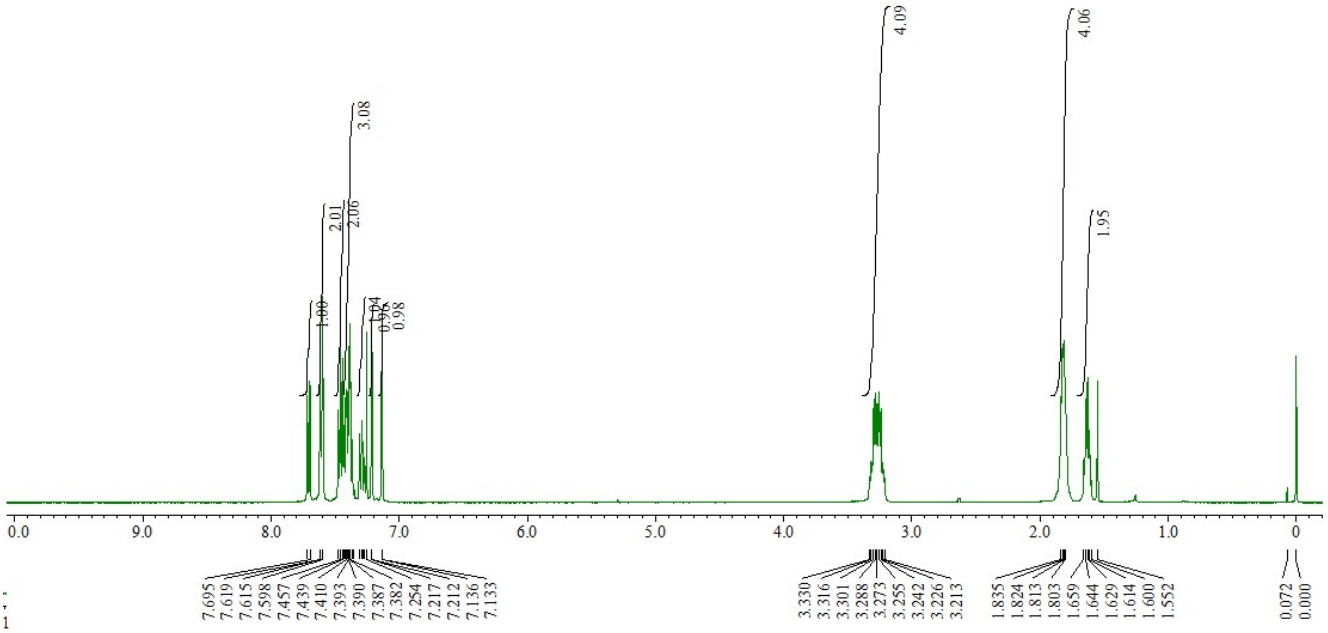

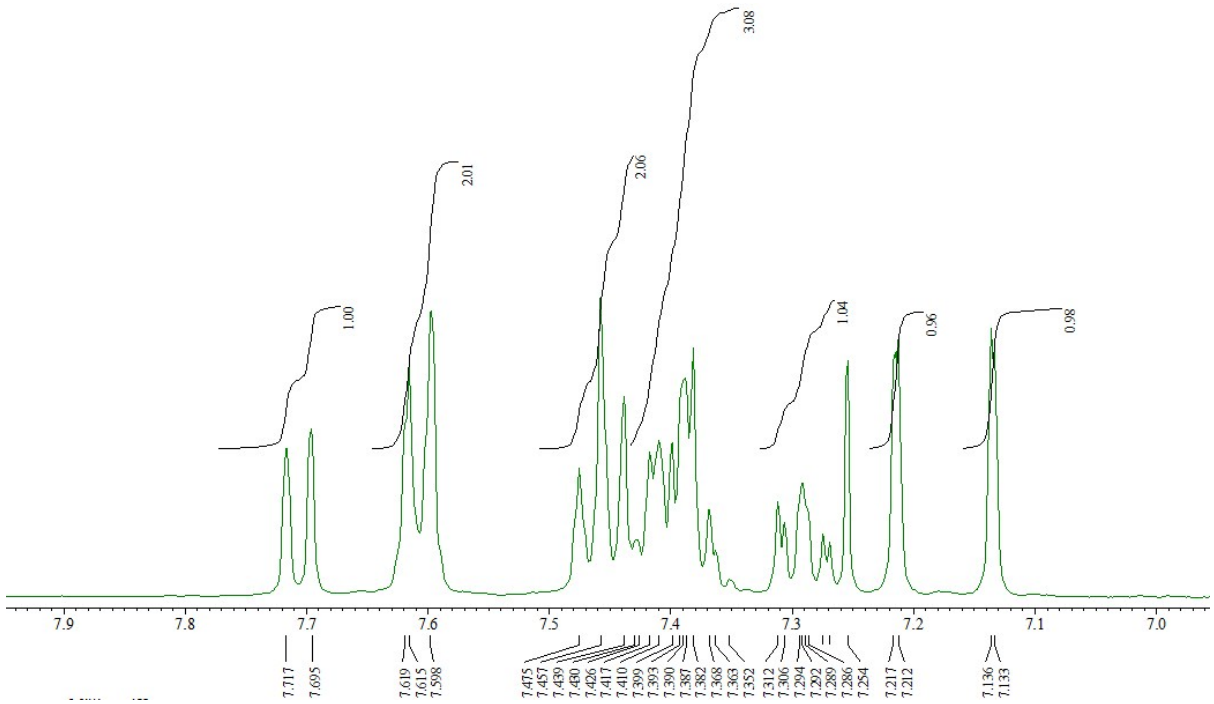

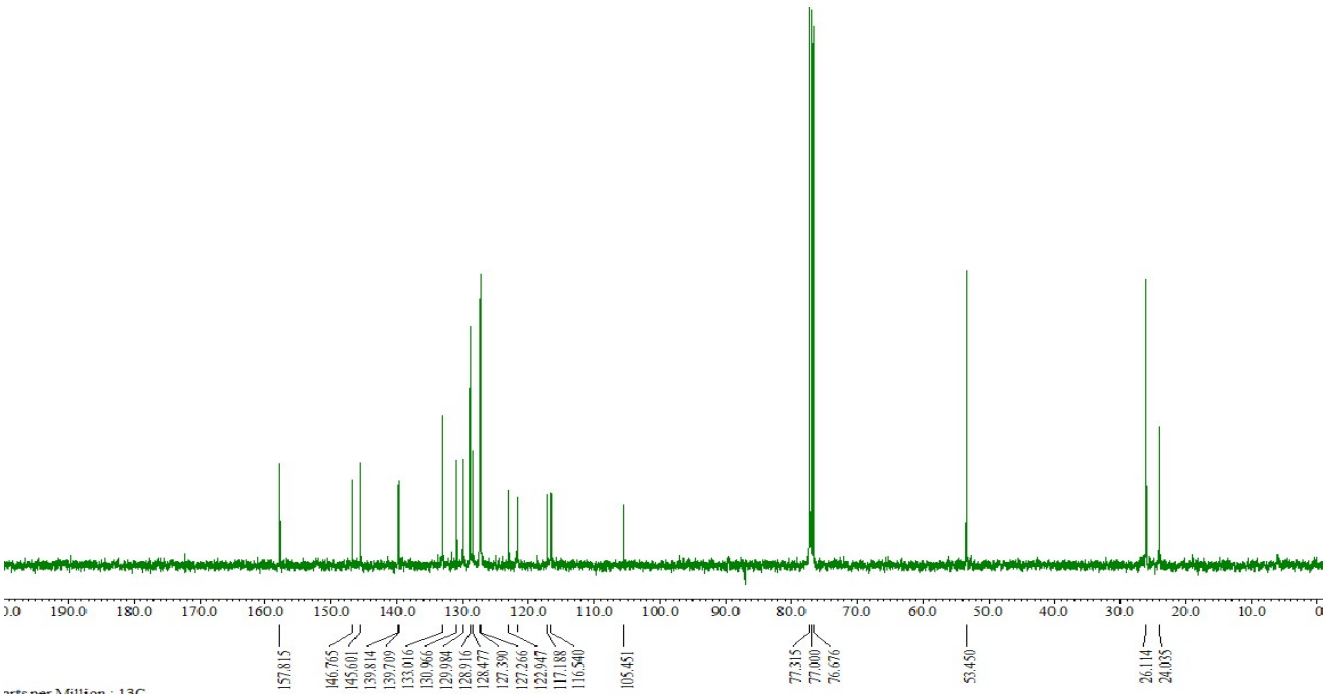

Fig.3. $^{1}H,^{1}H$ of aromatic region &^{13}C-NMR spectra of **6a**.

`

6b. 2''-bromo-5'-(pyrrolidin-1-yl)-[1,1':3',1''-terphenyl]-4'-carbonitrile

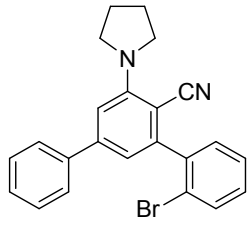

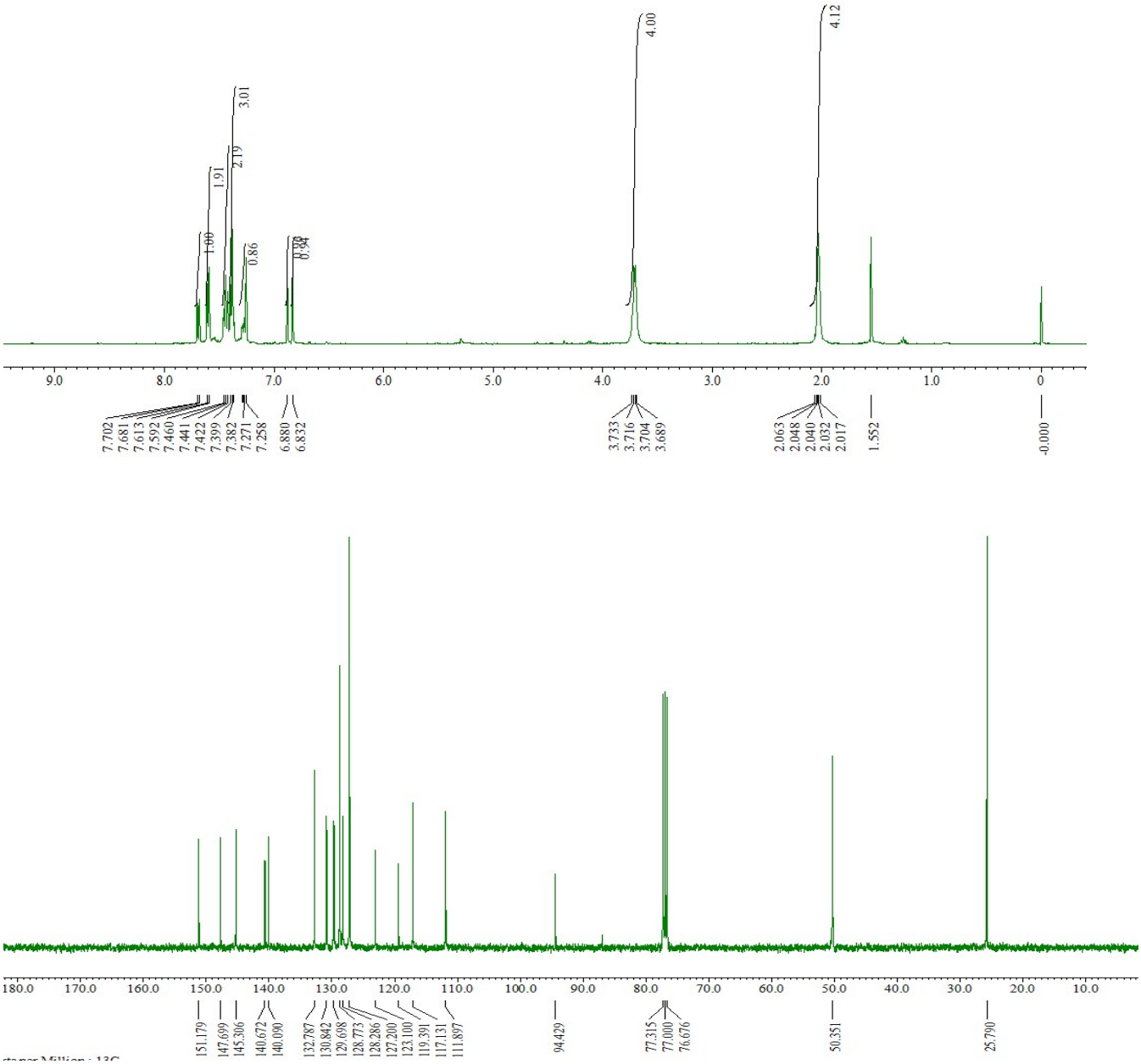

Fig. 4.^{1}H &^{13}C-NMR spectra of **6b**.

`

6c. 2''-bromo-5'-morpholino-[1,1':3',1''-terphenyl]-4'-carbonitrile

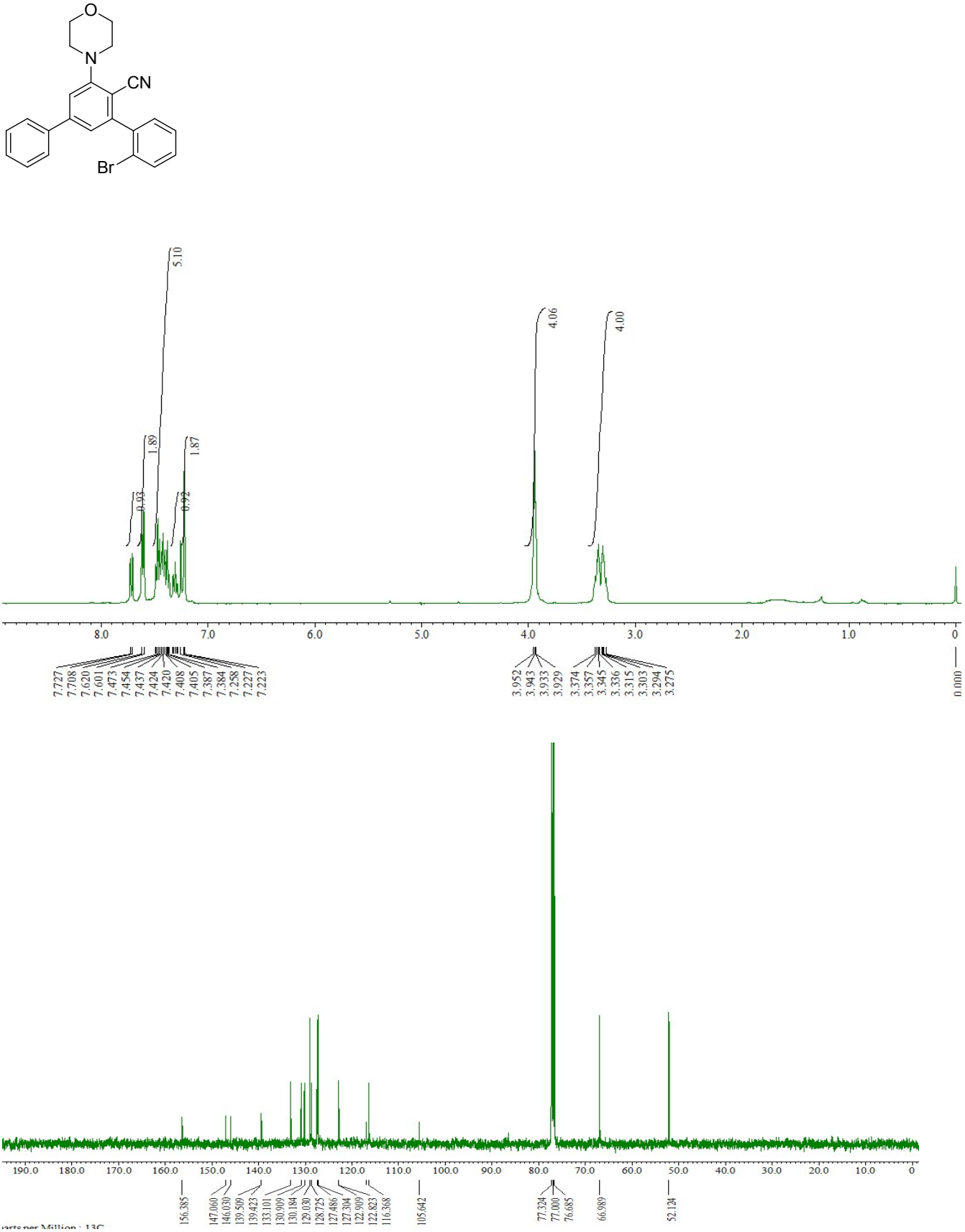

Fig.5. ^{1}H &^{13}C-NMR spectra of **6c**.

`

6d. 2''-bromo-4-methyl-5'-(piperidin-1-yl)-[1,1':3',1''-terphenyl]-4'-carbonitrile

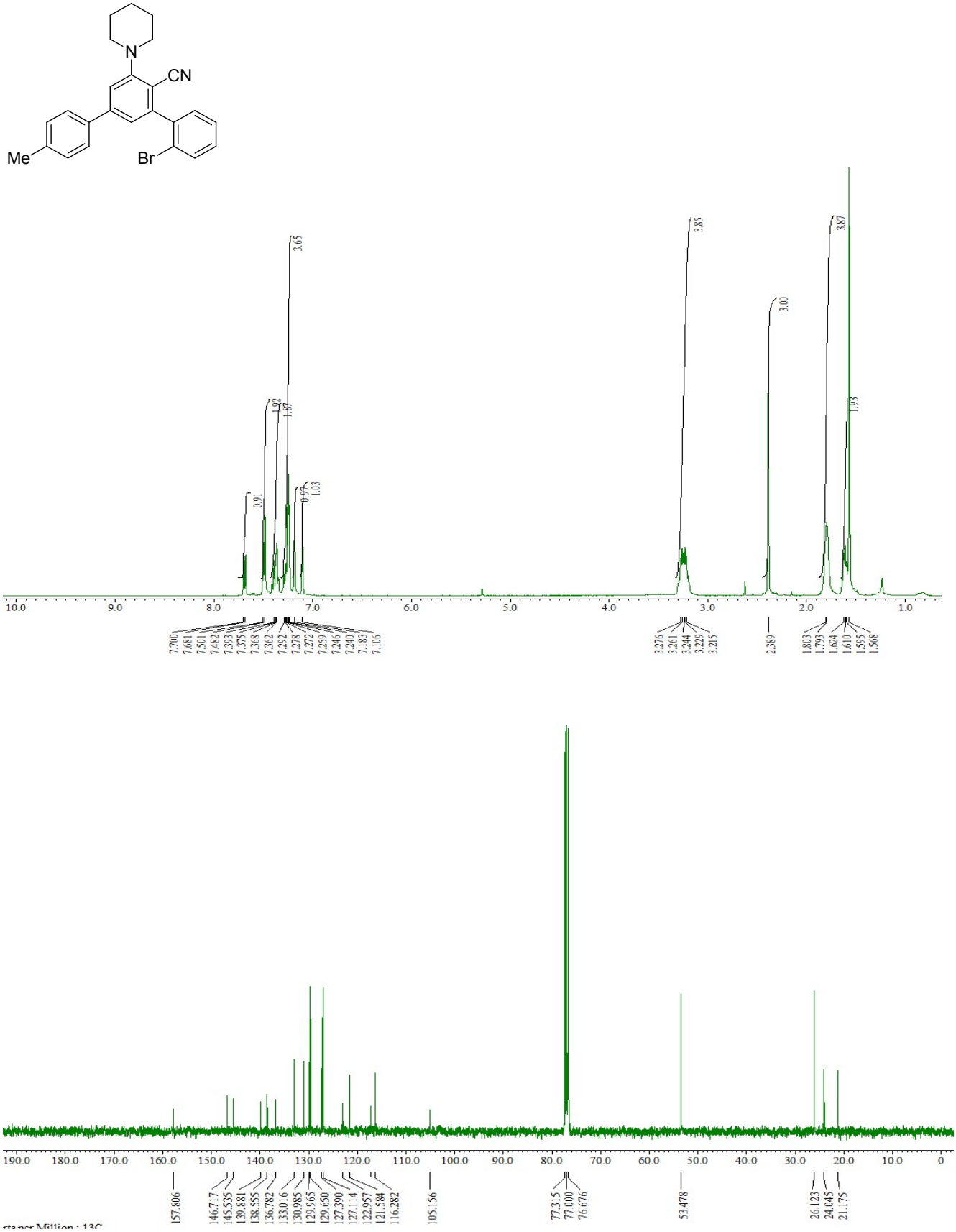

Fig.6.[1]H &[13]C-NMR spectra of **6d**.

`

6e. 2''-bromo-4-methyl-5'-(pyrrolidin-1-yl)-[1,1':3',1''-terphenyl]-4'-carbonitrile

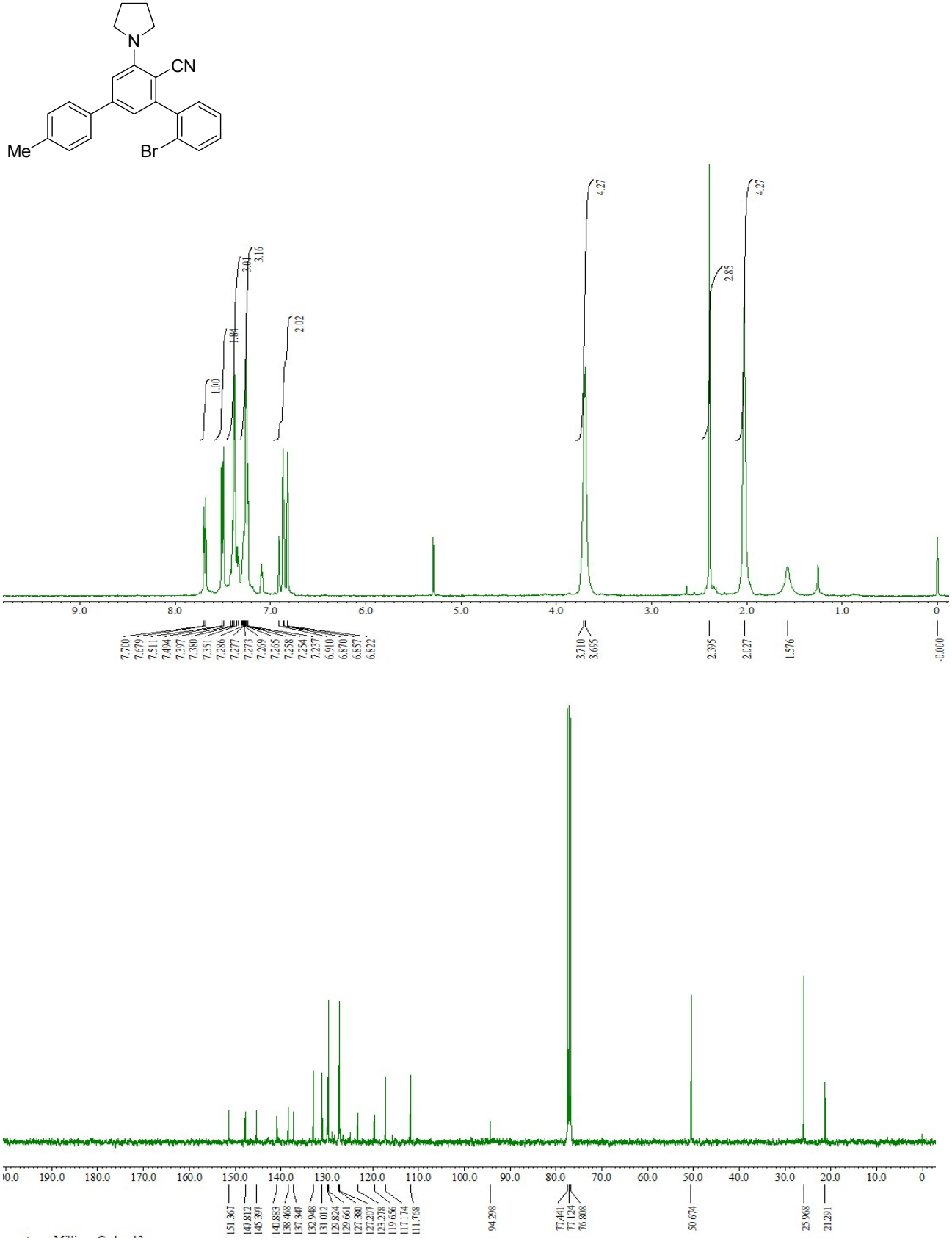

Fig.7. ^{1}H &^{13}C-NMR spectra of **6e**.

`

6f. 2''-bromo-4-methyl-5'-morpholino-[1,1':3',1''-terphenyl]-4'-carbonitrile

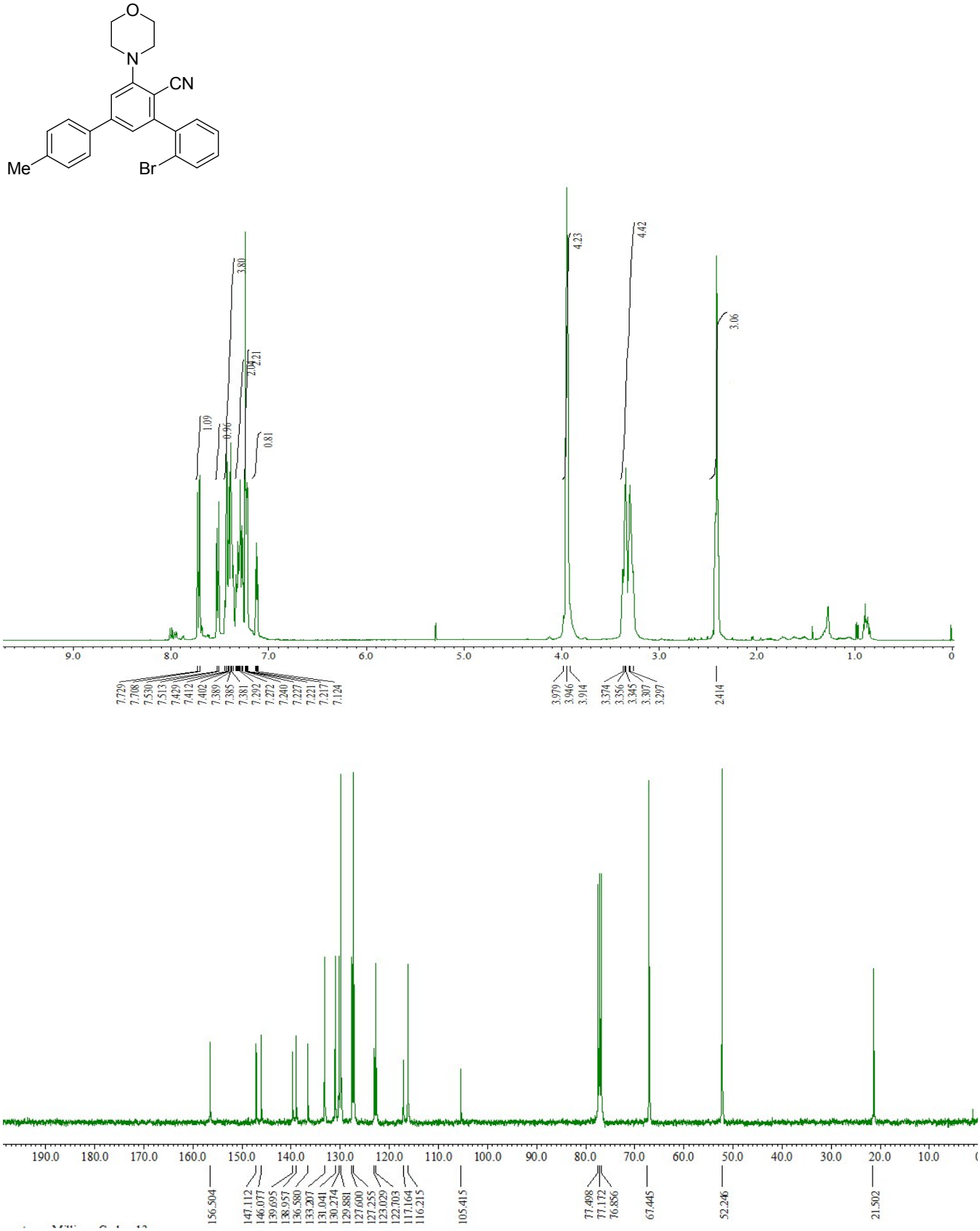

Fig.8.^{1}H &^{13}C-NMR spectra of **6f**.

6g. 2''-bromo-4-methoxy-5'-(piperidin-1-yl)-[1,1':3',1''-terphenyl]-4'-carbonitrile

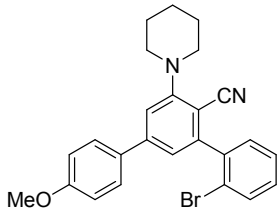

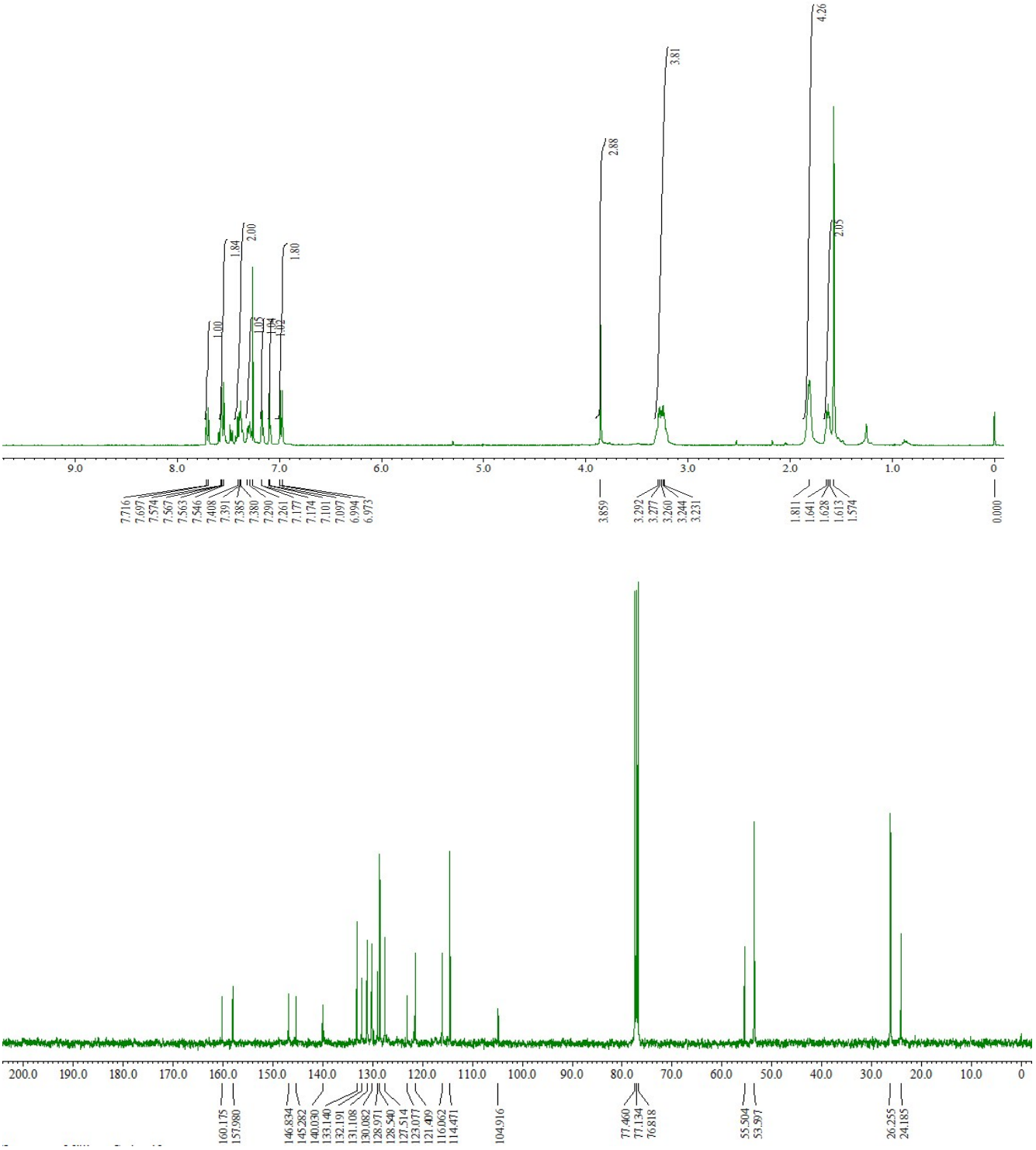

Fig.9.^{1}H &^{13}C-NMR spectra of **6g**.

`

6h. 2''-bromo-4-methoxy-5'-(pyrrolidin-1-yl)-[1,1':3',1''-terphenyl]-4'-carbonitrile

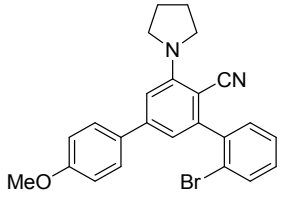

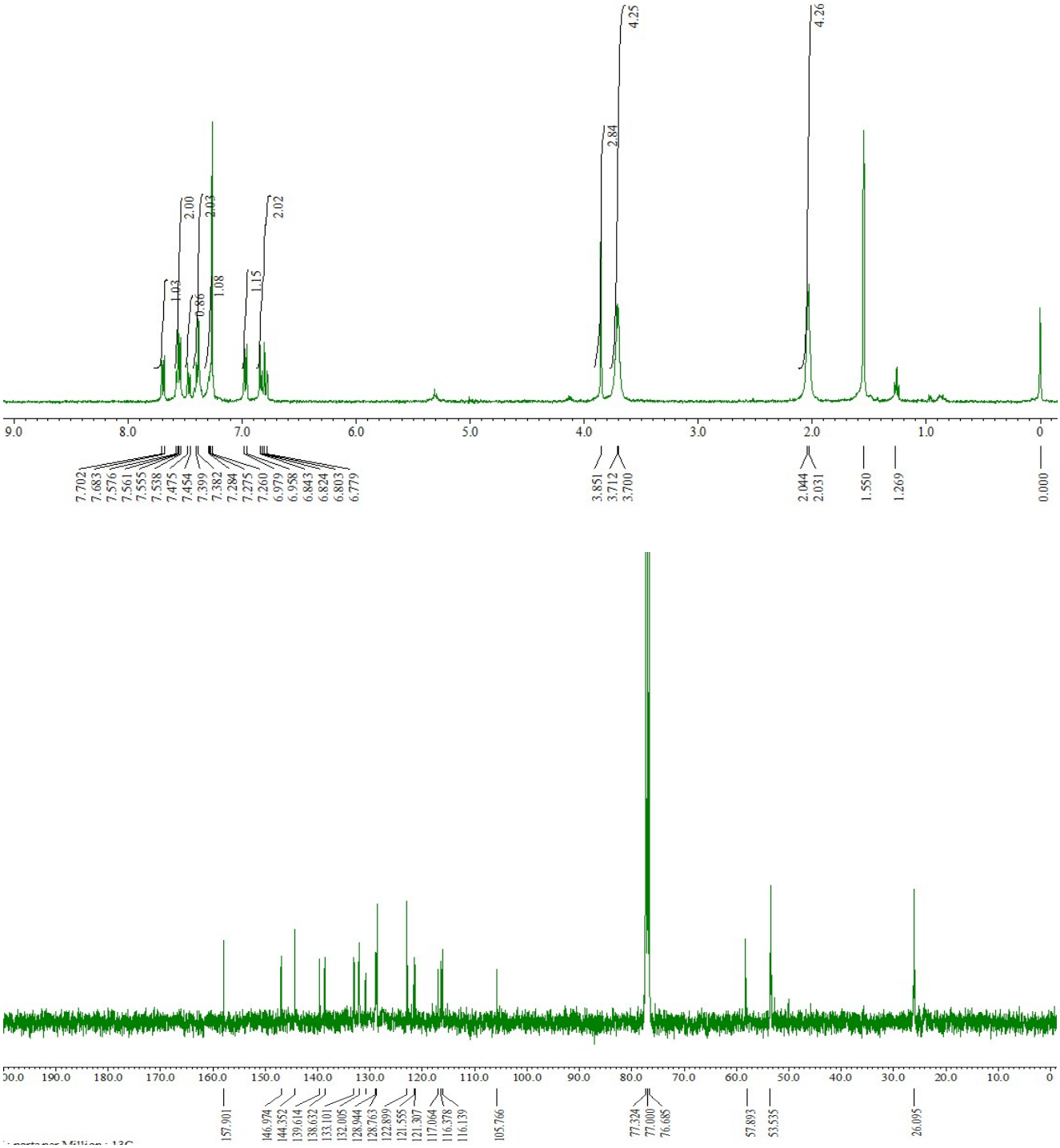

Fig.10.^{1}H &^{13}C-NMR spectra of **6h**.

`

6i. 2''-bromo-4-chloro-5'-morpholino-[1,1':3',1''-terphenyl]-4'-carbonitrile

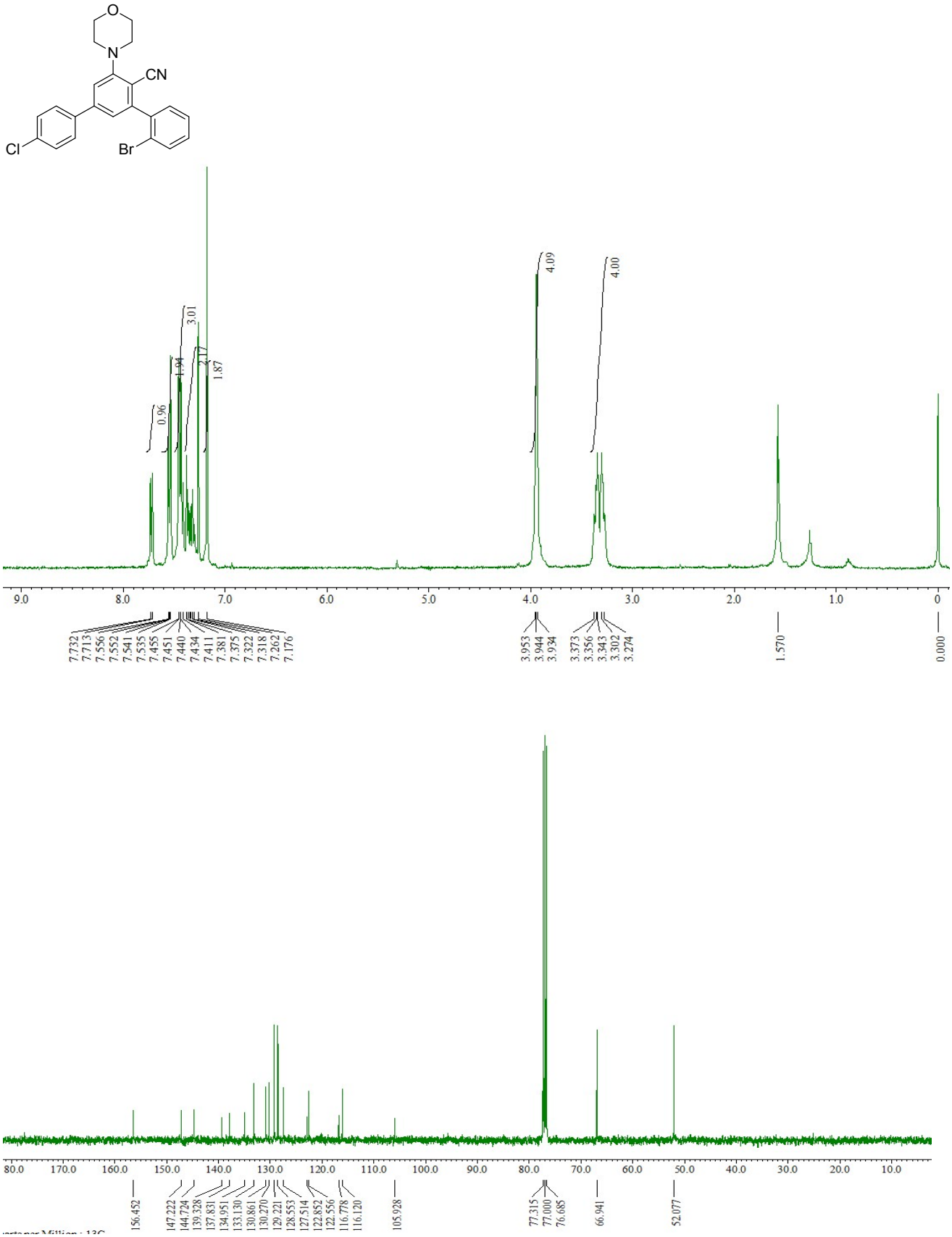

Fig.11.[1]H &[13]C-NMR spectra of **6i**.

`

6j.2'-bromo-5-(naphthalen-2-yl)-3-(piperidin-1-yl)-[1,1'-biphenyl]-2-carbonitrile

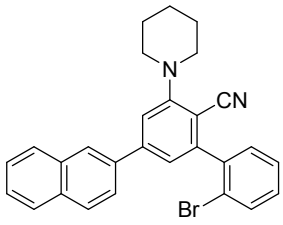

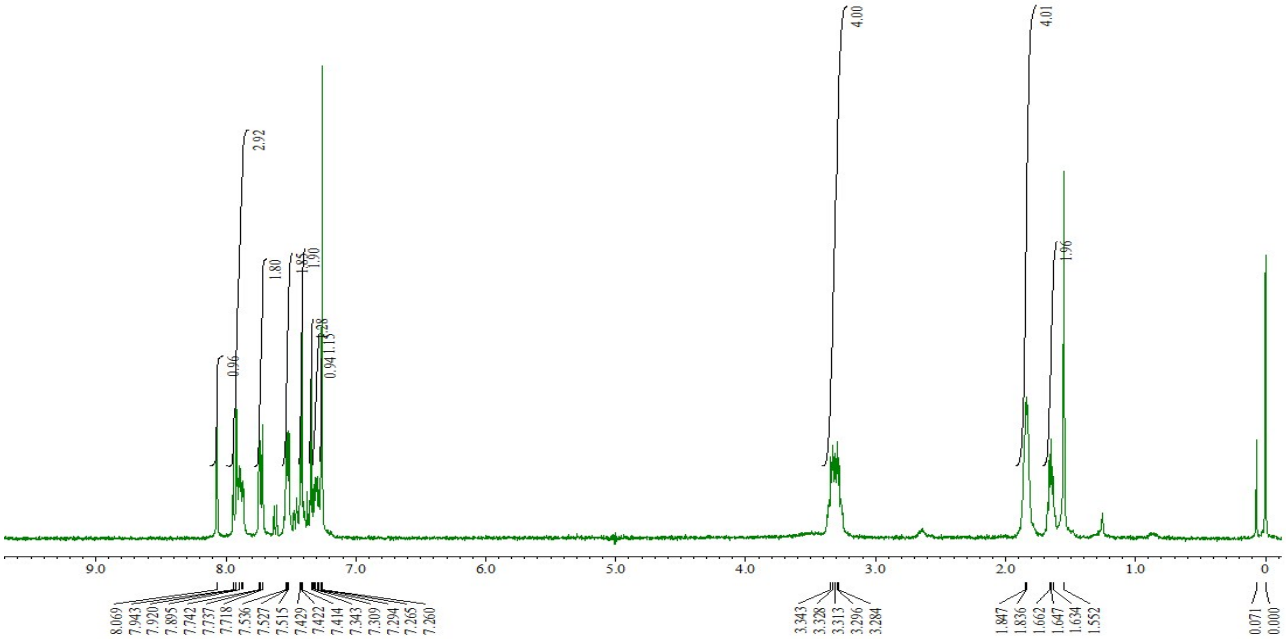

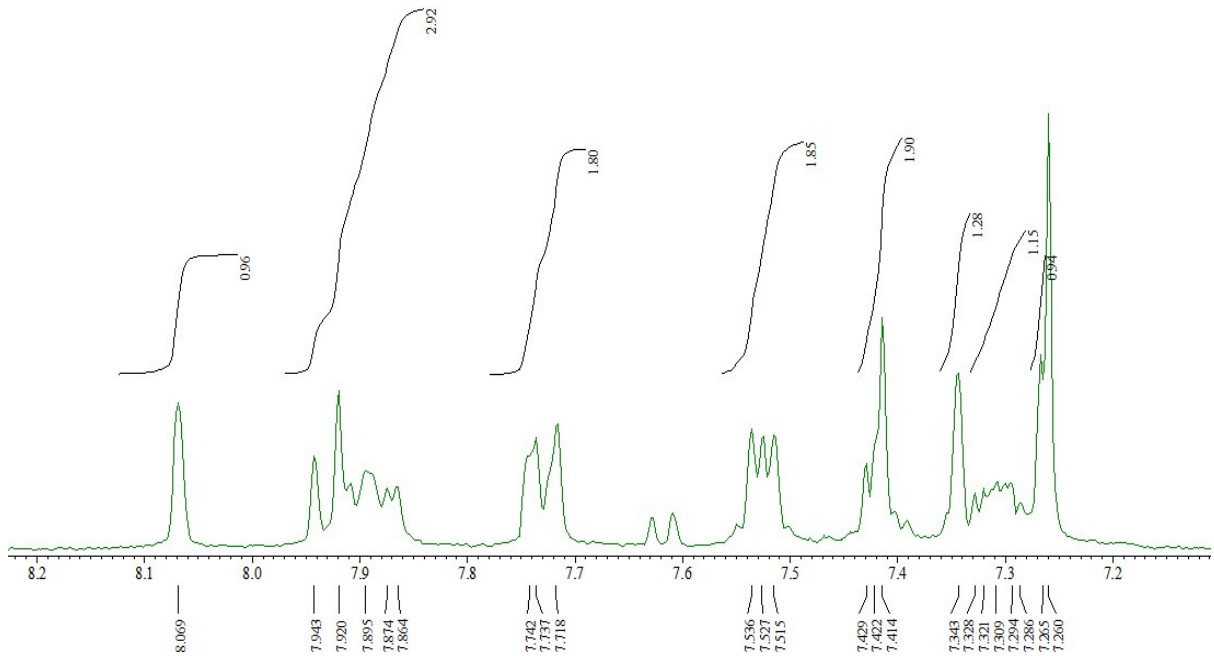

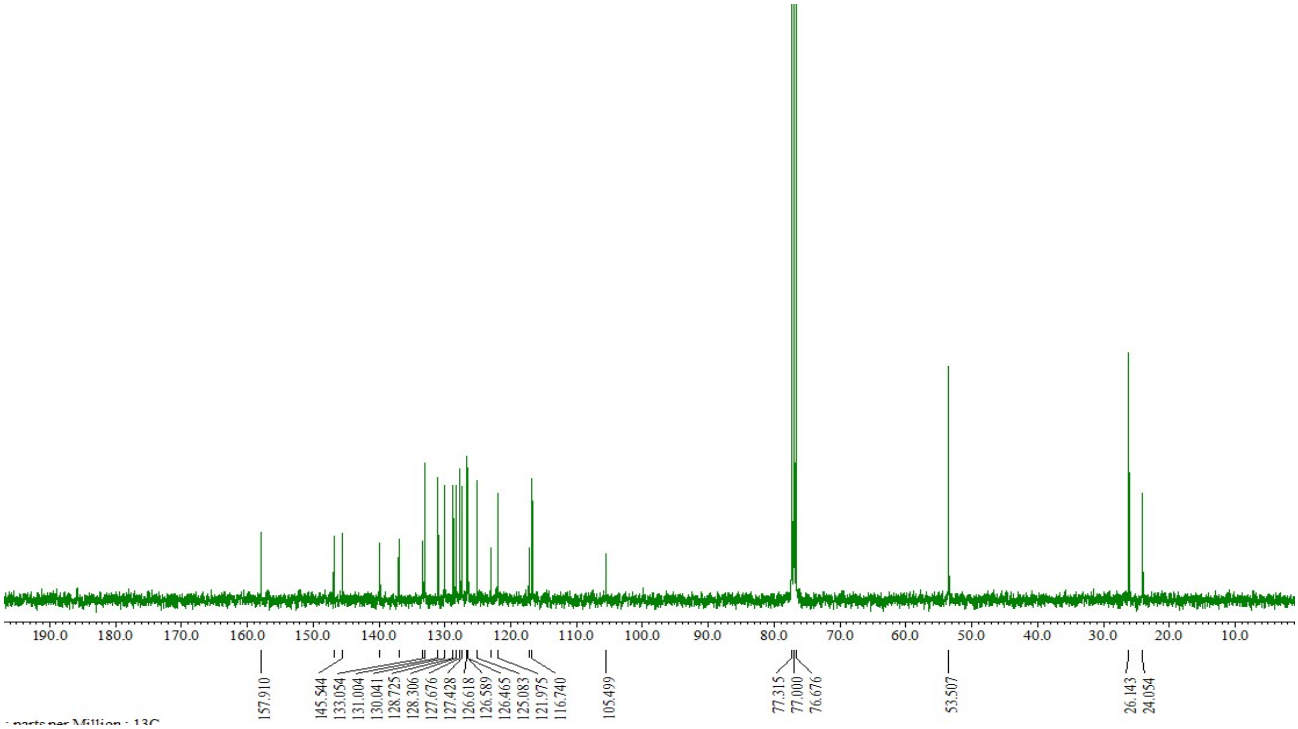

Fig.12.^{1}H,^{1}H of aromatic region&^{13}C-NMR spectra of **6j**.

`

6k. 2'-bromo-3-(piperidin-1-yl)-5-(thiophen-2-yl)-[1,1'-biphenyl]-2-carbonitrile

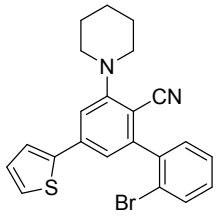

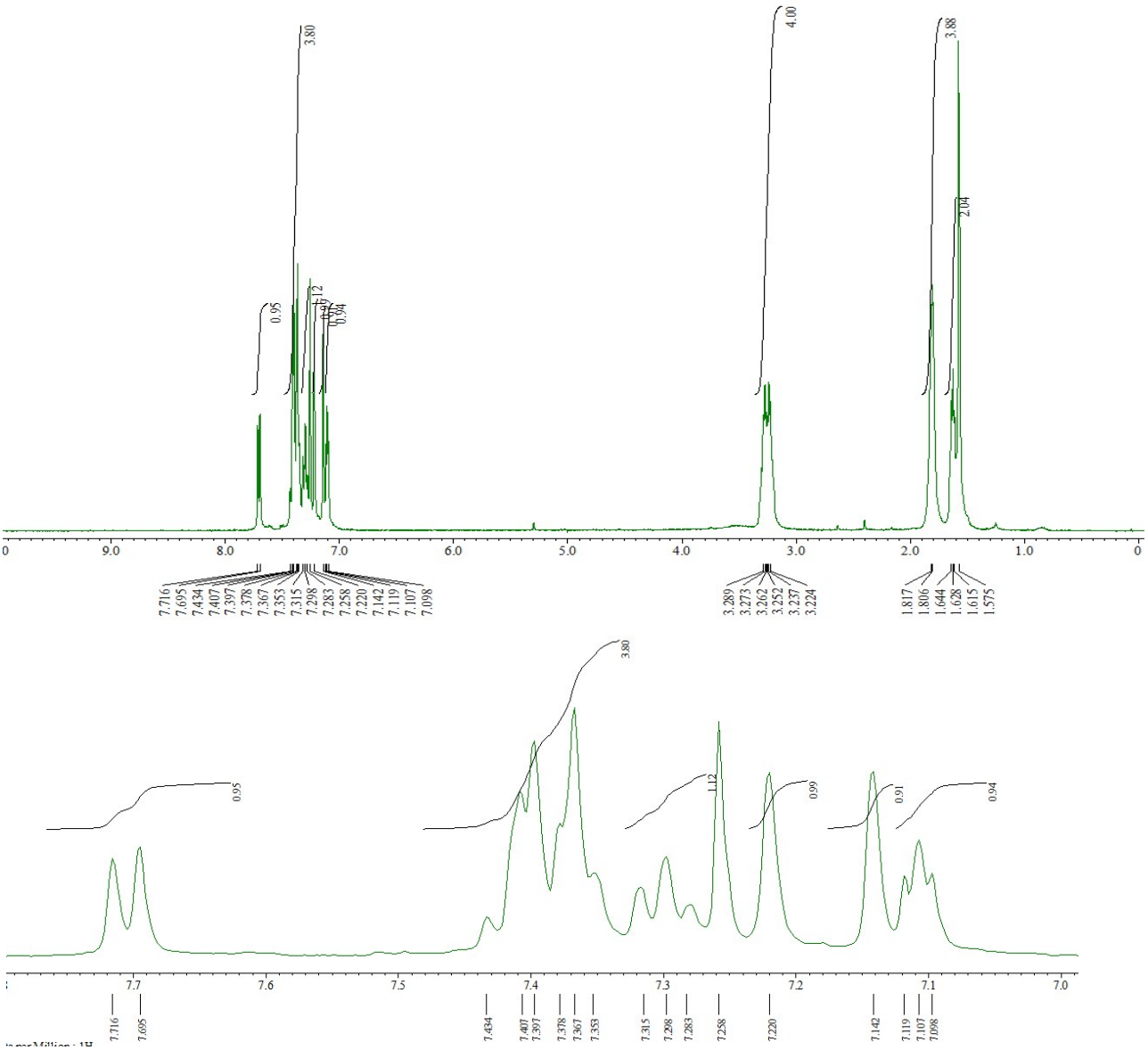

`

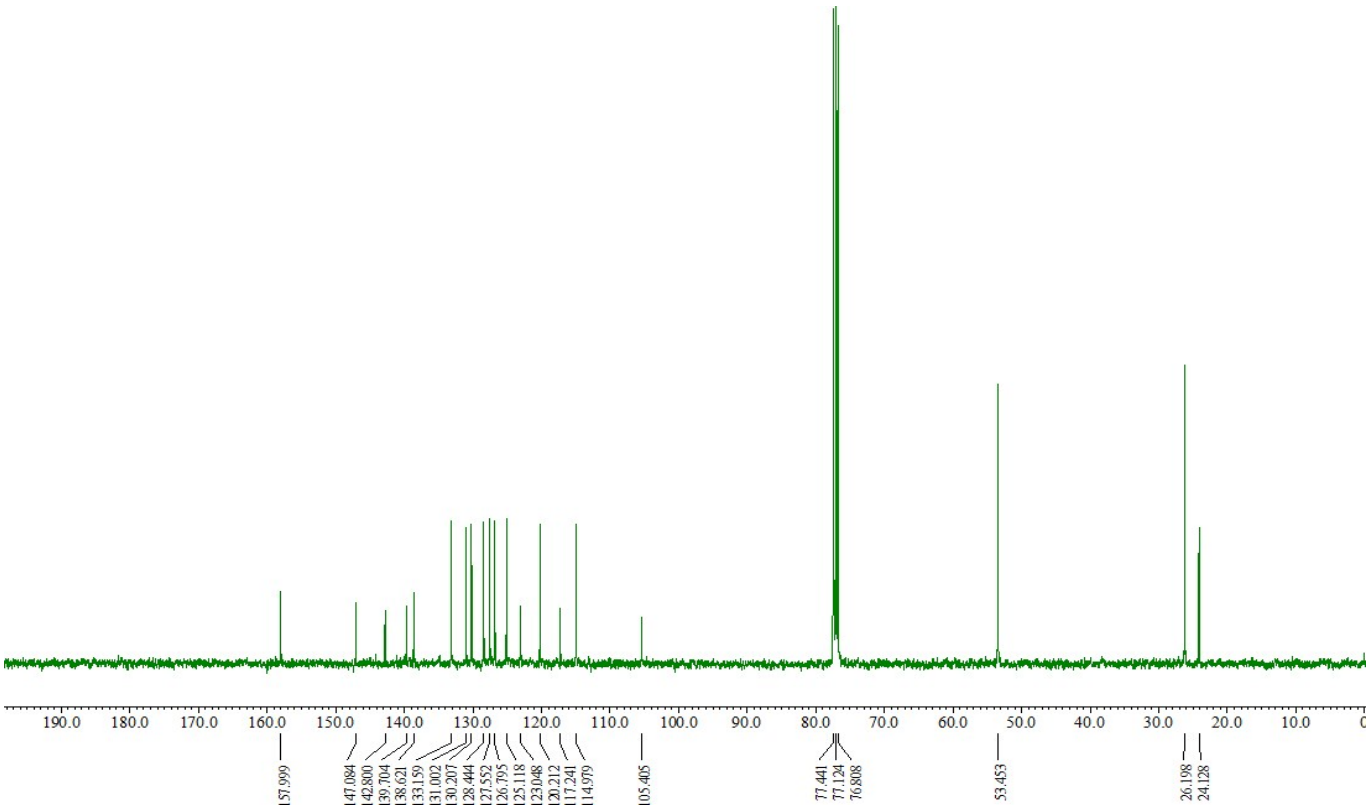

Fig.13.^{1}H,^{1}H of aromatic region&^{13}C-NMR spectra of **6k**.

`

6l. 2'-bromo-3-(pyrrolidin-1-yl)-5-(thiophen-2-yl)-[1,1'-biphenyl]-2-carbonitrile

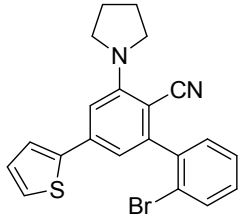

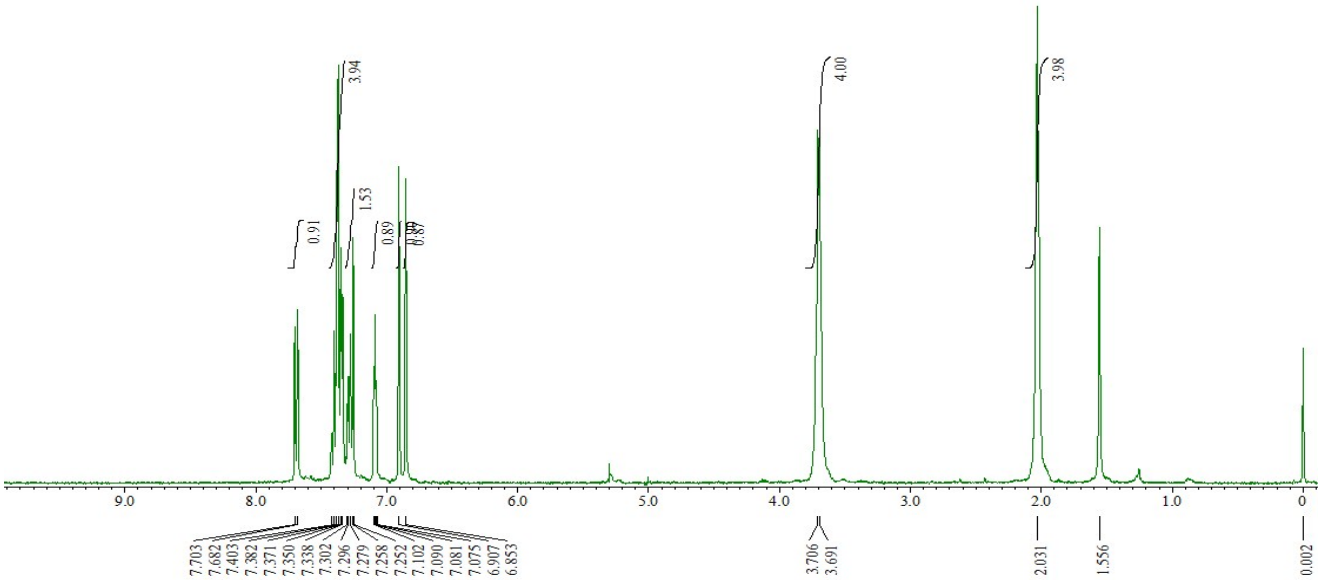

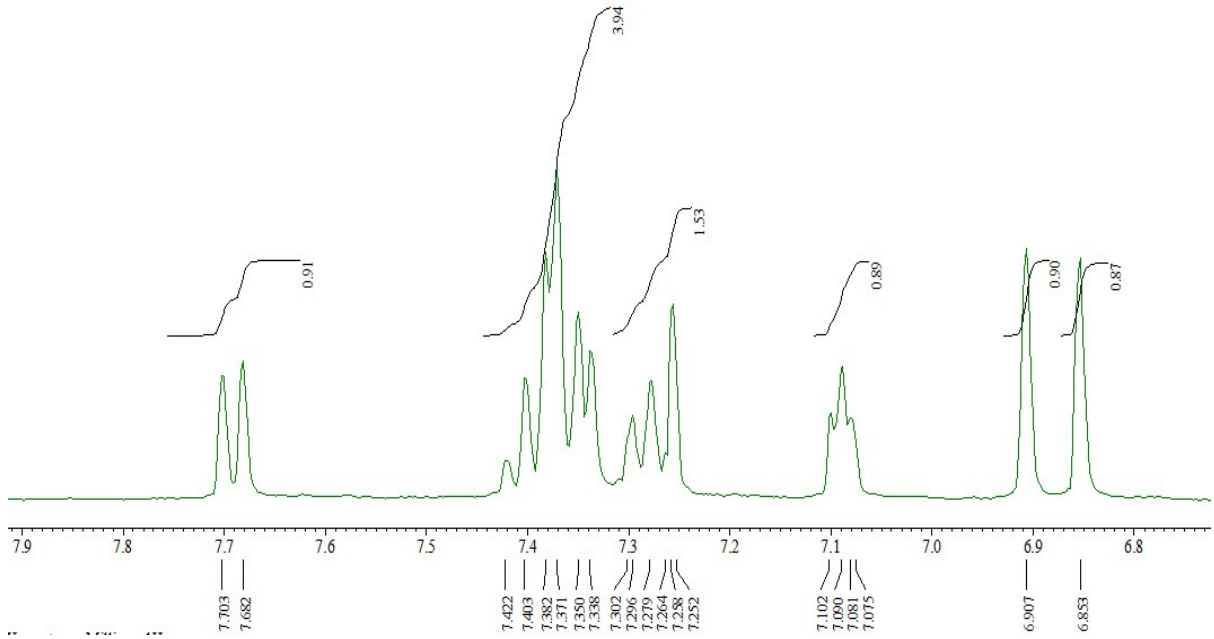

`

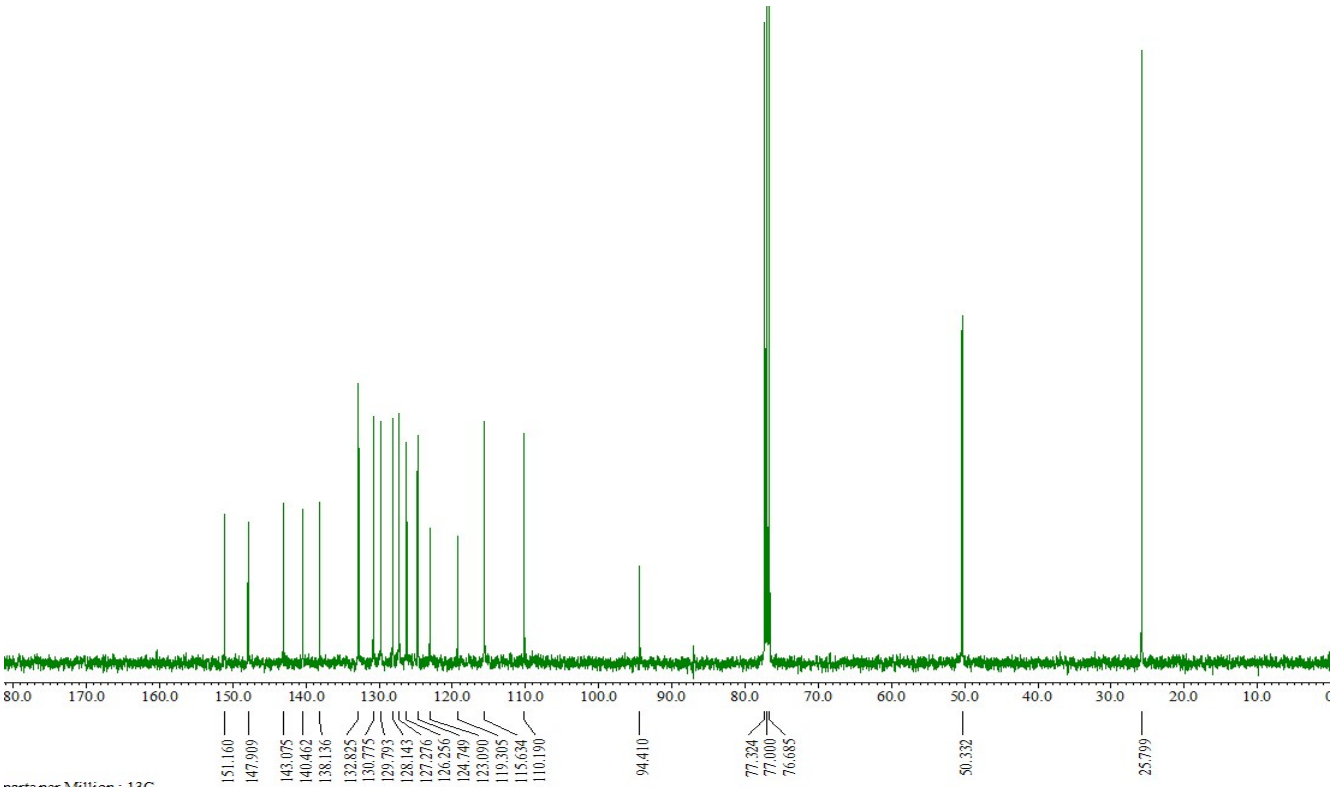

Fig.14. ^{1}H, ^{1}H of aromatic region&^{13}C-NMR spectra of **6l**.

`

6m. 3-(2-bromophenyl)-1-(piperidin-1-yl)-9,10-dihydrophenanthrene-2-carbonitrile

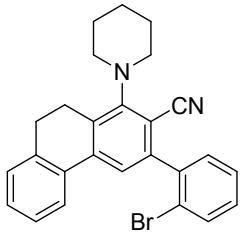

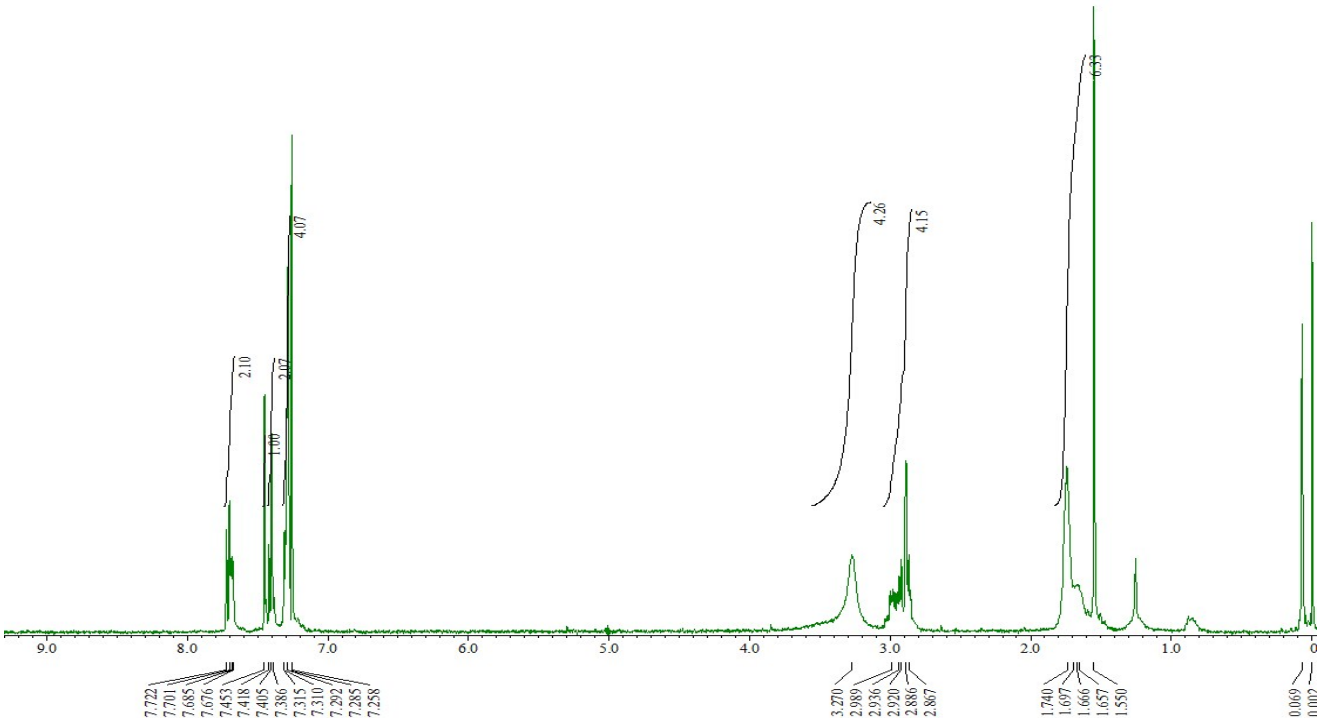

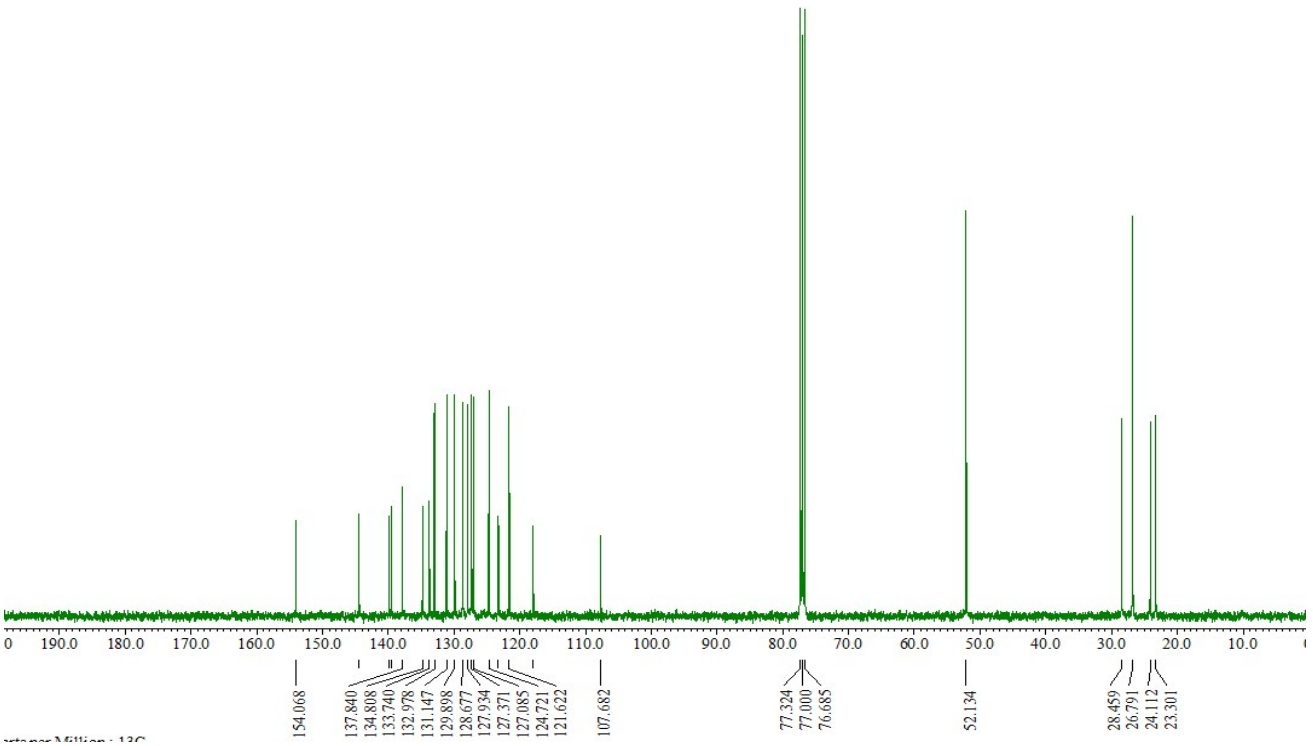

Fig.15.^{1}H &^{13}C-NMR spectra of **6m**.

6n. 3-(2-bromophenyl)-7-methoxy-1-(piperidin-1-yl)-9,10 dihydrophenanthrene-2-carbonitrile

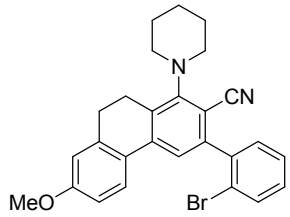

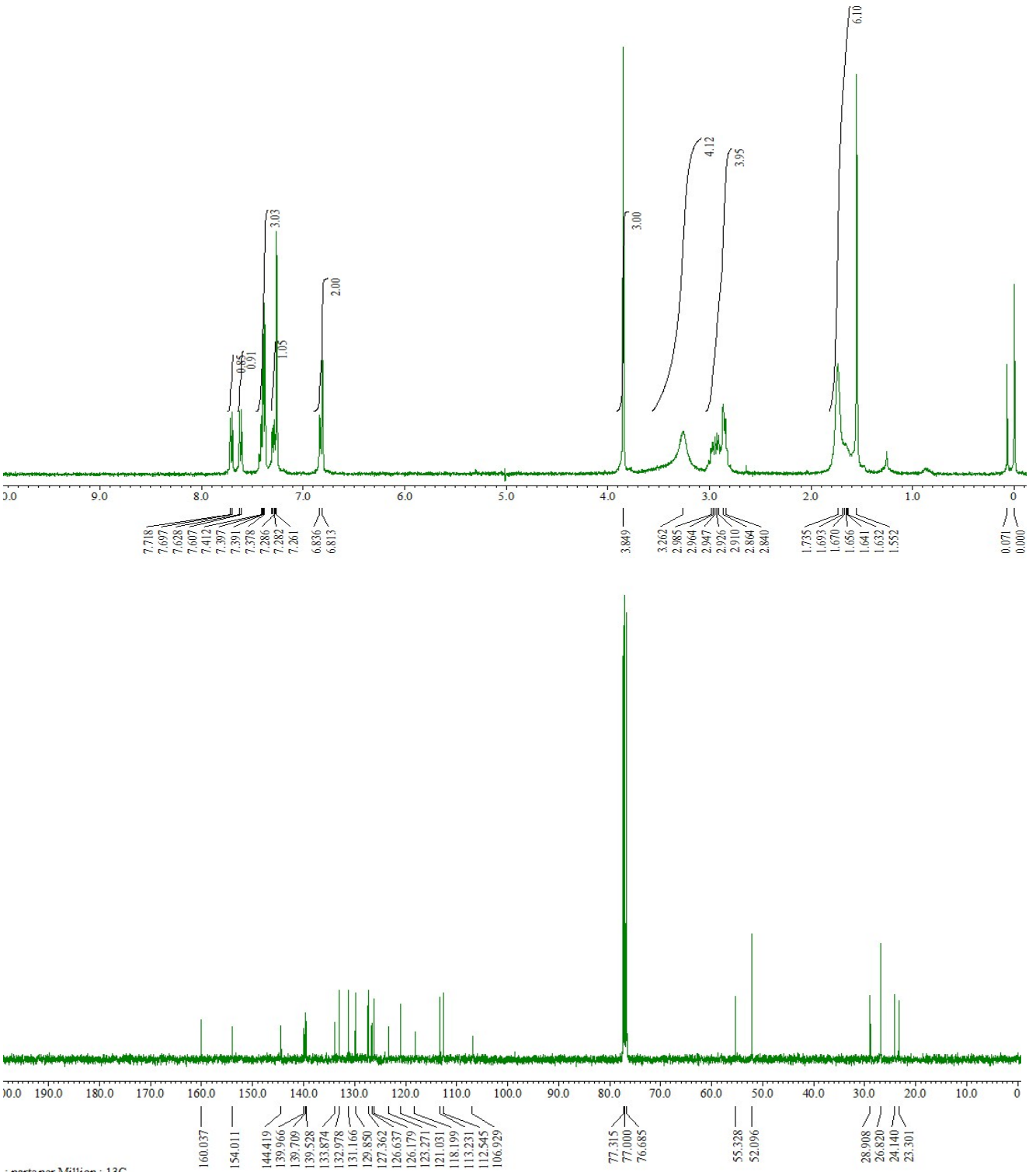

Fig.16.[1]H &[13]C-NMR spectra of **6n**.

6o. 3-(2-bromophenyl)-7-methoxy-1-(pyrrolidin-1-yl)-9,10-dihydrophenanthrene-2-carbonitrile

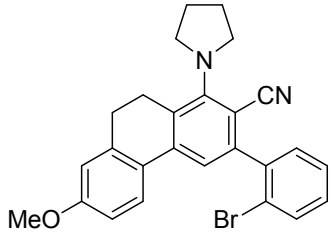

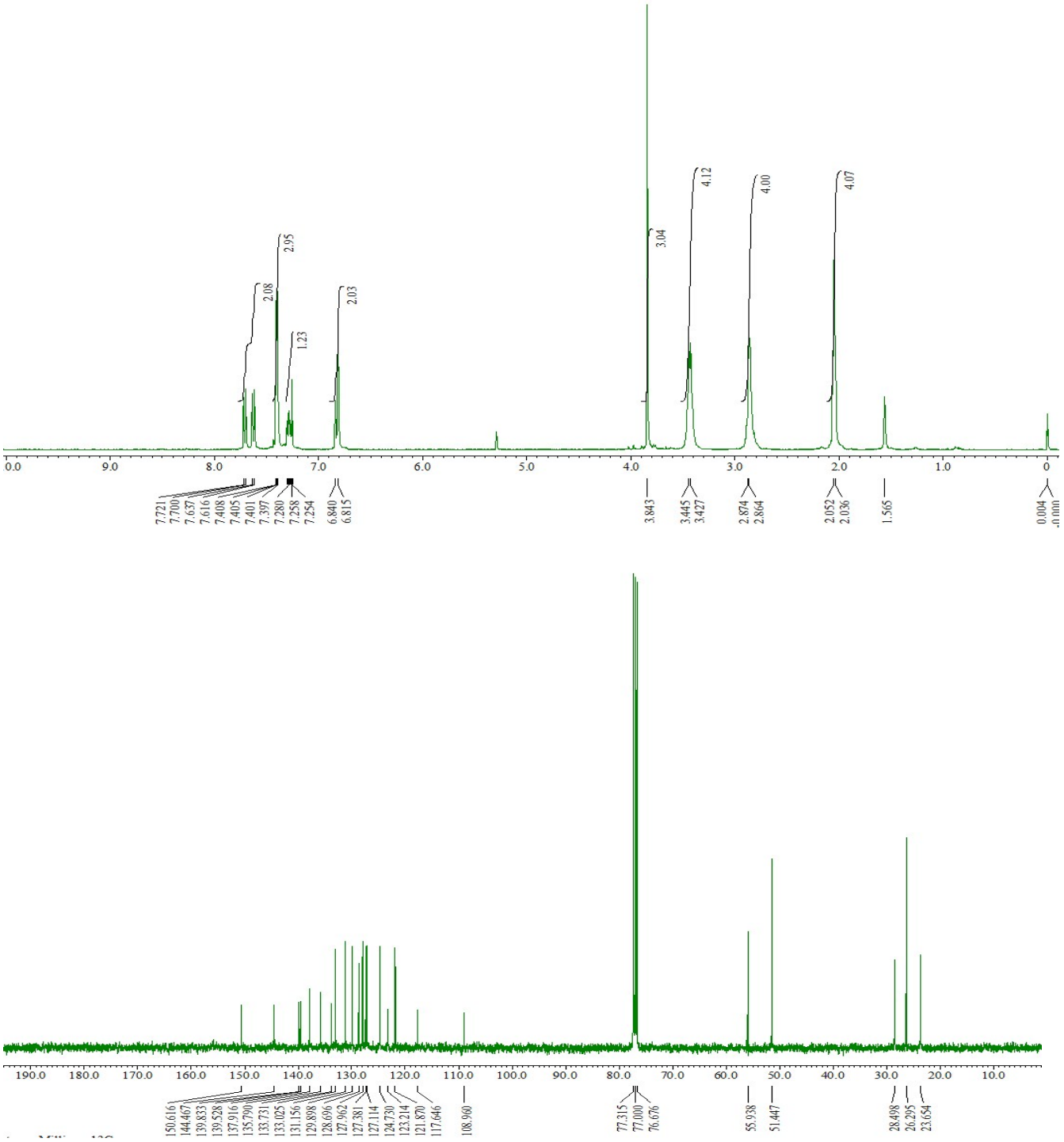

Fig.17.[1]H &[13]C-NMR spectra of **6o**.

`

6p. 2''-fluoro-4-methyl-5'-(piperidin-1-yl)-[1,1':3',1''-terphenyl]-4'-carbonitrile

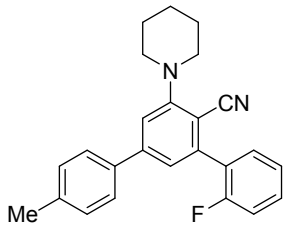

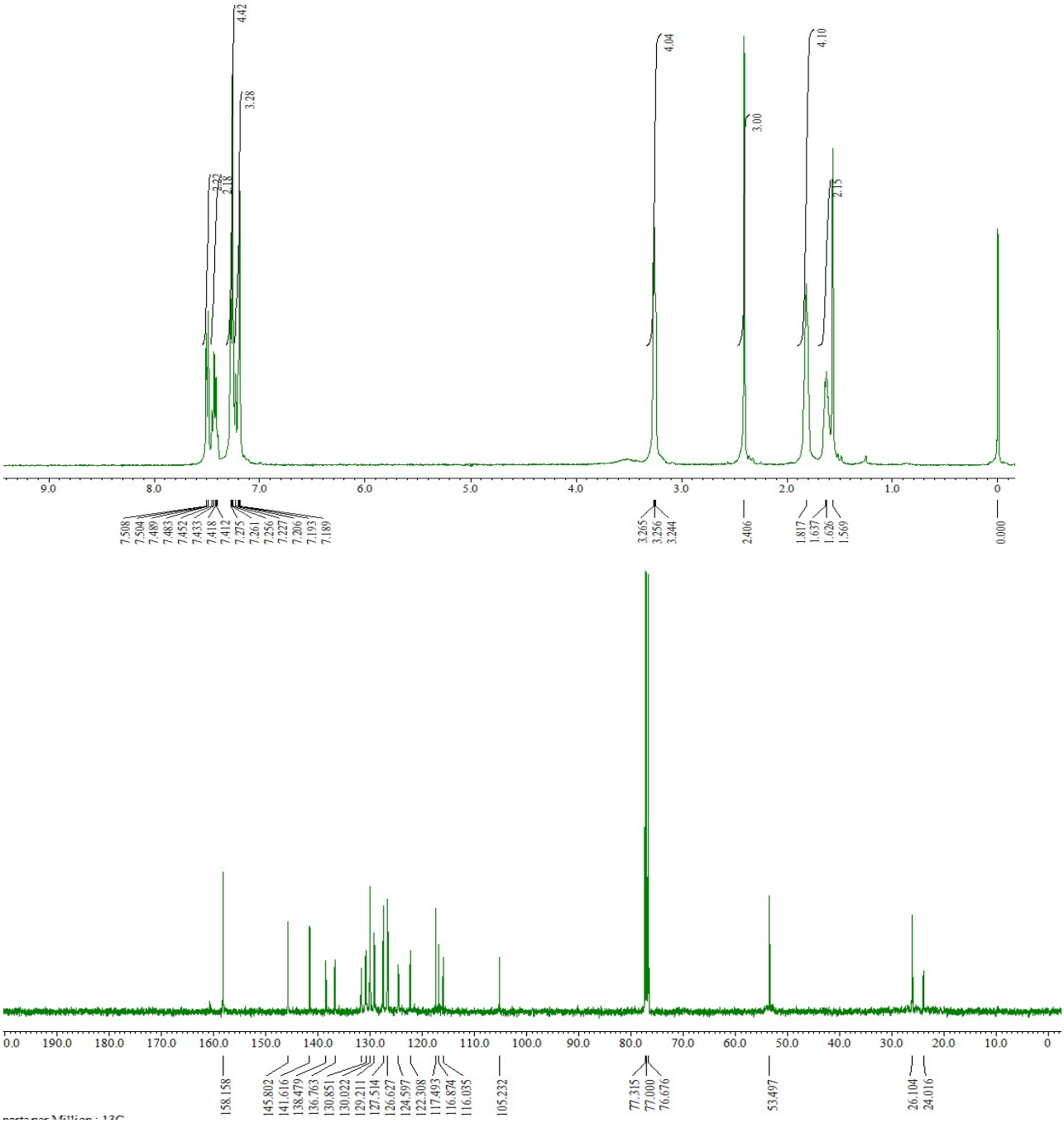

Fig.18.[1]H &[13]C-NMR spectra of **6p**.

`

6q. 2''-chloro-4-methyl-5'-(piperidin-1-yl)-[1,1':3',1''-terphenyl]-4'-carbonitrile

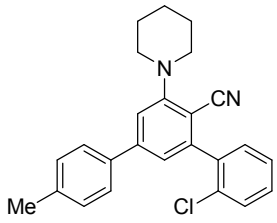

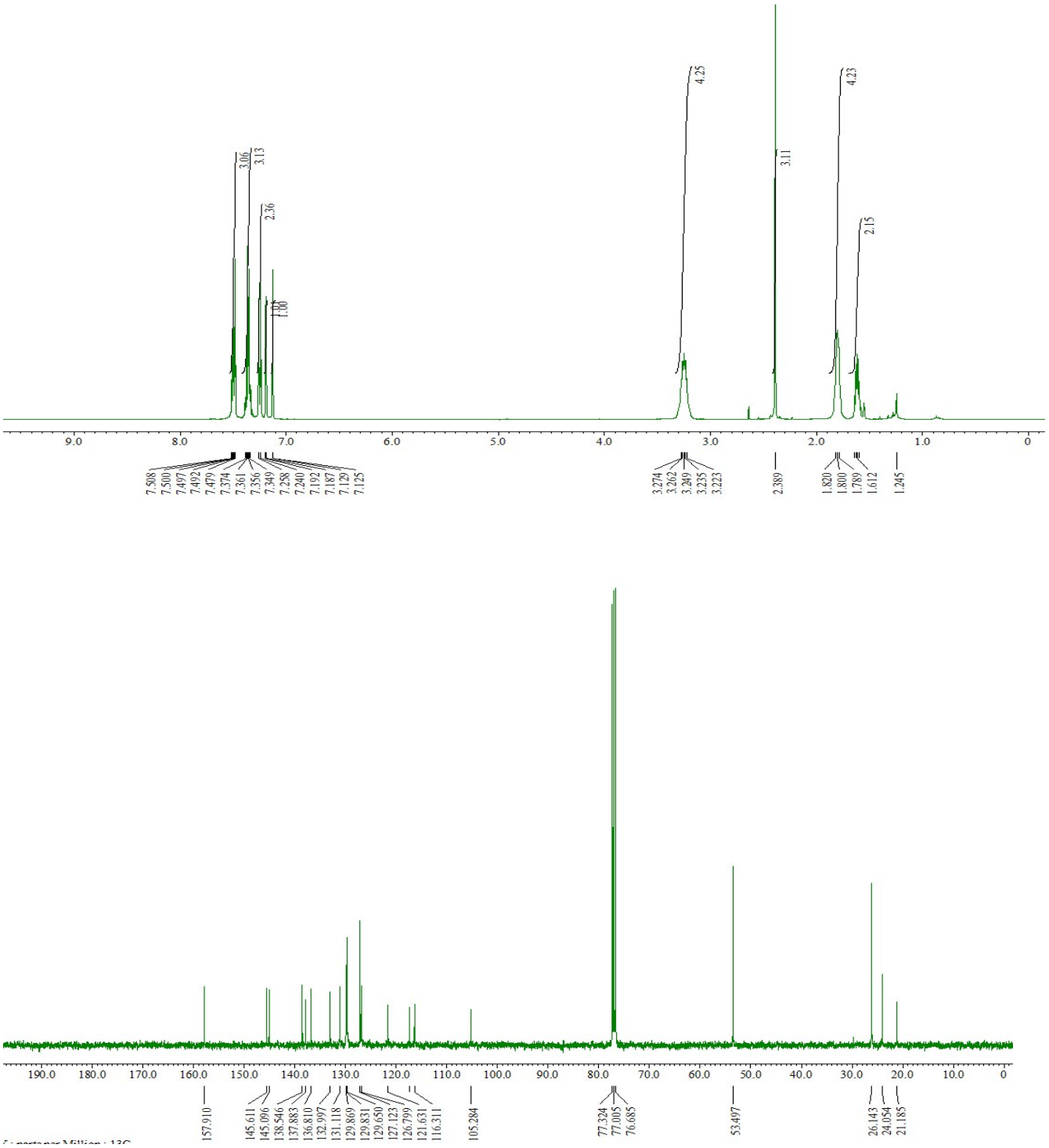

Fig.19.[1]H &[13]C-NMR spectra of **6q**.

6r. 2'-fluoro-3-(piperidin-1-yl)-5-(thiophen-2-yl)-[1,1'-biphenyl]-2-carbonitrile

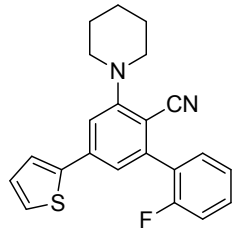

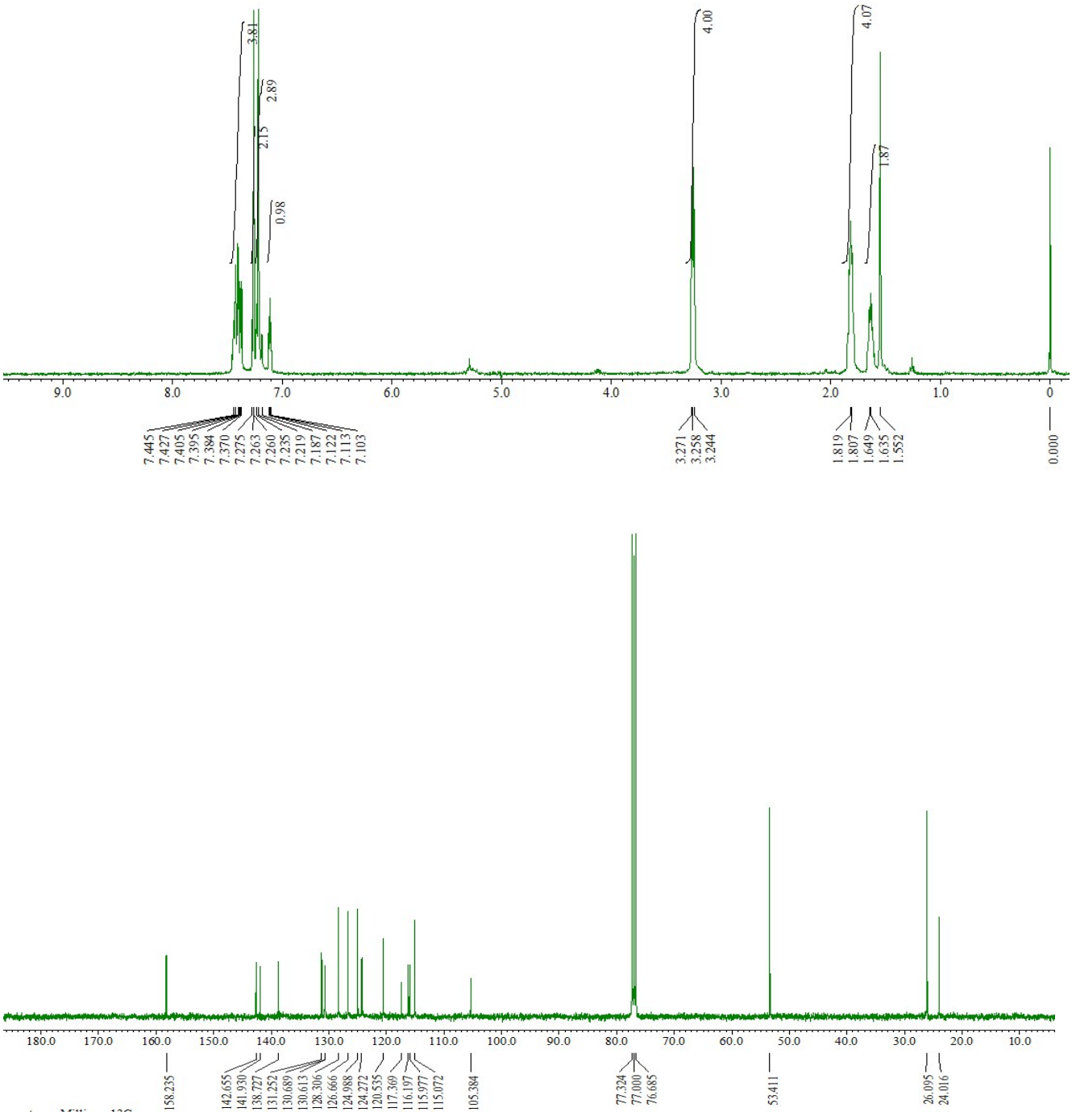

Fig.20.^{1}H &^{13}C-NMR spectra of **6r**.

`

6s. 2'-chloro-3-(piperidin-1-yl)-5-(thiophen-2-yl)-[1,1'-biphenyl]-2-carbonitrile

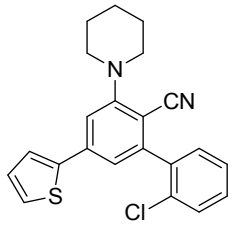

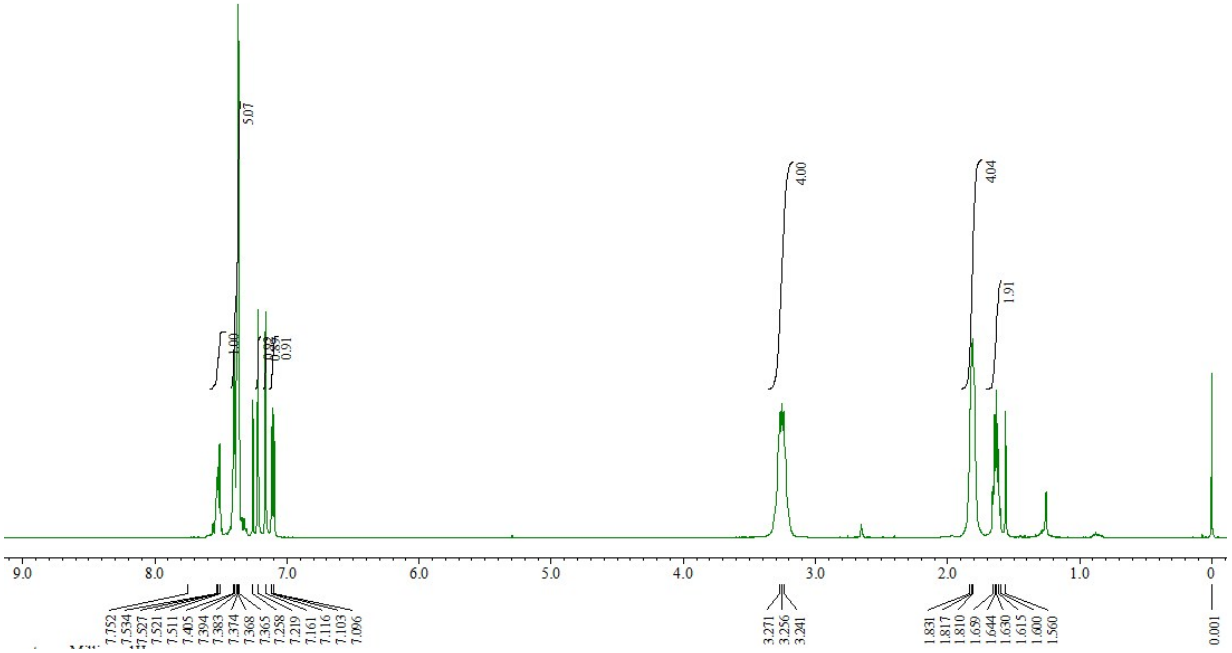

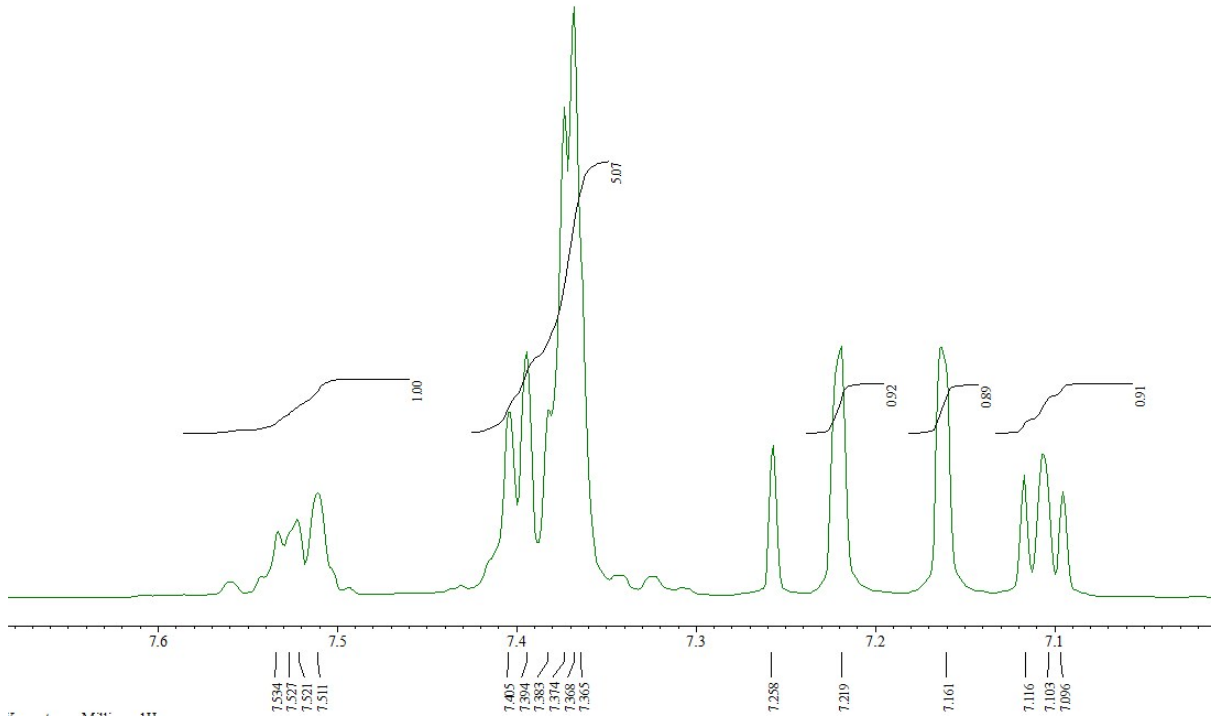

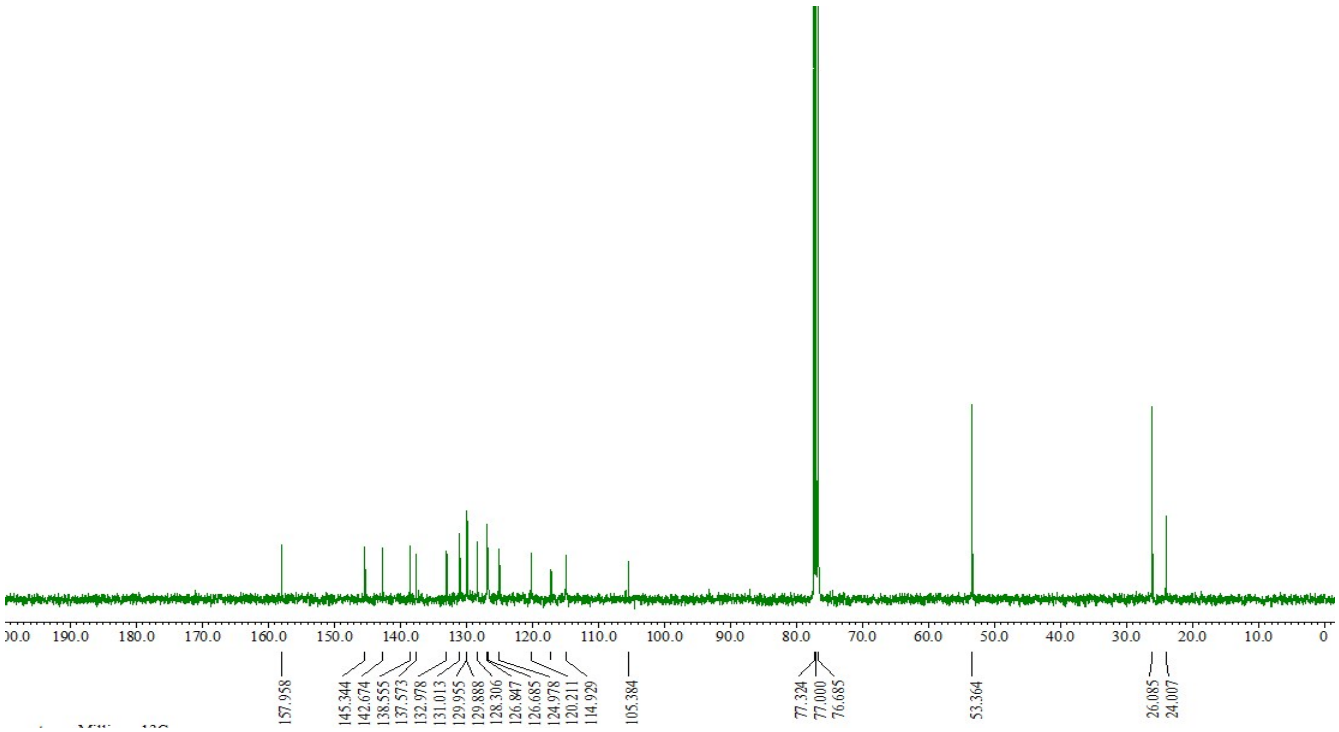

Fig.21.^{1}H,^{1}H of aromatic region&^{13}C-NMR spectra of **6s**.

`

8a. 3-phenyl-1-(piperidin-1-yl)-9H-fluoren-9-one

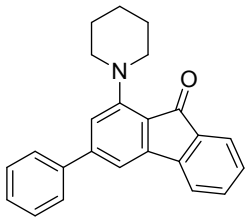

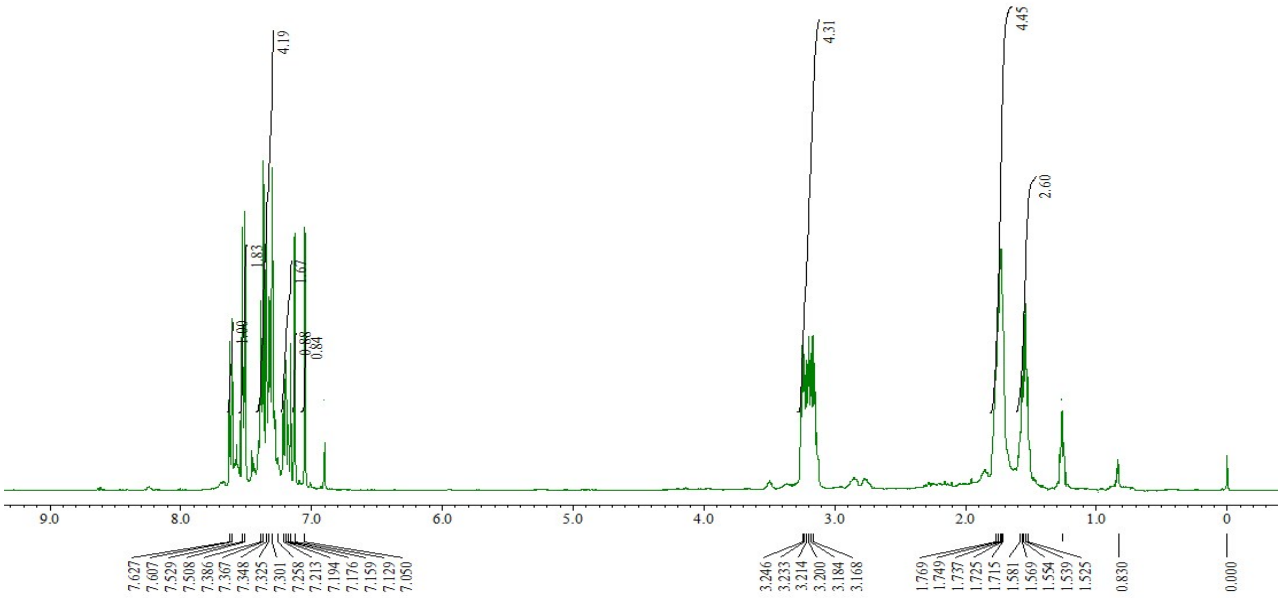

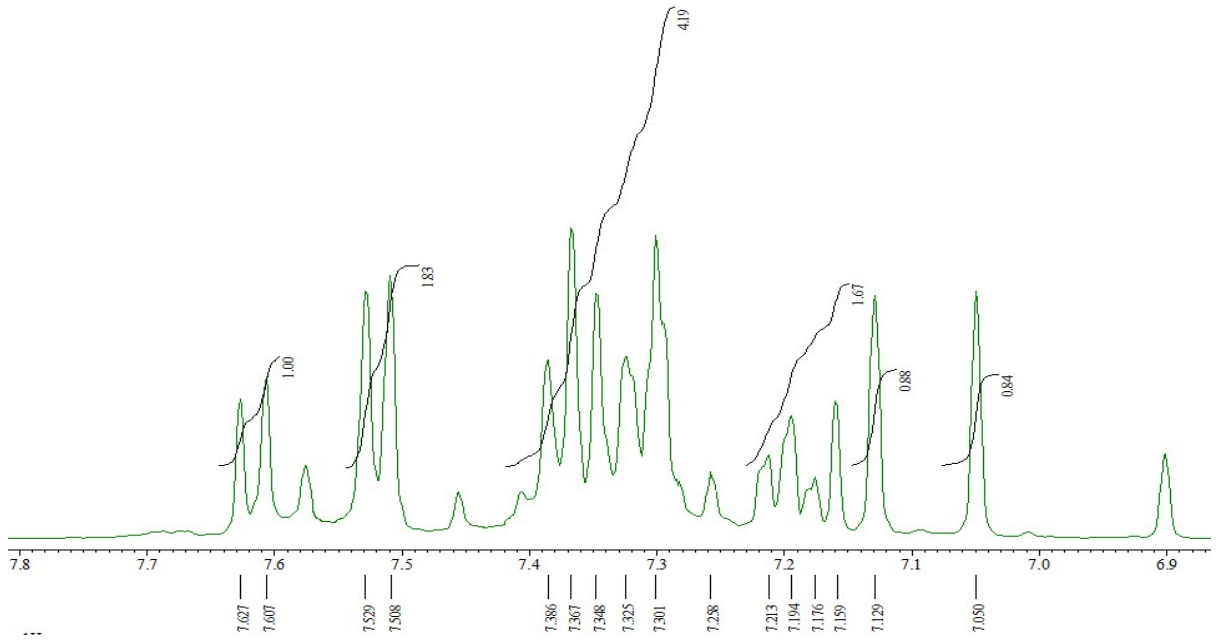

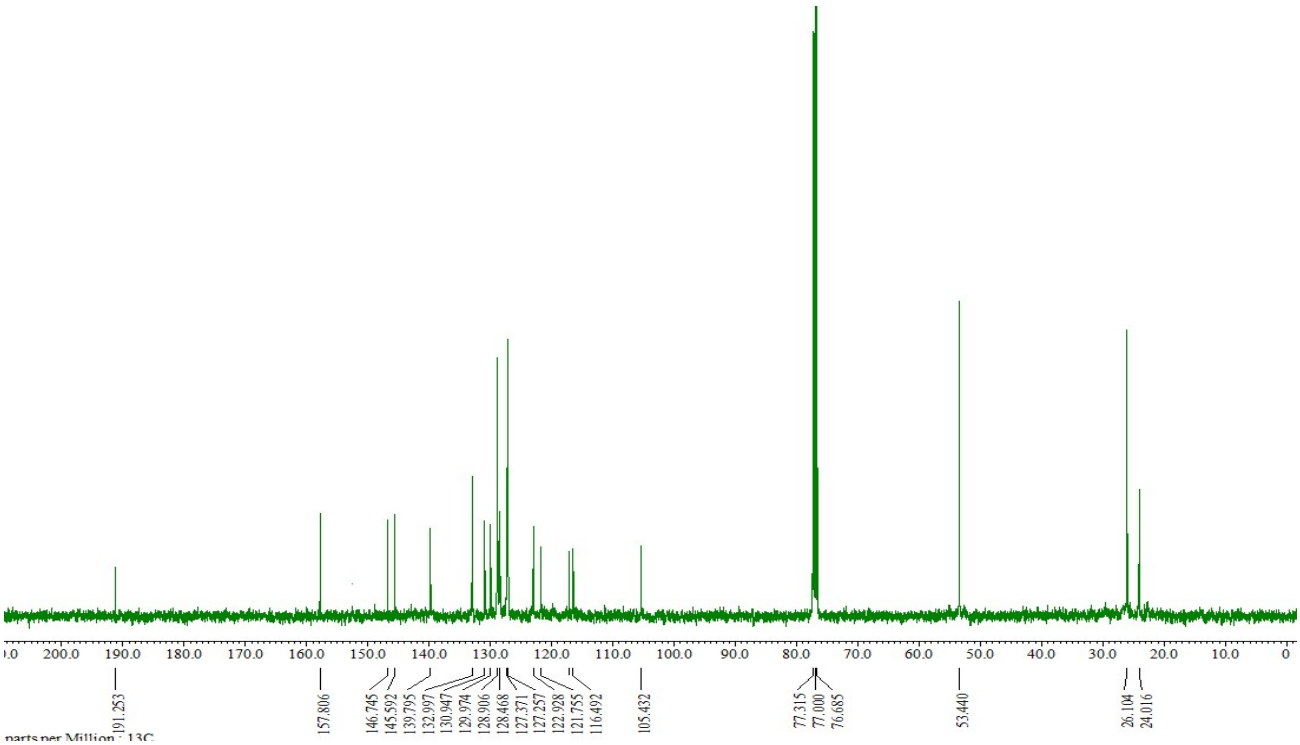

Fig.22.^{1}H,^{1}H of aromatic region&^{13}C-NMR spectra of **8a**.

`

8b. 3-phenyl-1-(pyrrolidin-1-yl)-9H-fluoren-9-one

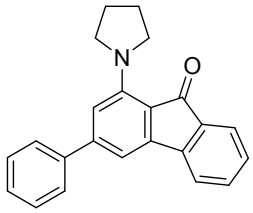

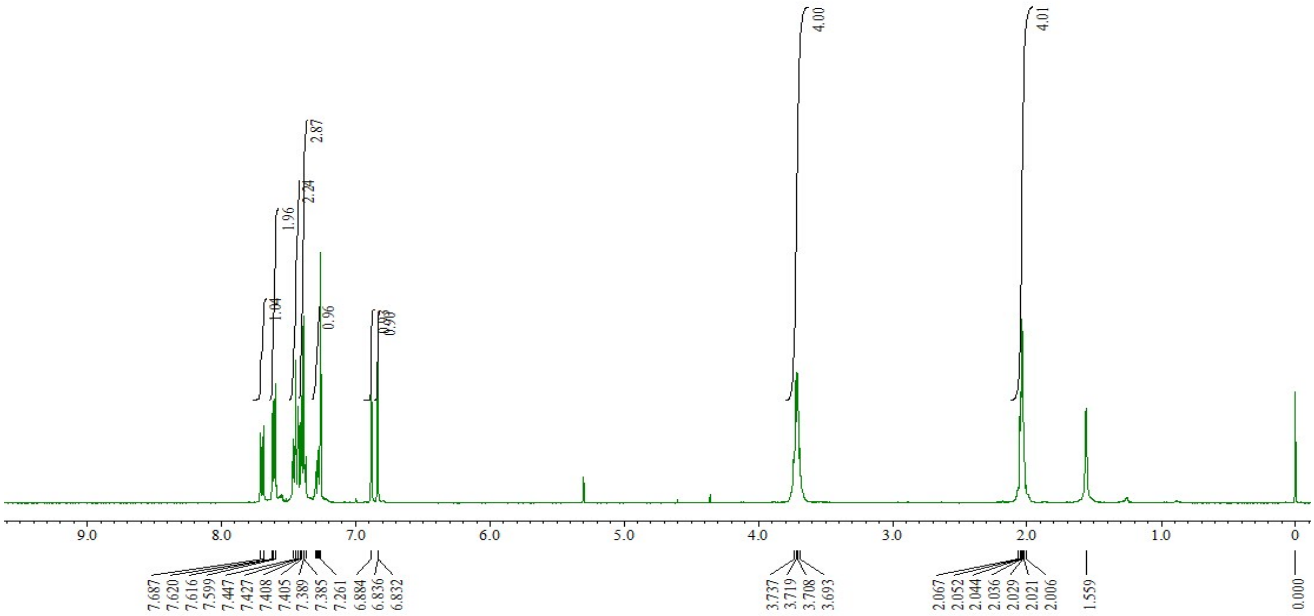

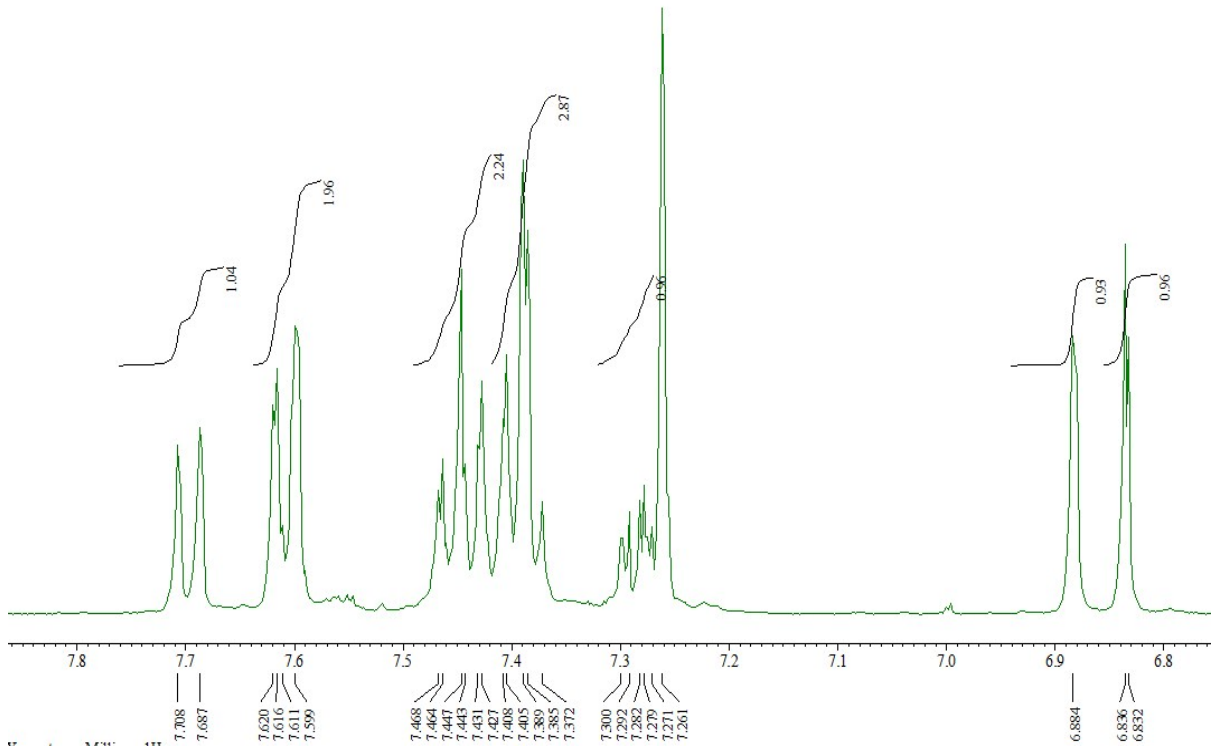

`

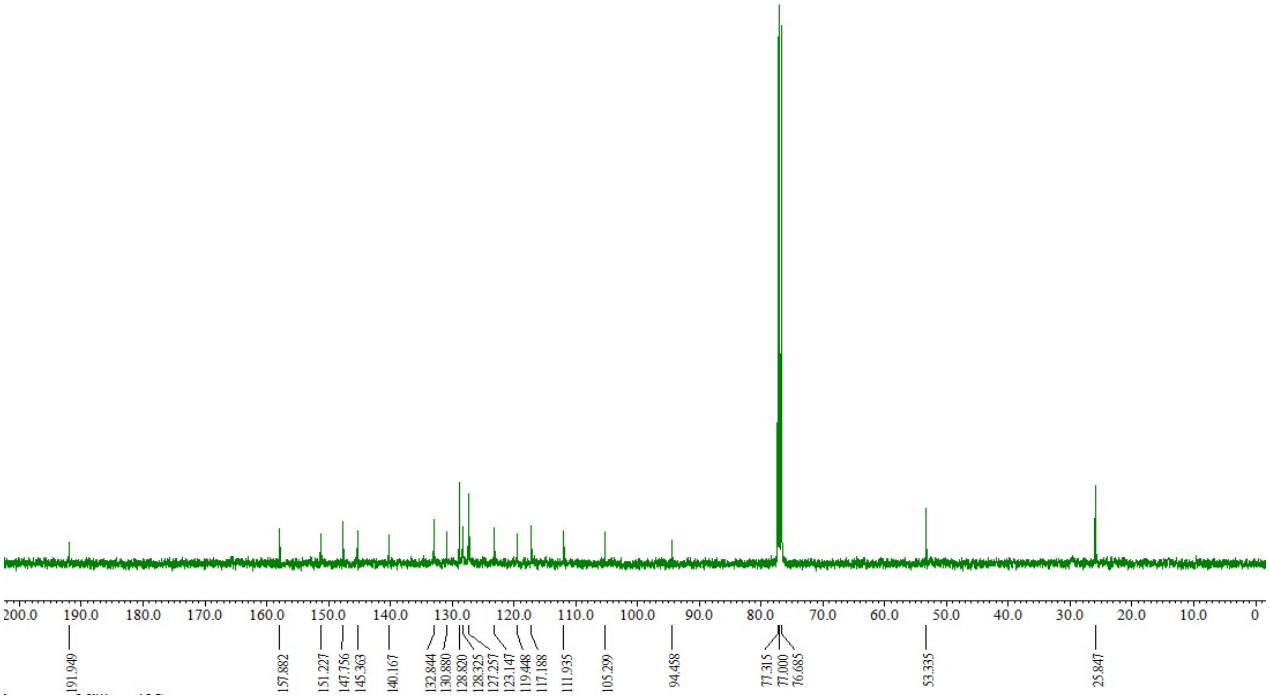

Fig.23.^{1}H,^{1}H of aromatic region&^{13}C-NMR spectra of **8b**.

`

8c. 1-morpholino-3-phenyl-9H-fluoren-9-one

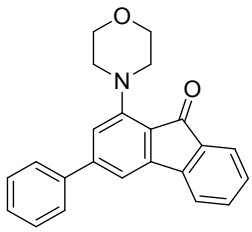

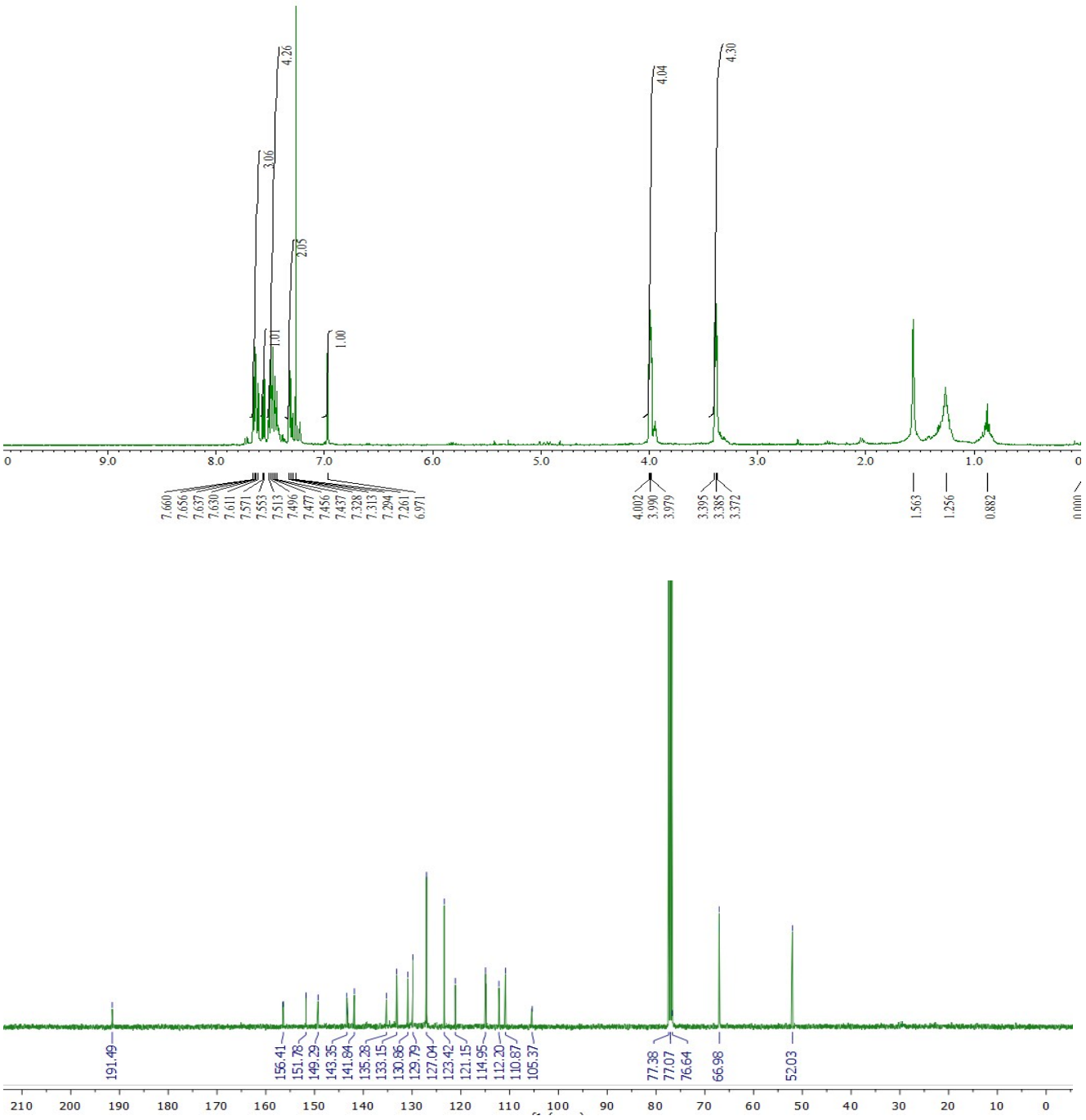

Fig.24.[1]H &[13]C-NMR spectra of **8c**.

`

8d. 1-(piperidin-1-yl)-3-(p-tolyl)-9H-fluoren-9-one

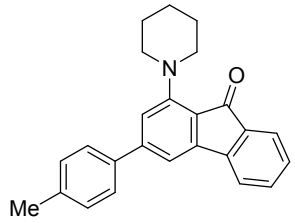

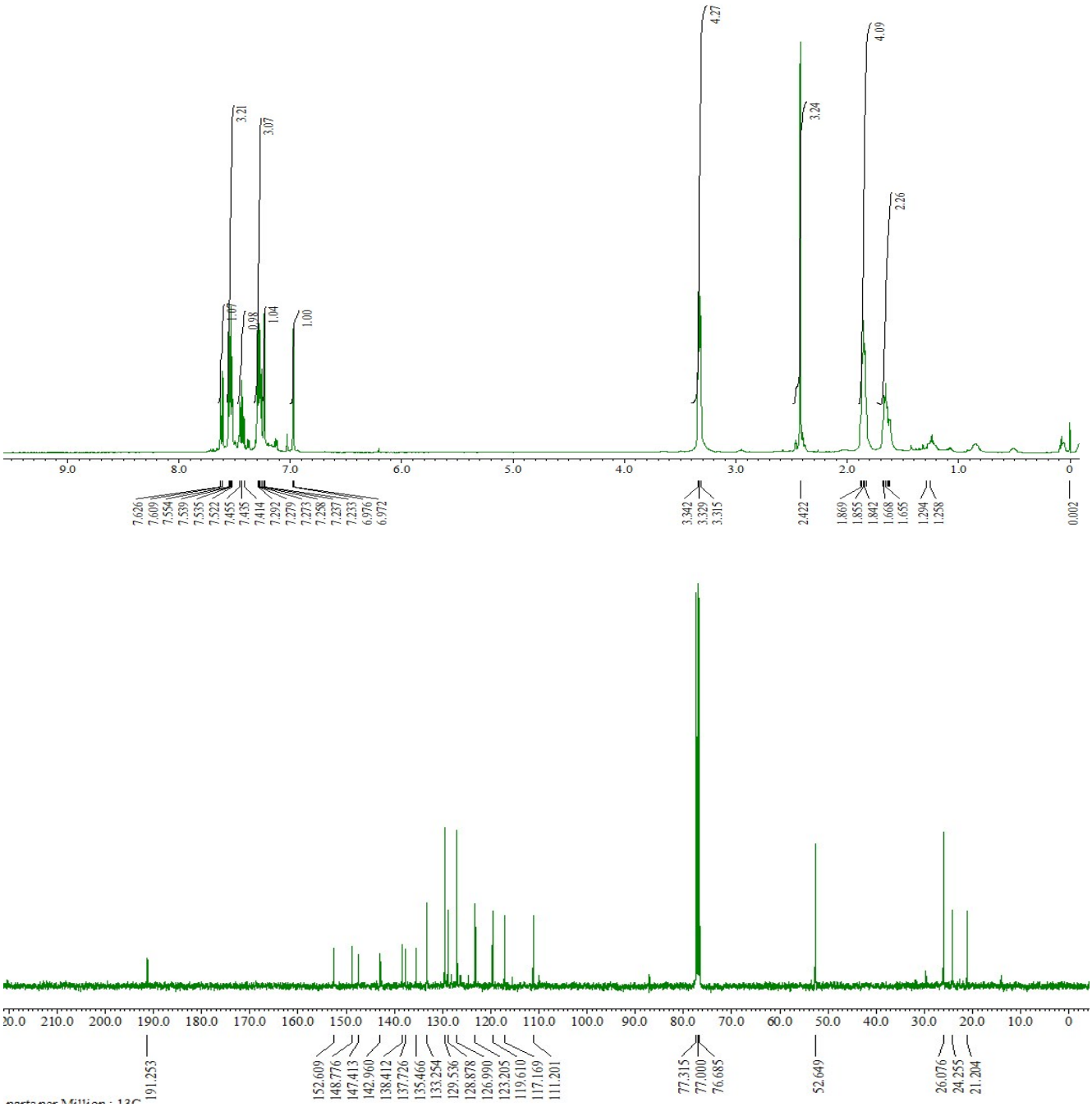

Fig.25.[1]H &[13]C-NMR spectra of **8d**.

`

8e. 1-(pyrrolidin-1-yl)-3-(p-tolyl)-9H-fluoren-9-one

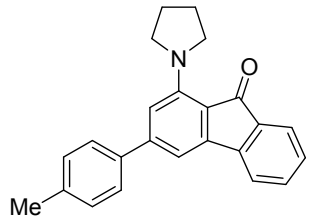

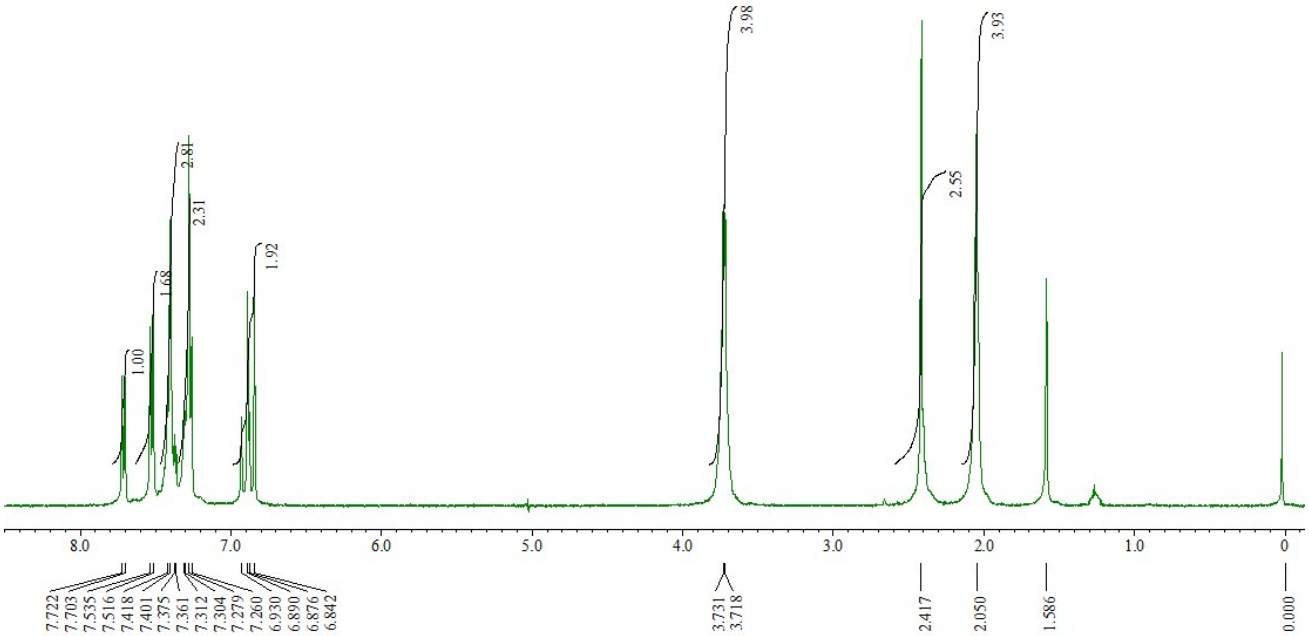

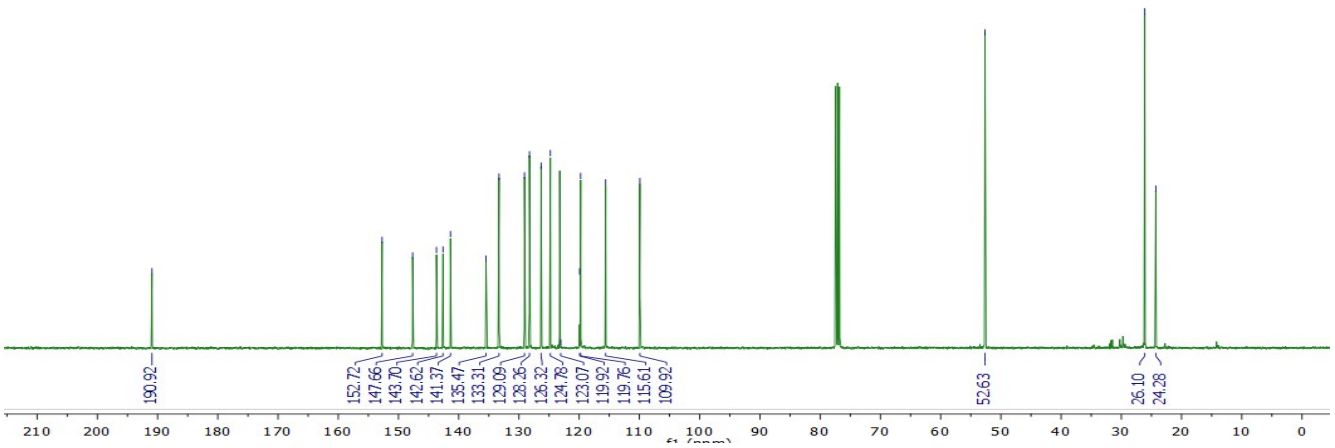

Fig.26.^{1}H &^{13}C-NMR spectra of **8e**.

`

8f. 1-morpholino-3-(p-tolyl)-9H-fluoren-9-one

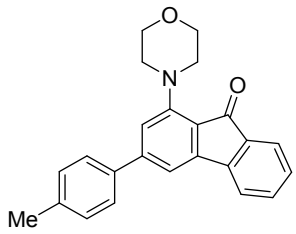

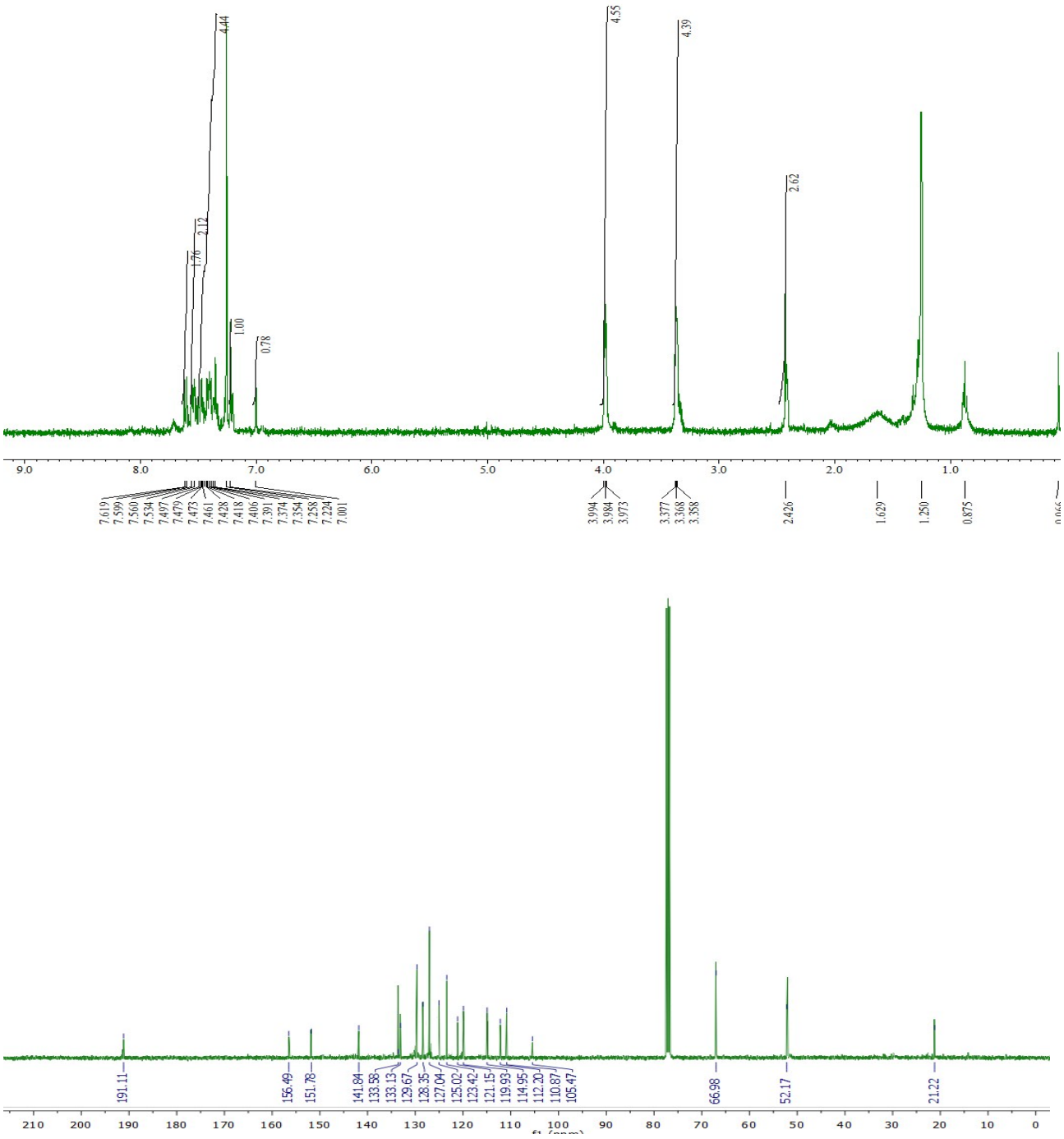

Fig.27.[1]H &[13]C-NMR spectra of **8f**.

`

8g. 3-(4-methoxyphenyl)-1-(piperidin-1-yl)-9H-fluoren-9-one

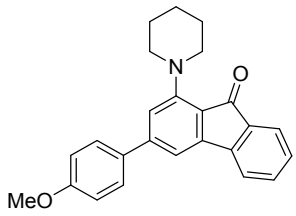

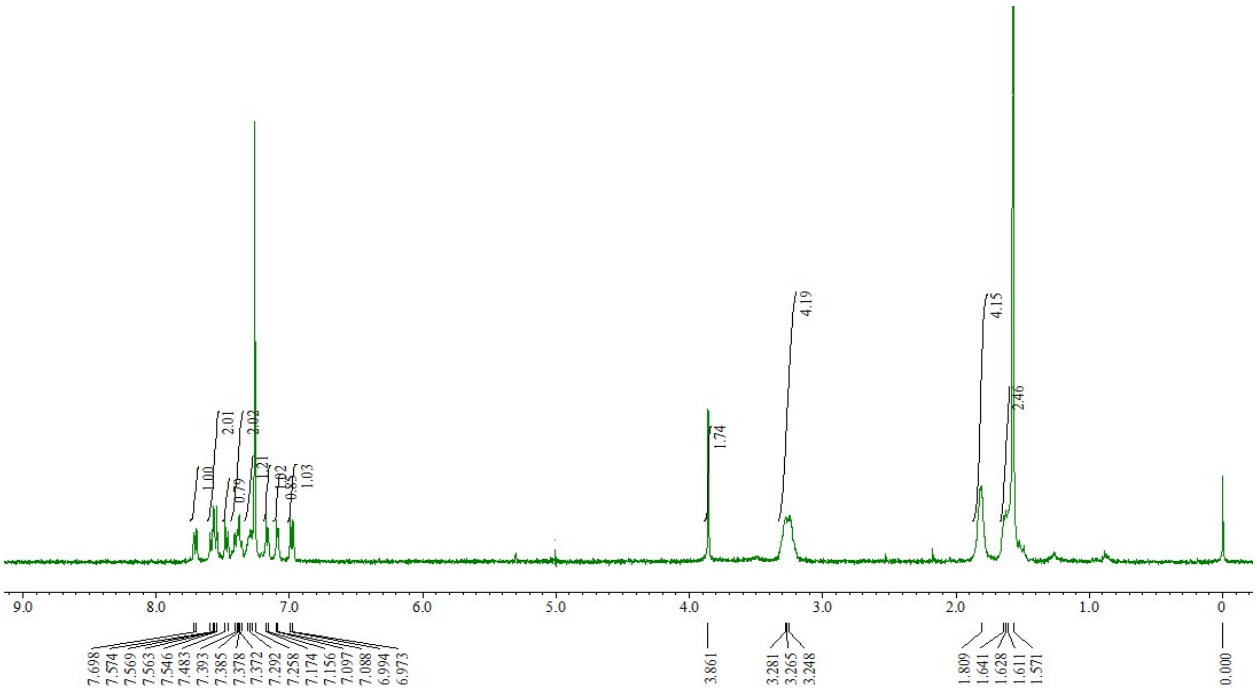

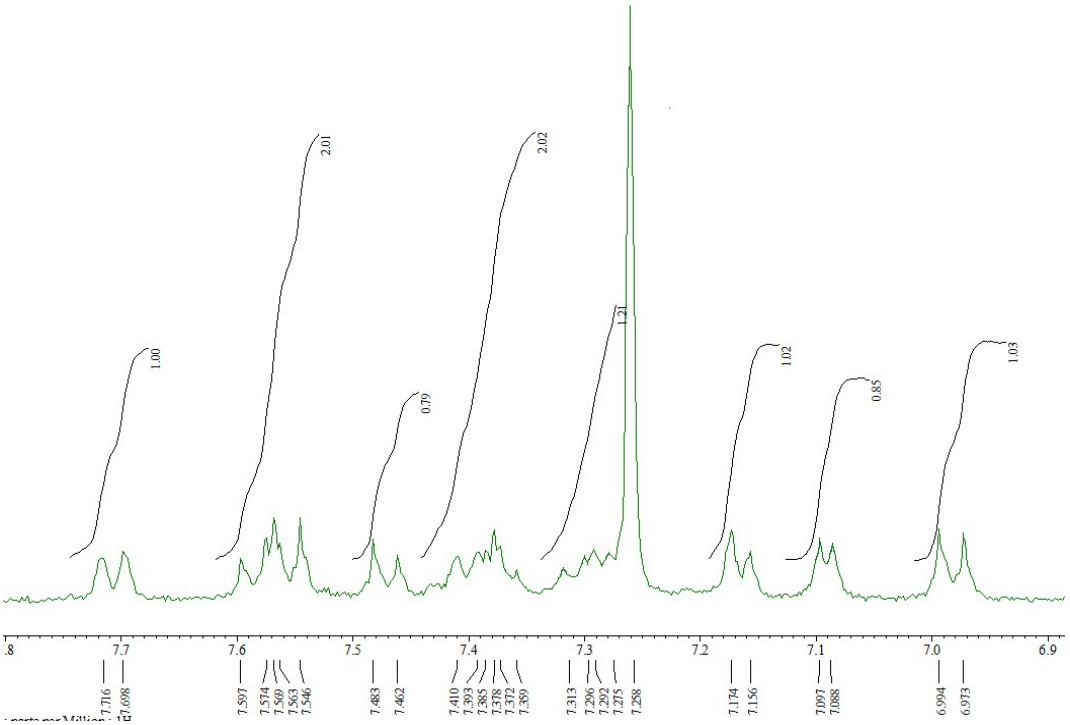

`

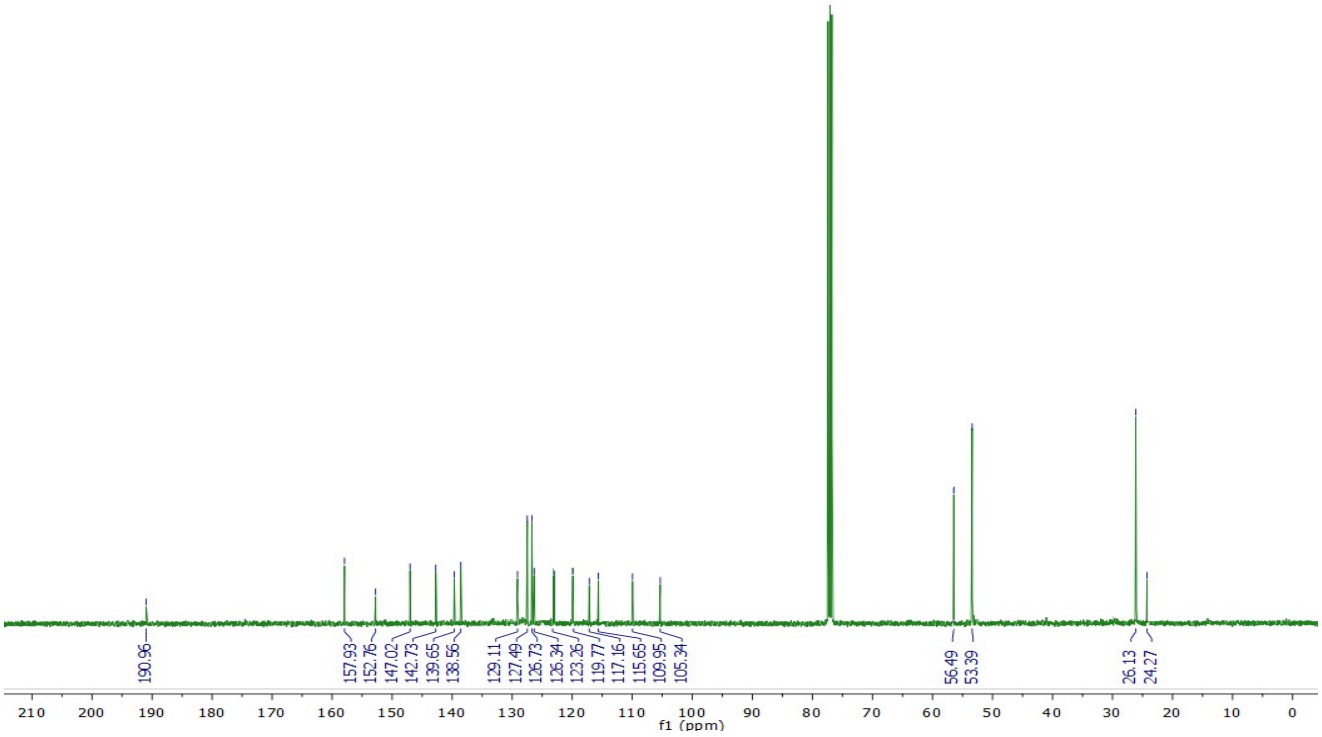

Fig.28.^{1}H,^{1}H of aromatic region&^{13}C-NMR spectra of **8g**.

8h. 3-(4-methoxyphenyl)-1-(pyrrolidin-1-yl)-9H-fluoren-9-one

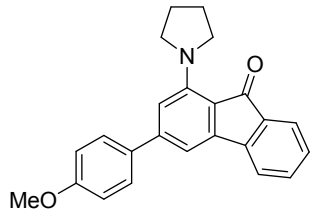

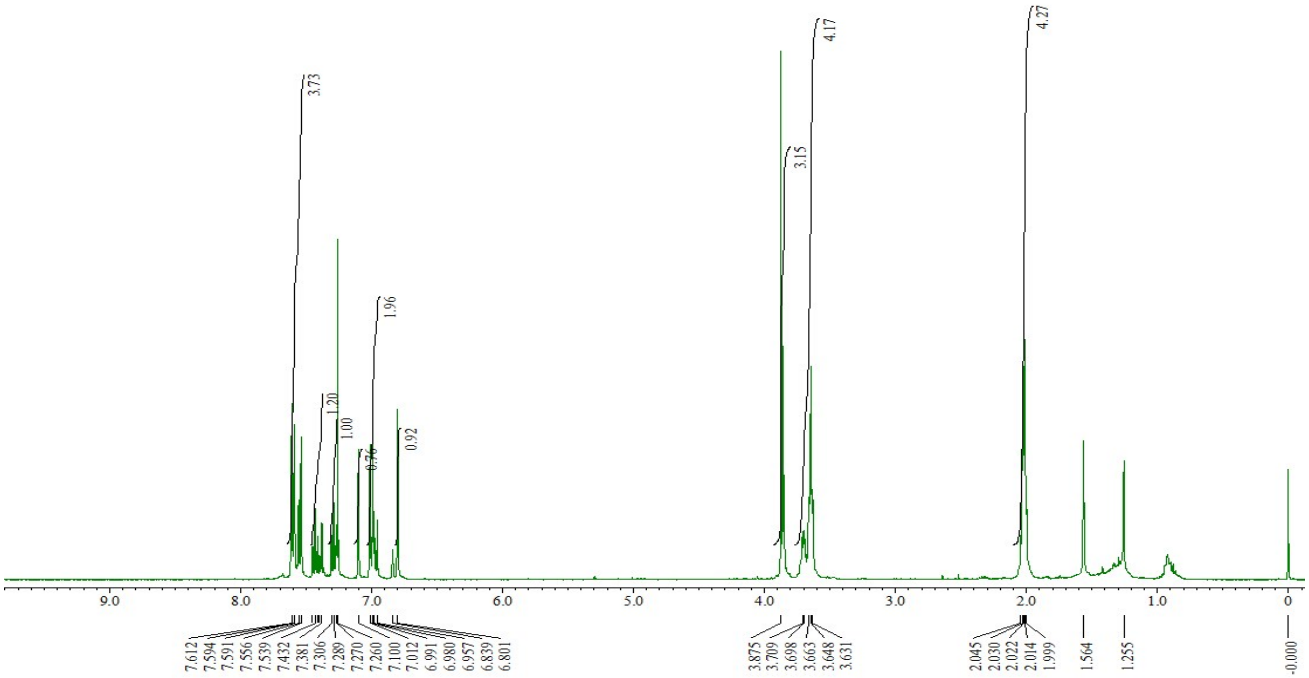

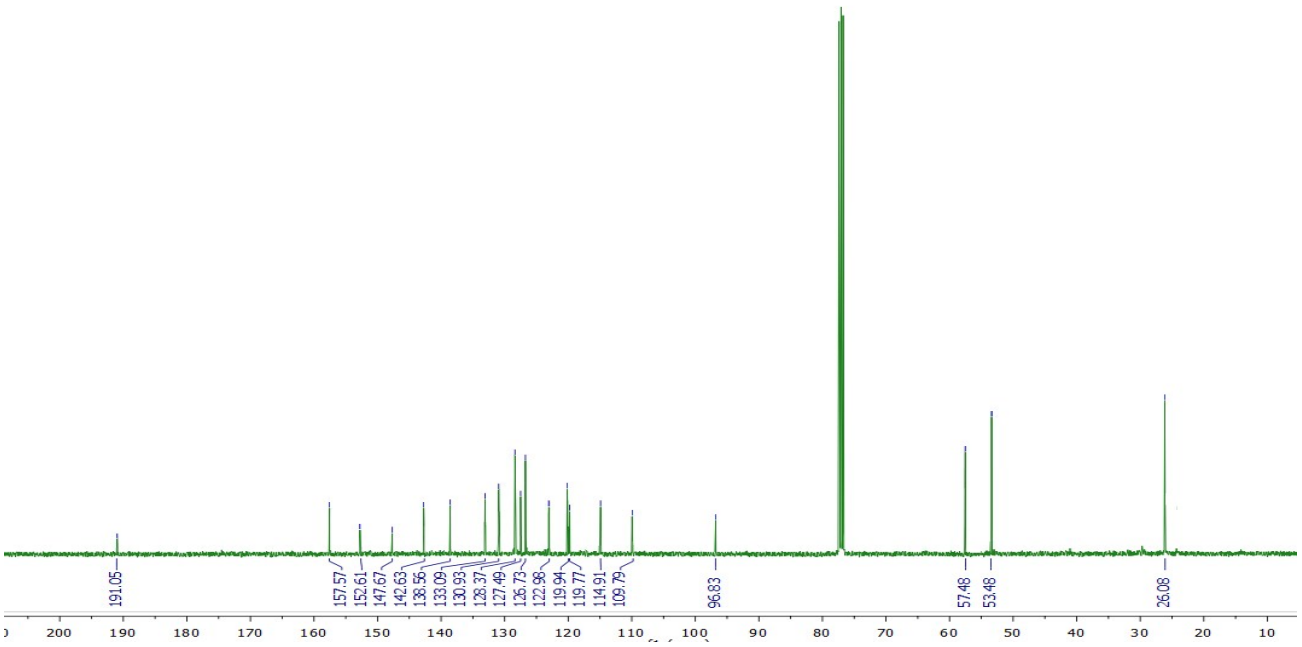

Fig.29.[1]H &[13]C-NMR spectra of **8h**.

8i. 3-(4-chlorophenyl)-1-morpholino-9H-fluoren-9-one

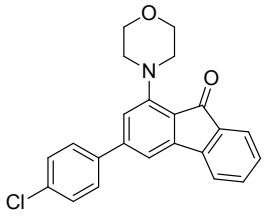

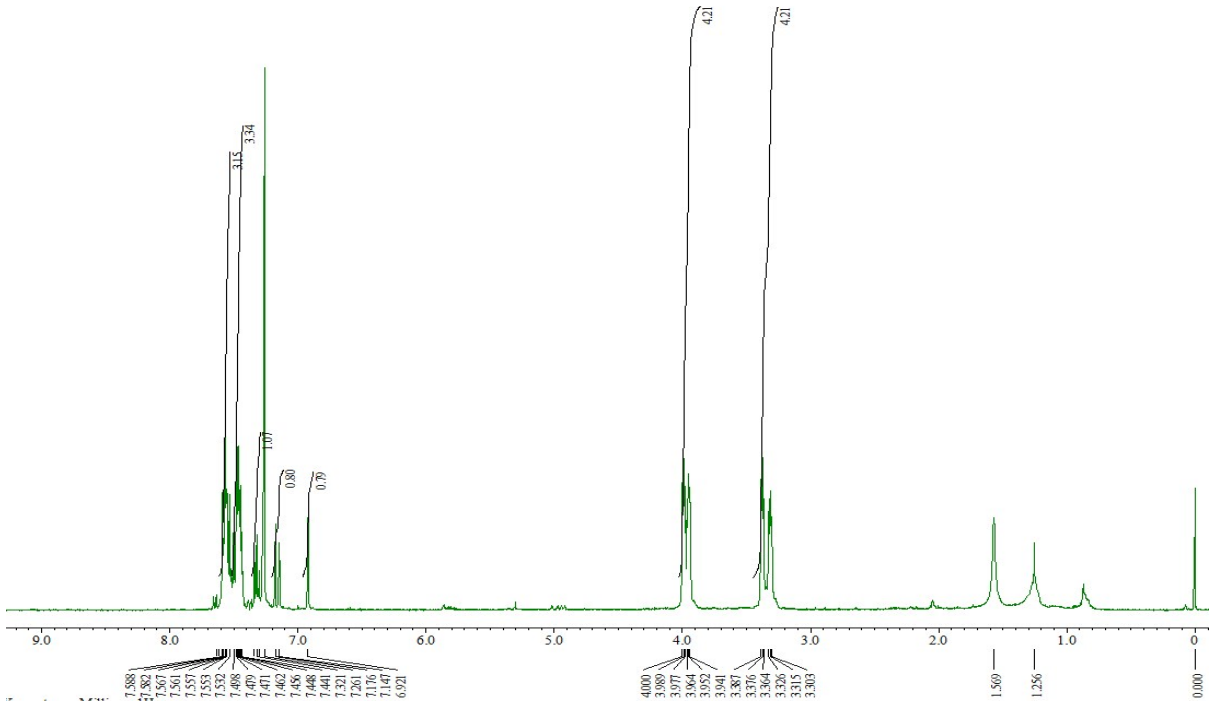

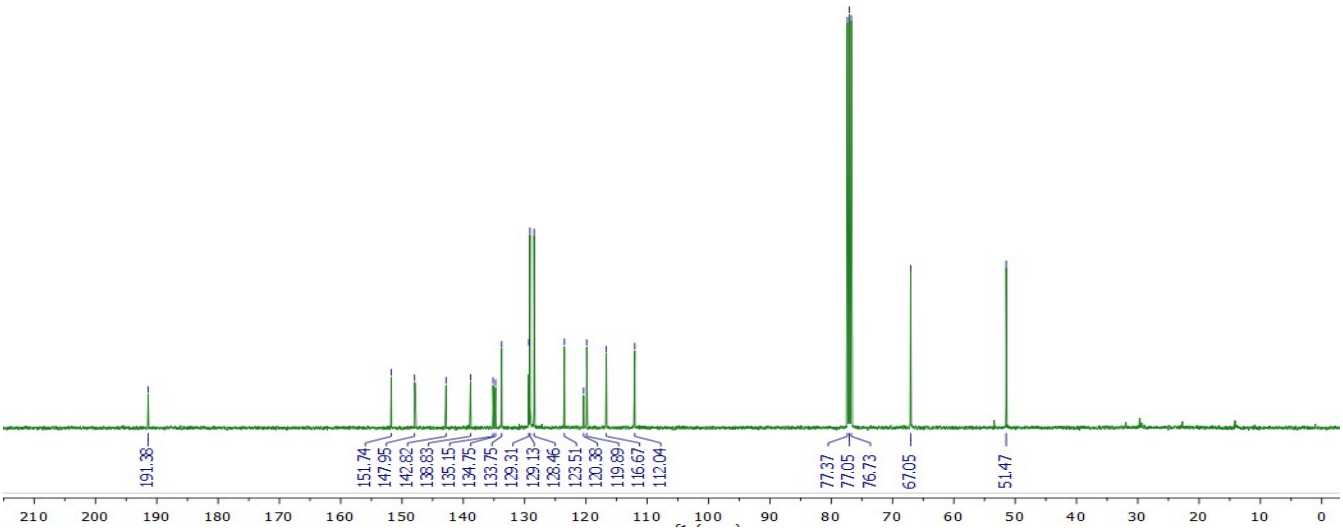

Fig.30.[1]H &[13]C-NMR spectra of **8i**.

8j. 3-(naphthalen-2-yl)-1-(piperidin-1-yl)-9H-fluoren-9-one

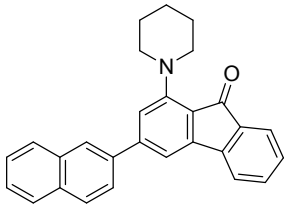

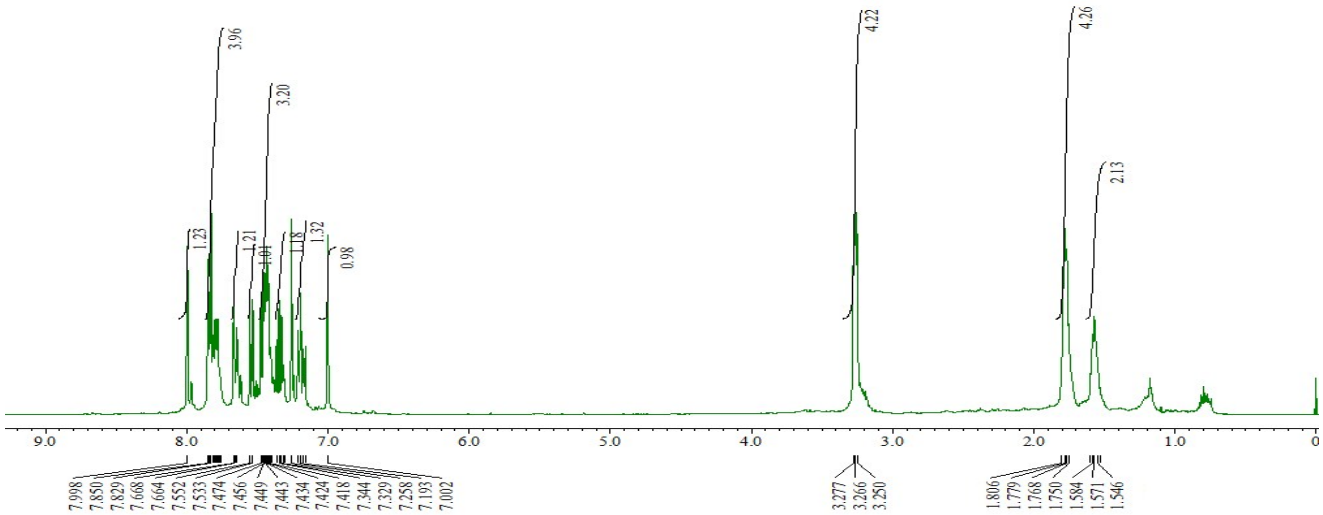

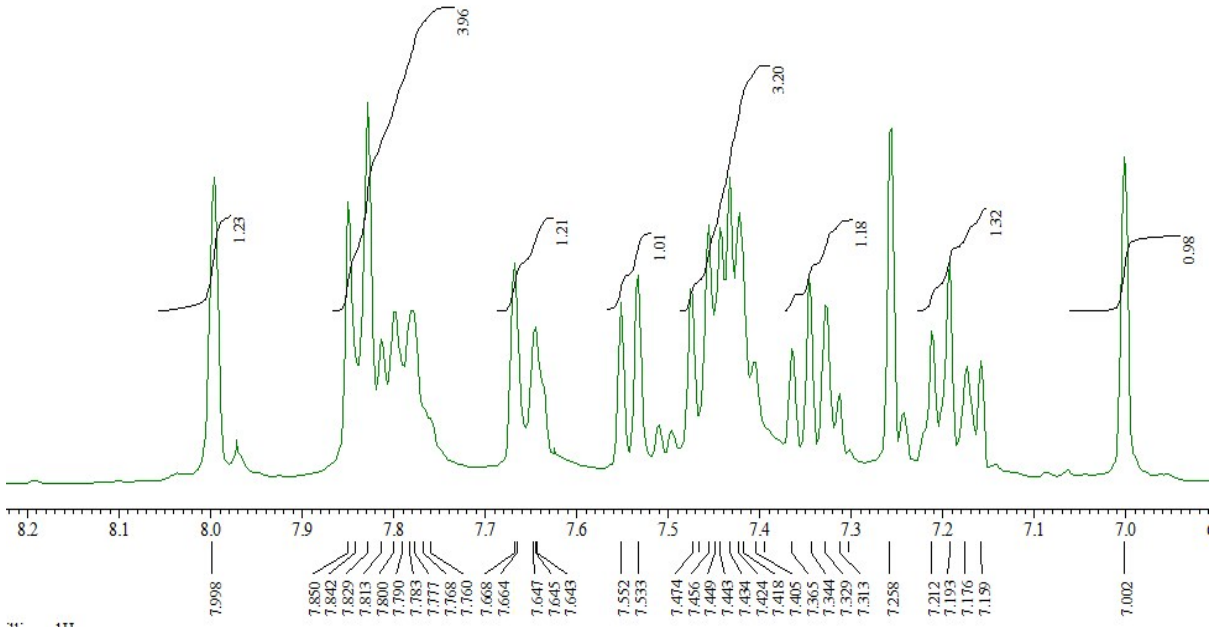

`

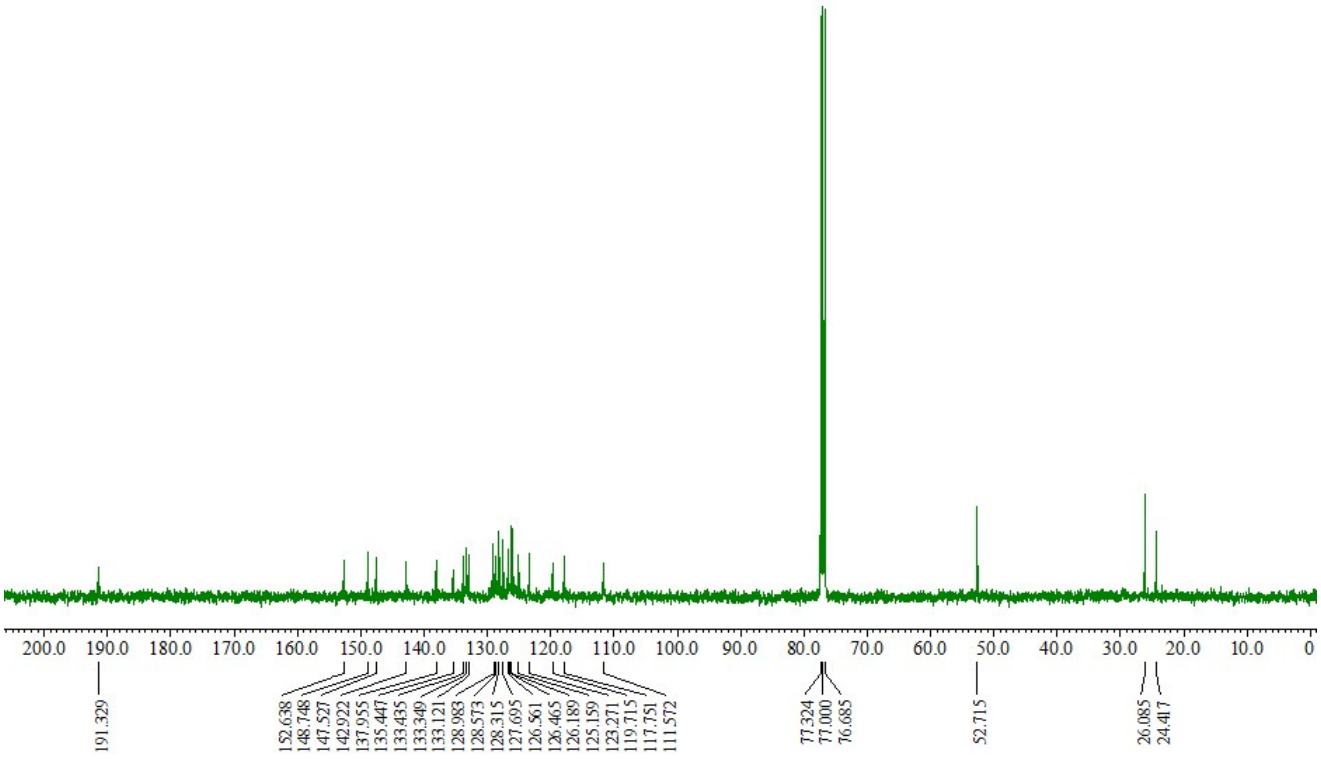

Fig. 31.[1]H, [1]H of aromatic region&[13]C-NMR spectra of **8j**.

`

8k. 1-(piperidin-1-yl)-3-(thiophen-2-yl)-9H-fluoren-9-one

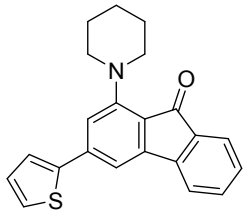

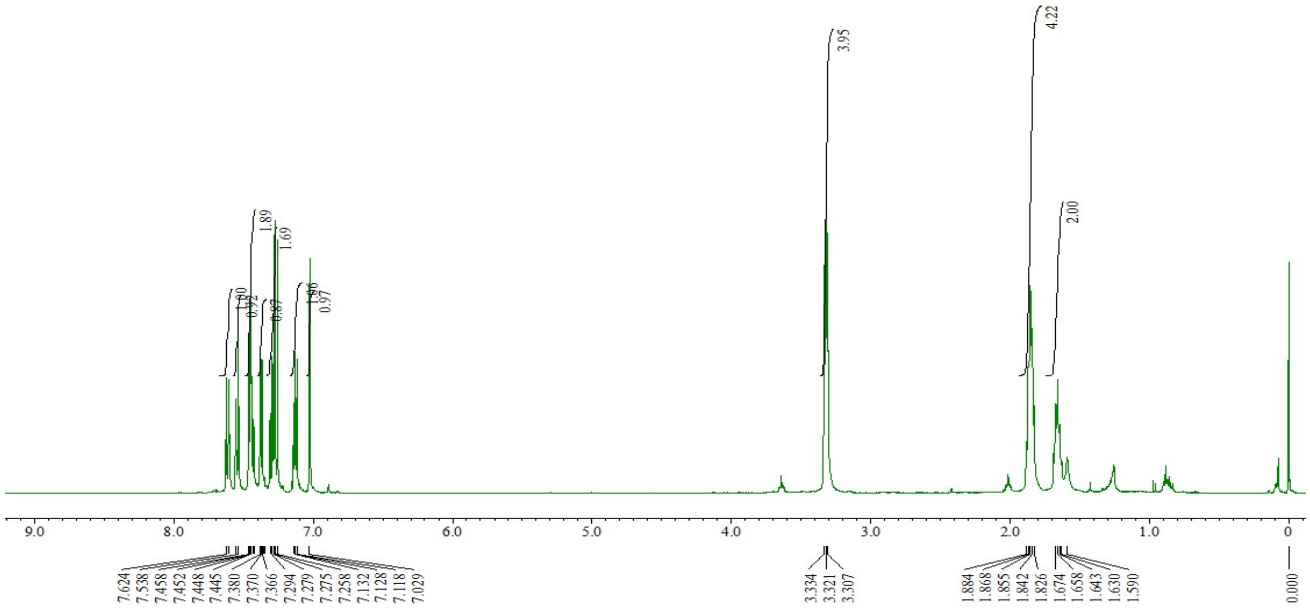

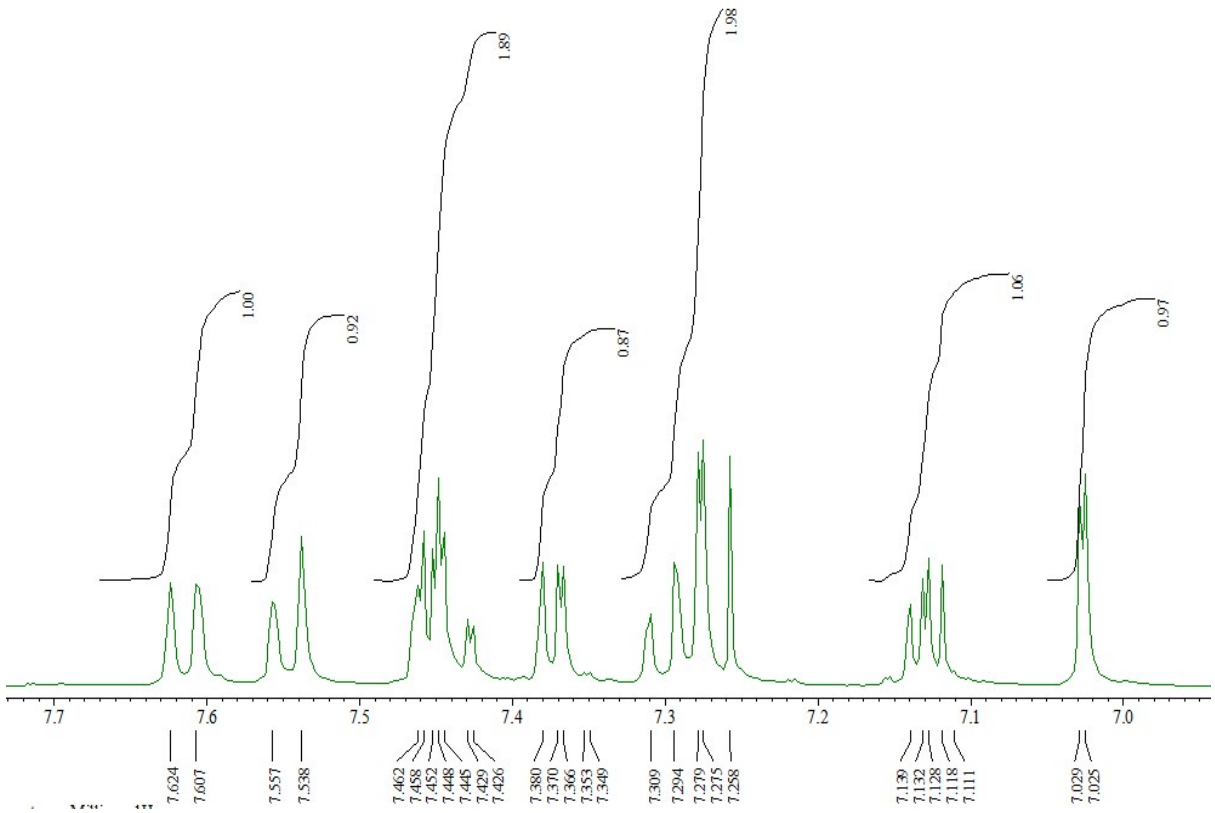

`

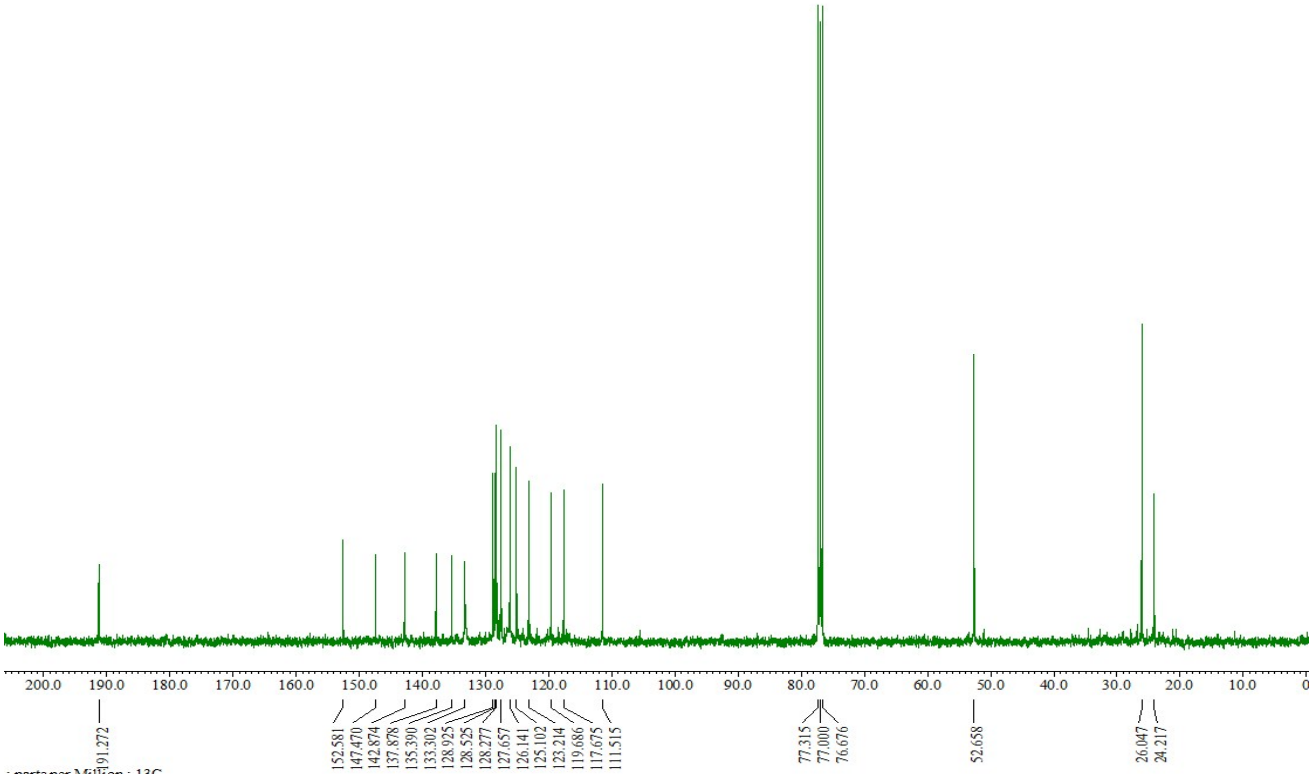

Fig.32.^{1}H, ^{1}H of aromatic region&^{13}C-NMR spectra of **8k**.

8l. 1-(pyrrolidin-1-yl)-3-(thiophen-2-yl)-9H-fluoren-9-one

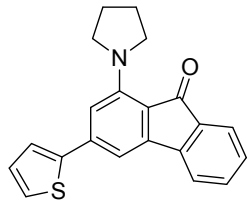

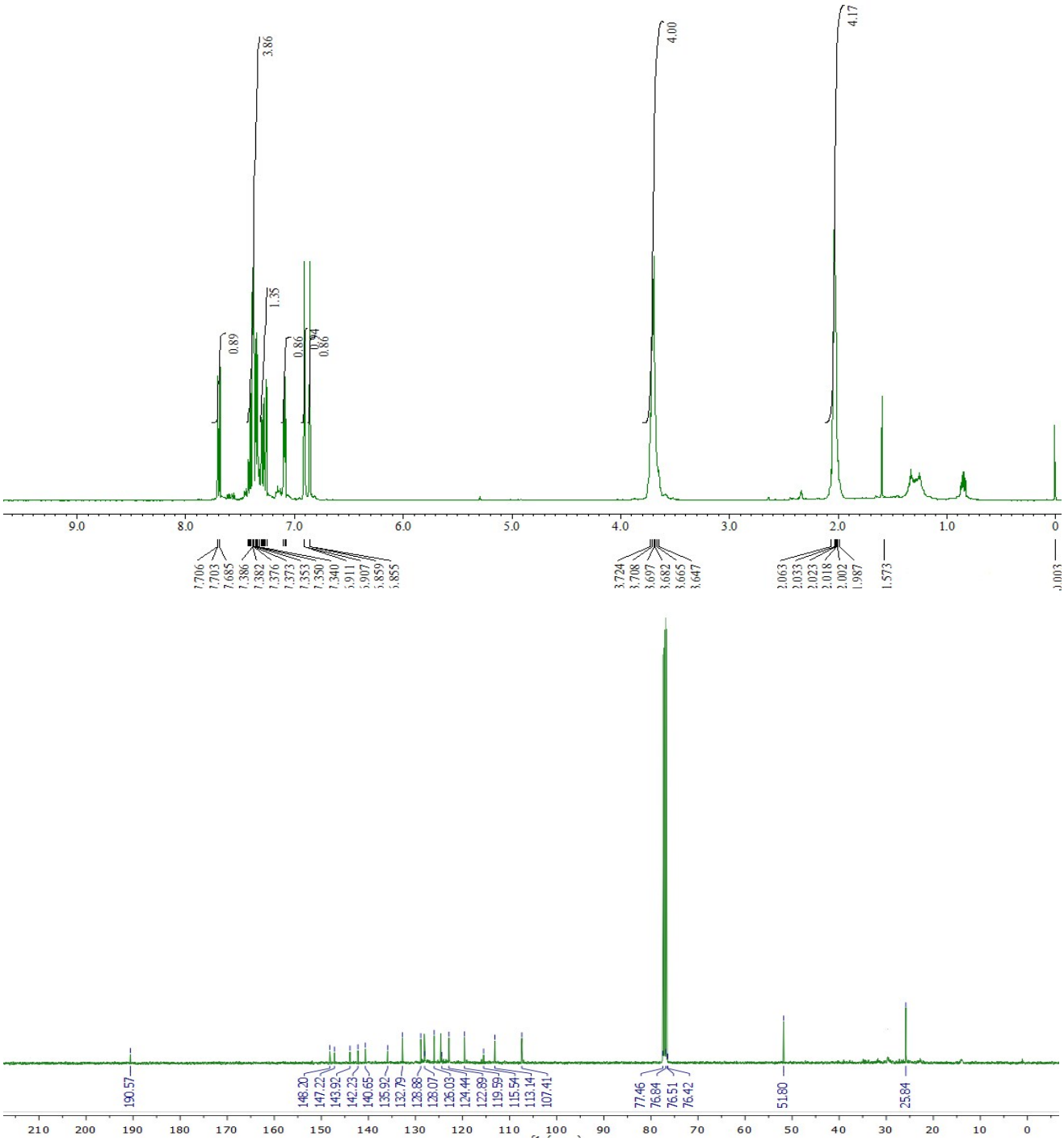

Fig.33.[1]H &[13]C-NMR spectra of **8l**.

`

8m. 7-(piperidin-1-yl)-5H-indeno[2,1-b]phenanthren-8(6H)-one

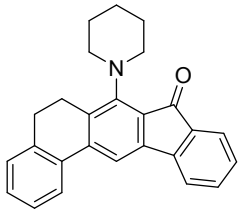

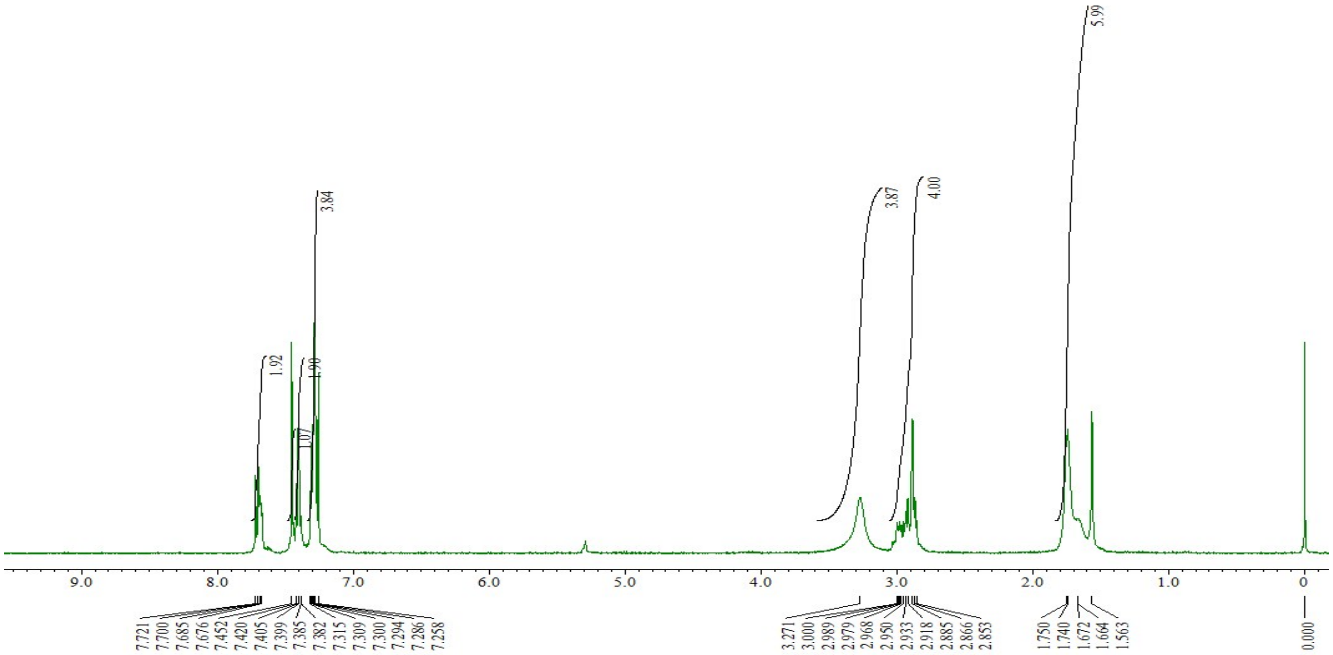

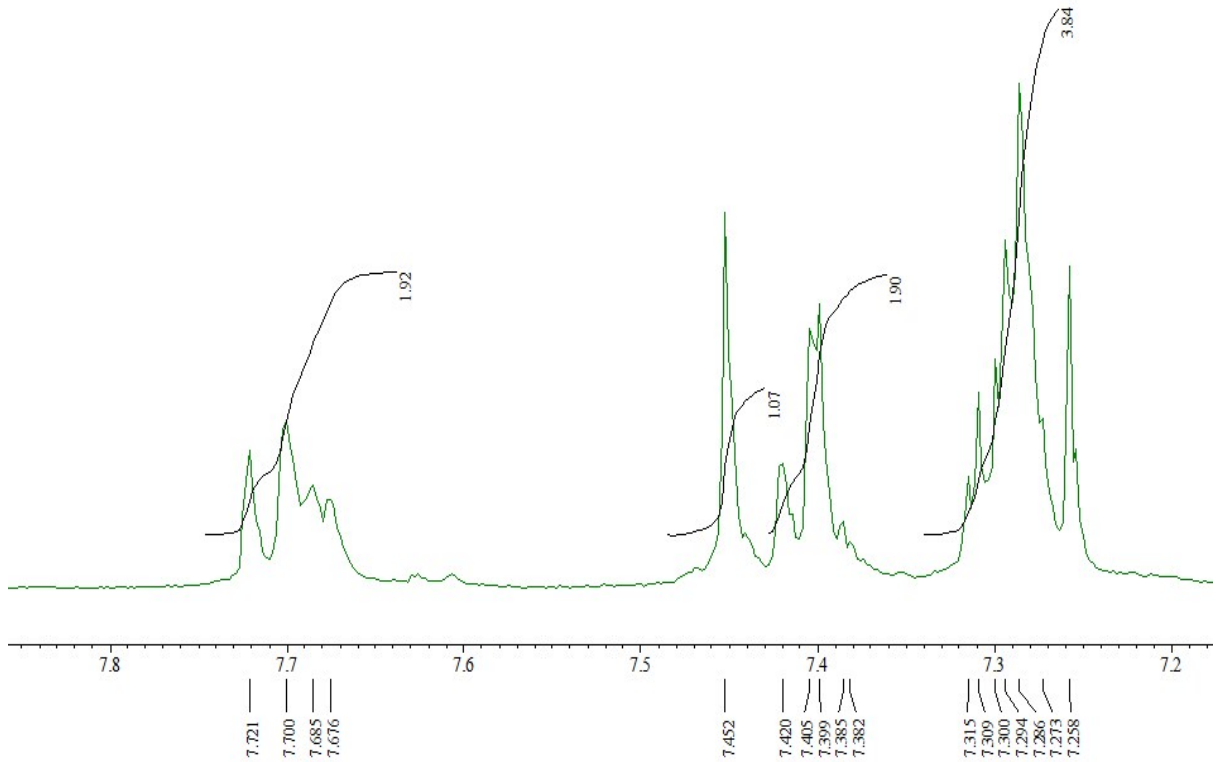

`

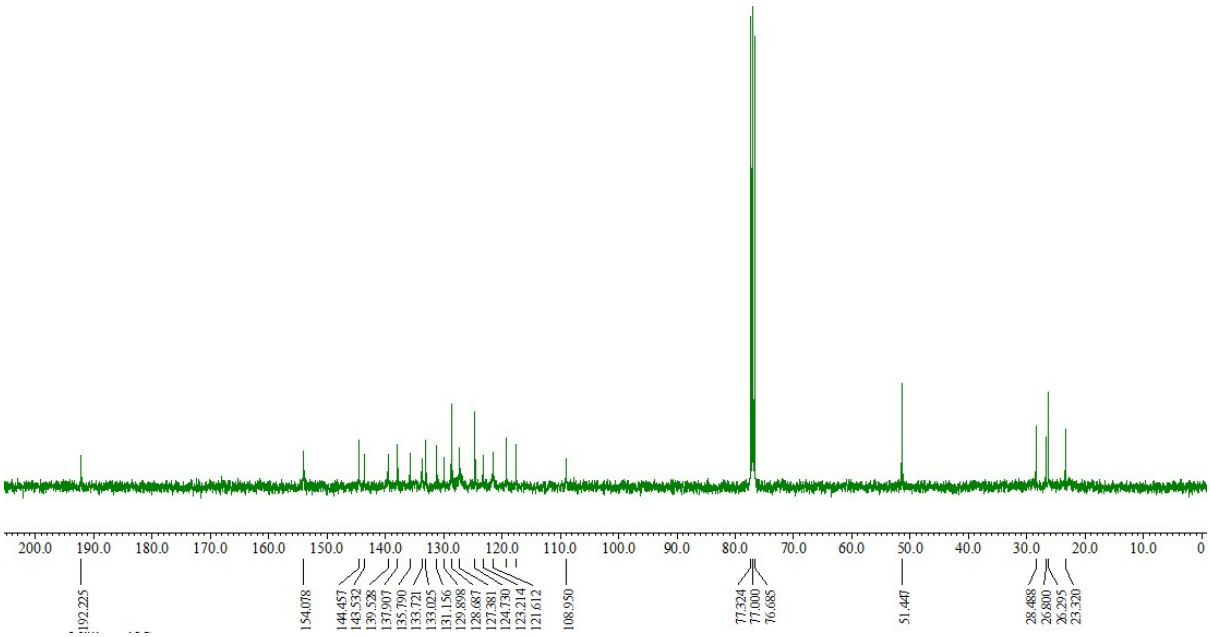

Fig.34.^{1}H,^{1}H of aromatic region&^{13}C-NMR spectra of **8m**.

`

8n. 3-methoxy-7-(piperidin-1-yl)-5H-indeno[2,1-b]phenanthren-8(6H)-one

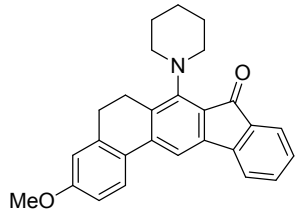

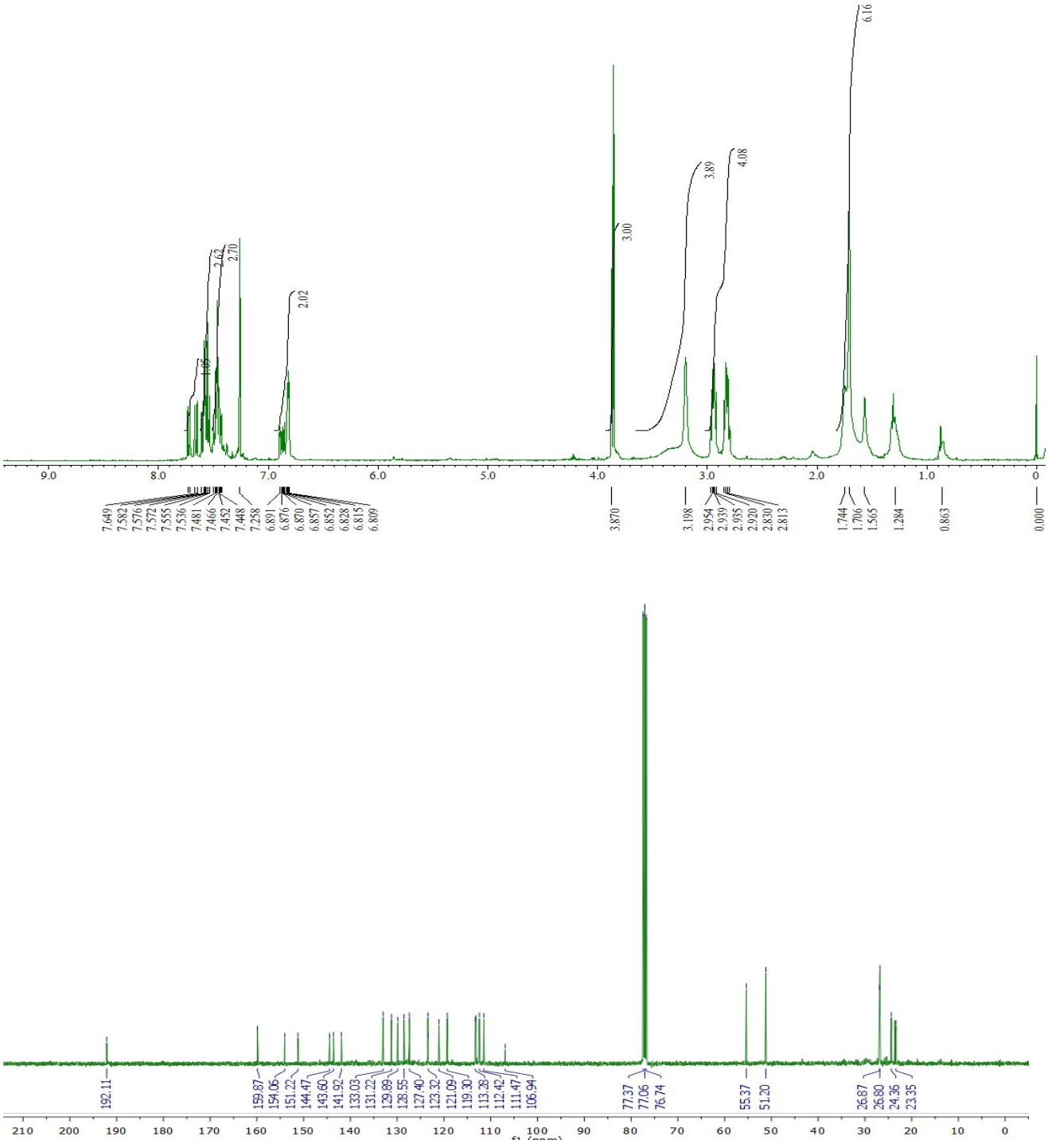

Fig.35.[1]H &[13]C-NMR spectra of **8n**.

`

8o. 3-methoxy-7-(pyrrolidin-1-yl)-5H-indeno[2,1-b]phenanthren-8(6H)-one

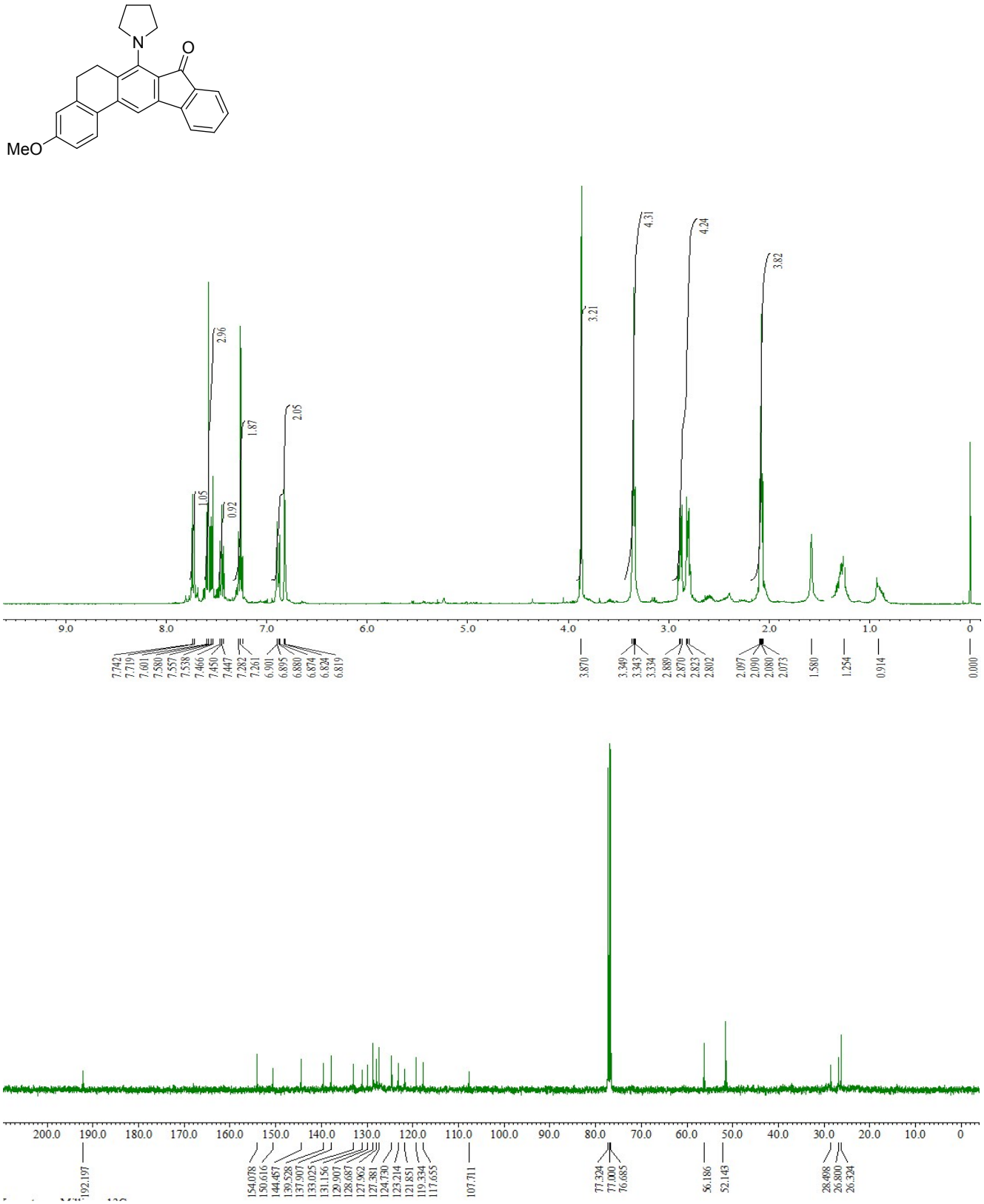

Fig. 36.[1]H &[13]C-NMR spectra of **8o**.

`

9. 4-methyl-5'-(piperidin-1-yl)-[1,1':3',1''-terphenyl]-4'-carbonitrile

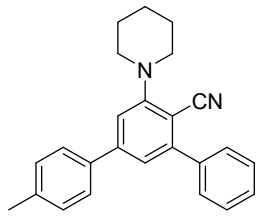

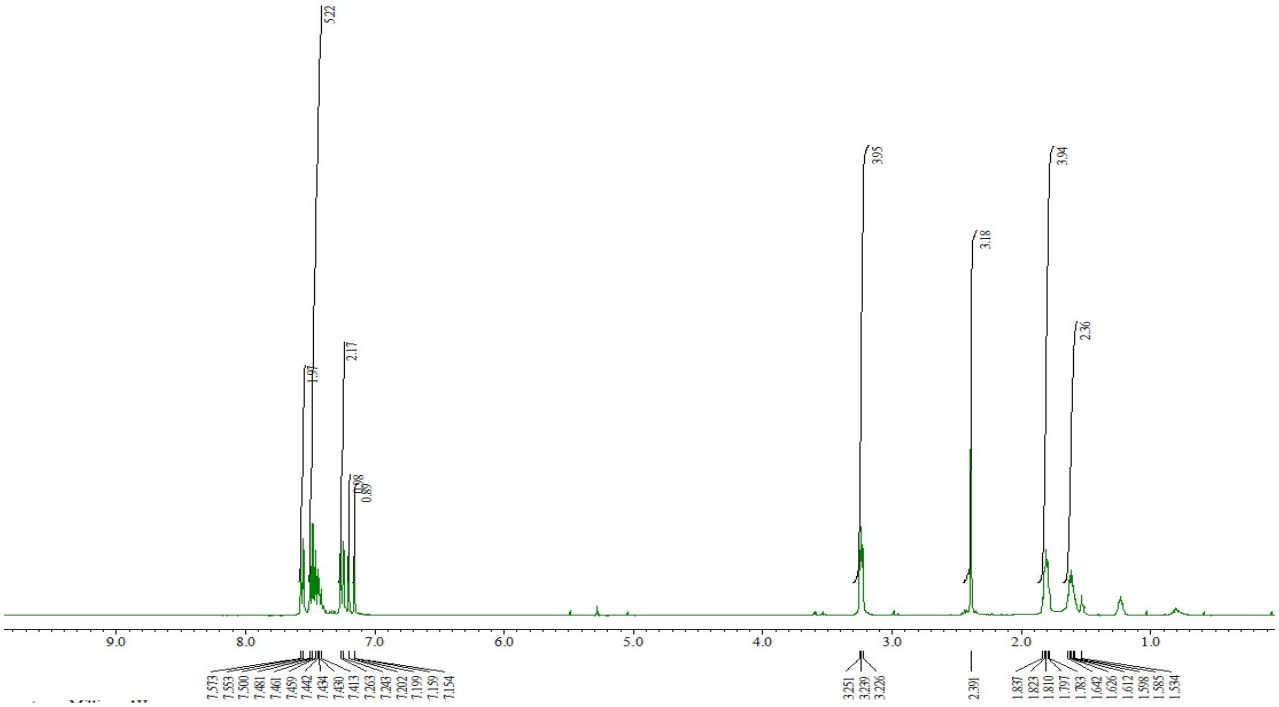

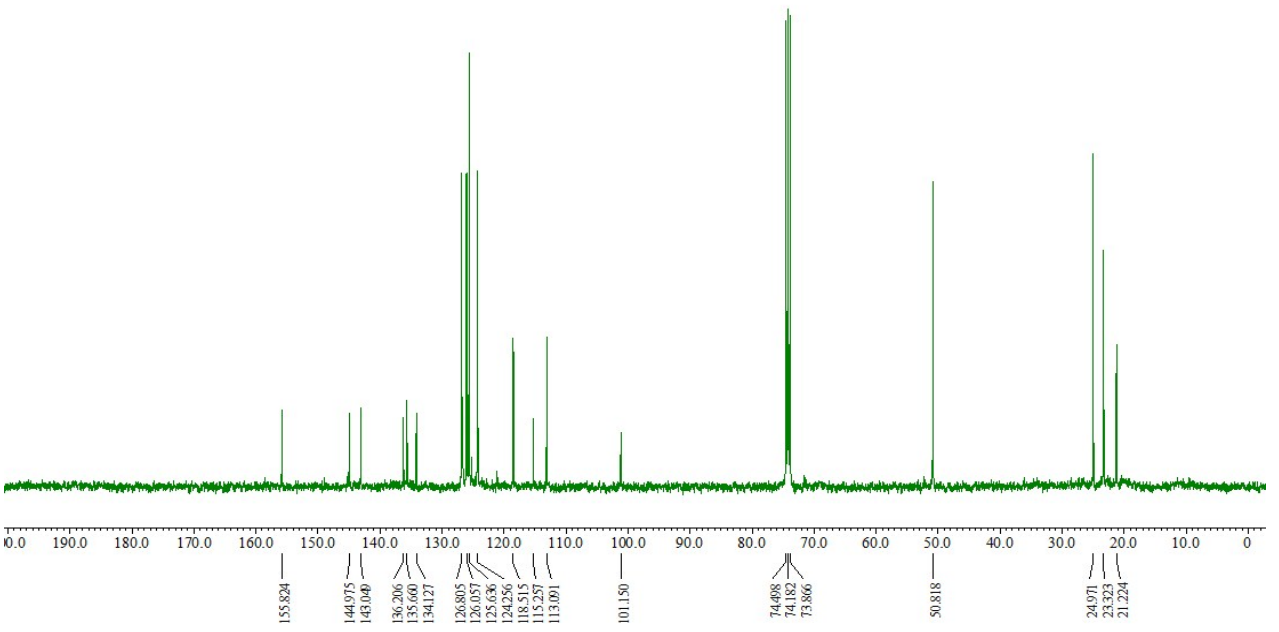

Fig. 37.[1]H &[13]C-NMR spectra of **9**.

`

10. 3-(piperidin-1-yl)-5-(thiophen-2-yl)-[1,1'-biphenyl]-2-carbonitrile-2'-d

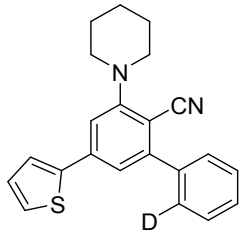

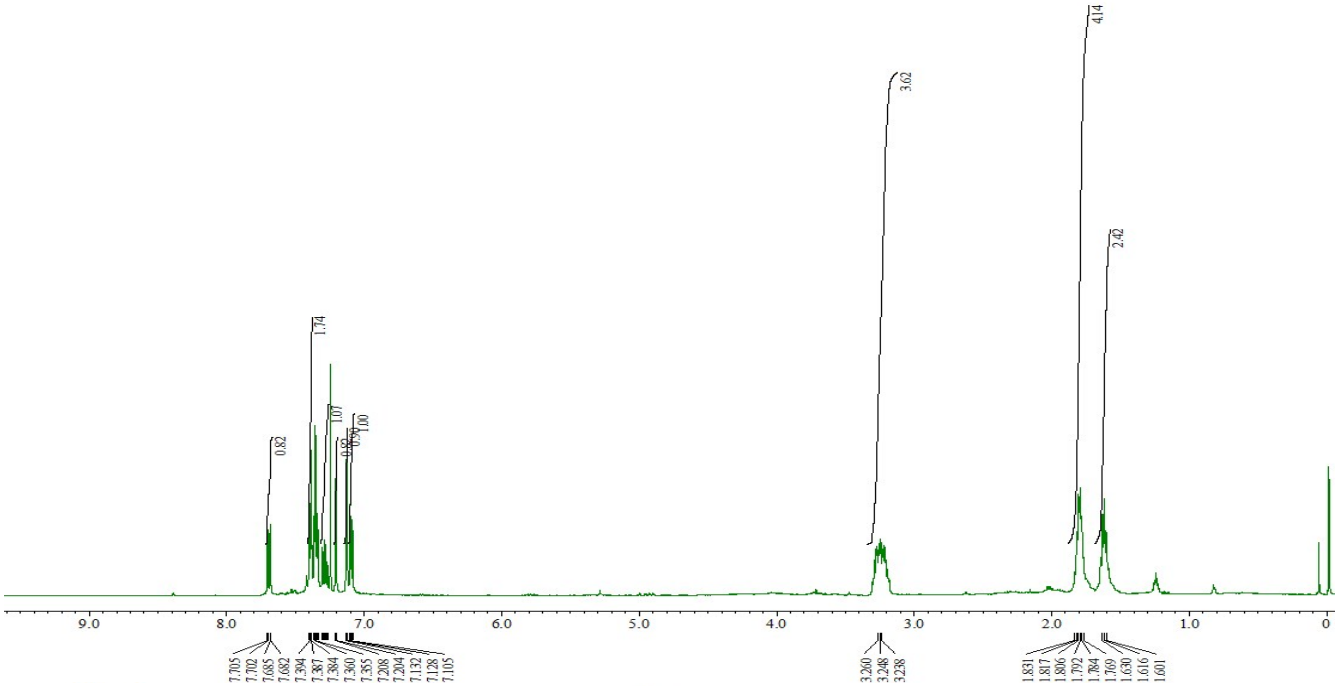

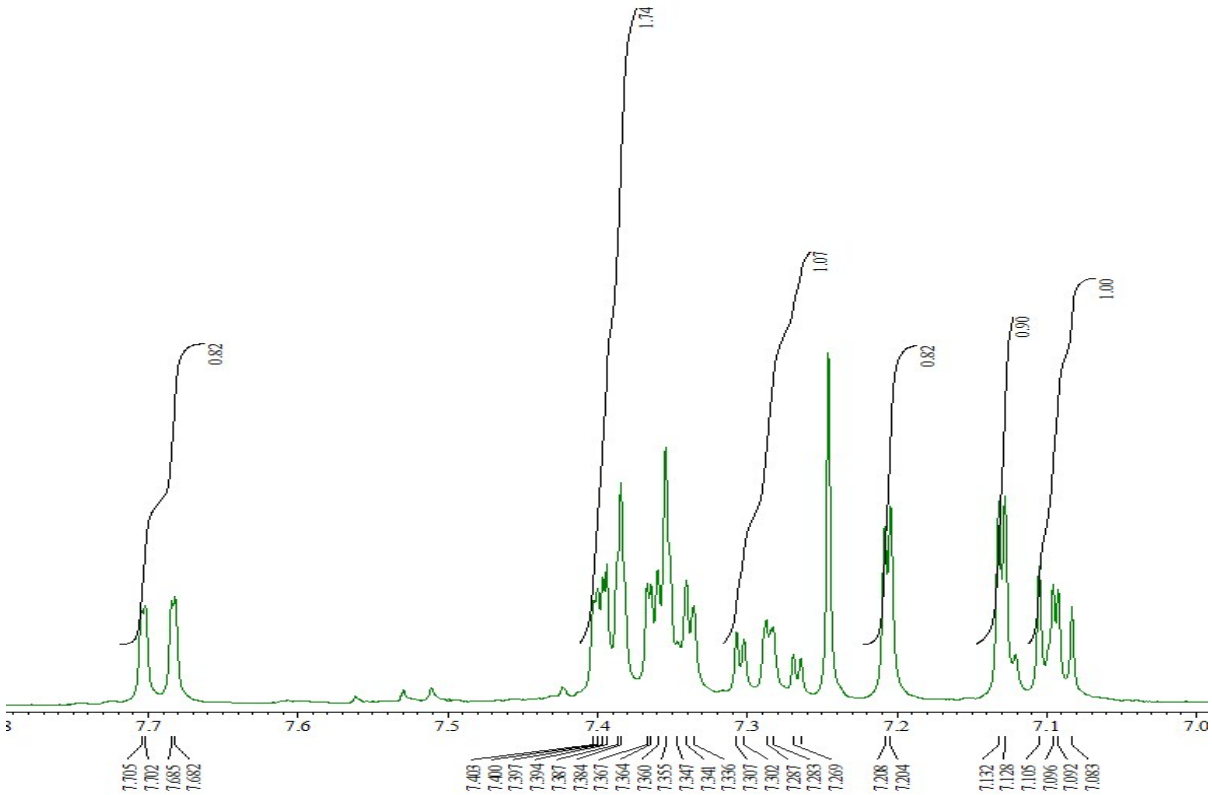

`

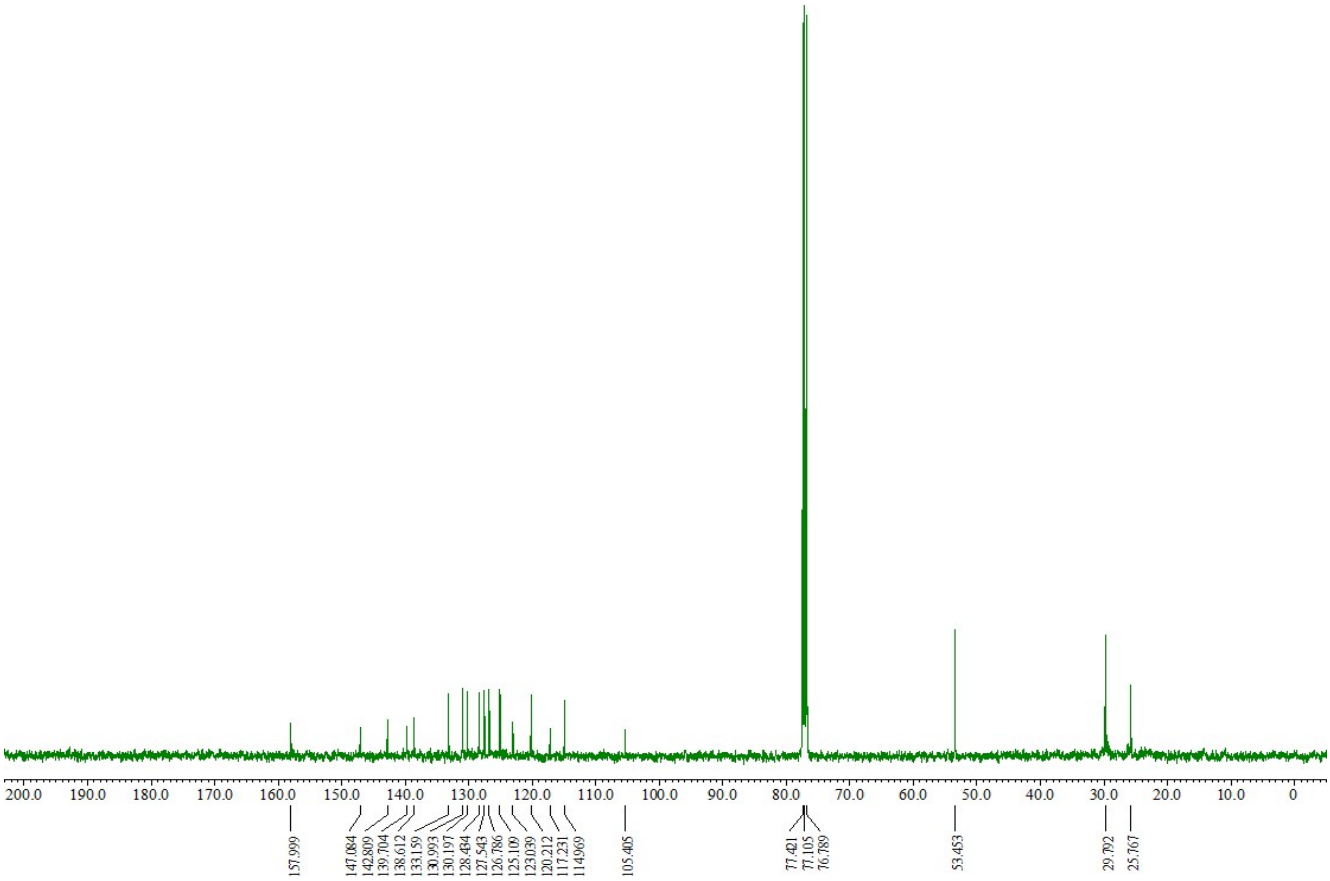

Fig. 38.[1]H, [1]H of aromatic region &[13]C-NMR spectra of **10**.

References:

1. *CrysAlis CCD, RED version 1.711.13, copyright*1995-2003, Oxford Diffraction Poland Sp.
2. A. Altomare, G. Cascarano, C. Giacovazzo, A. Guagliardi, *J. Appl. Crystallogr.*1993, ***26***, 343.
3. G. M. Sheldrick, *F^2 SHELXL-2014/7: Program for the Solution of Crystal Structures; University of Göttingen: Göttingen, Germany,*2014.
4. G. M. Sheldrick, *Crystal structure refinement with SHELXL, Acta Cryst.*2015, ***C71***, 3.
5. G. M. Sheldrick, *A short history of SHELX*2008, ***64***, 112.
6. L. Farrugia, *WinGX, An Integrated System of Windows Program for Solution, Refinement and Analysis of Single-Crystal X-ray Diffraction Data, version 1.70. 01;*2005.
7. F. Macrae Clare,J. Bruno Ian, A. Chisholm James, R. Edgington Paul, McCabe Patrick; Pidcock Elna, e. a. *Mercury CSD 2.0e new features for the visualization and investigation of crystal structures.*2008, ***41***, 466.